Delft University of Technology

Building Safety with Nature

A System Analysis of Dynamic Double Dike Systems

MSc. Thesis

M.D.M. Jansen

Building Safety with Nature

A System Analysis of Dynamic Double Dike Systems

by

M.D.M. Jansen

to obtain the degree of Master of Science
at the Delft University of Technology,
to be defended publicly on Tuesday June 15, 2023 at 04:00 PM.

Student number:	4464850	
Project duration:	May, 2022 – March, 2023	
Thesis committee:	Prof. dr. ir. S. N. Jonkman,	TU Delft
	Dr. ir. B. van Prooijen,	TU Delft
	Dr. ir. V. Vuik,	TU Delft & HKV lijn in het water

This thesis is confidential and cannot be made public until June 15, 2023.

Cover: Koen van Asselt

TU Delft

HKV LIJN IN WATER

Preface

Before you lies the thesis: ”Building with nature: A System Analysis of Dynamic Double Dike Systems”. This thesis has been written in partial fulfillment of the requirements for the degree of Master of Science in Hydraulic Engineering at the Delft University of Technology. The research was performed in close collaboration with HKV lijn in water and is part of the project ’Dynamic Dike Systems’ initiated by the Royal Netherlands Institute for Sea Research (NIOZ).

Of course, this could not have been realised without the support of others. I would like to thank my supervisors for their constructive feedback and guidance; especially Vincent Vuik, as my daily supervisor, for your time and effort, critical thinking along and giving me confidence throughout my thesis.

To all colleagues and students at HKV Lijn in water: thank you for providing an enjoyable workplace for me to write my thesis. I really appreciated the discussions and enjoyable lunch moments.

The journey of writing this thesis was not without any personal challenges and set backs. So, to my dear friends and family: your support served me well, not only throughout my thesis, but my entire university life. Last, but not least, to Chantal: your loving care has enabled me to get the most out of myself everyday, as always.

I hope you enjoy reading.

M.D.M. Jansen
Delft, June 2023

Summary

Sea level rise and land subsidence increasingly put more pressure on Dutch flood protections. Additional to regular dike reinforcements, new, more nature-based, solutions are considered, such as a double dike system (DDS). Such system, consisting of two parallel dikes in combination with an interdike area in the form of a salt marsh, offers the opportunity to adapt via hydro-morphological processes to sea level changes. An increased bed level of the interdike area of a double dike system potentially positively affects wave attenuation. Furthermore, if the second (landward) dike breaches, the elevated salt marsh of the interdike limits breach growth and discharge through the breach. However, previous studies show that it is hard to prove the feasibility and effectiveness regarding flood safety of a DDS relative to a single dike and an in-depth hydraulic engineering substantiation for flood risk reduction is lacking. The objective of this research was to investigate which factors determine the effectiveness of a DDS, with the focus on the dynamic development of the system. This leads to the following research question:

Under which circumstances can a double dike system be an effective alternative to a regular dike reinforcement?

It is possible to distinguish three distinct systems based on the function of the first (seaward) dike: dynamic open DDS, dynamic closable DDS, and static closed DDS. This distinction is primarily based on the degree to which water is permitted to pass through the first dike under both normal and extreme conditions via an opening in the dike. This interaction between the outerdike area and interdike is unobstructed for a dynamic open DDS and almost nonexistent for a static closed DDS. To achieve a more hybrid approach, dynamic closable DDS utilizes adjustable structures like tidal culverts to regulate the inflow. Under normal tidal conditions, the permitted inflow governs the sediment supply and the potential for accretion of the bed level in the interdike area. Depending on the design of the system, during extreme storm conditions, the first dike can act as primary flood defense or as breakwater that provides shelter for the second (landward) dike.

This research focused on an open dynamic DDS system, allowing for maximum potential bed level accretion of the interdike area. In doing so, the first dike functions as a breakwater and failure of the system occurs when the second dike is breached. Due to the unrestricted in- and outflow, the assumption is made that water levels are uniform and equal to the hydraulic conditions outside the system.

The double dike systems are analysed with the help of two approaches: failure probability approach and local individual risk (LIR) approach. The first approach compares systems based on equal probability of failure. The second approach compares systems based on an equal LIR of 10^{-5} per year and includes the expected mortality in case of flooding. Systems have been compared to each other with the help of calculated dike heights and total dike volumes.

Dikes were tested for failure due to overtopping or overflow. Therefore, a transmission model was applied to describe the transmission of waves through the system: wave transmission over the first dike, wave propagation in the interdike area and wave overtopping over the second dike. The probabilistic calculation method FORM was used to find the failure probability and design point. For the LIR approach, this model was extended with a 1D flood model to determine the flood characteristics and subsequent mortality fraction if failure of the dike

occurs. Figure 1 gives an overview of the dynamic open DDS and the implementation of the transmission model.

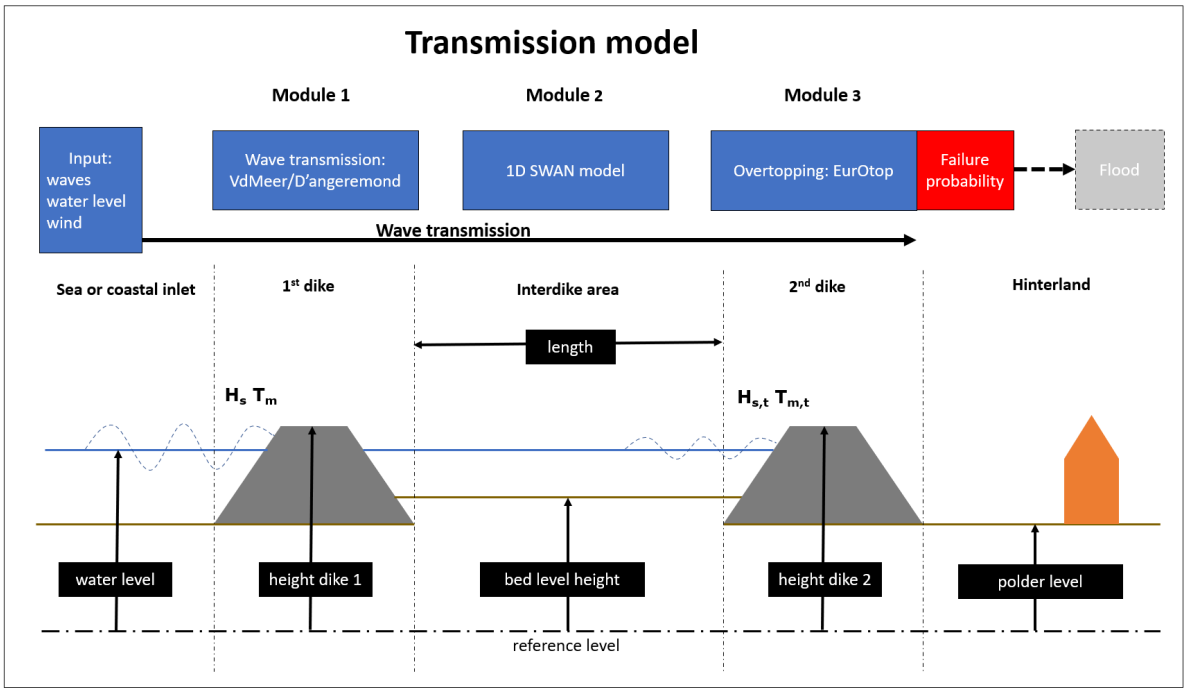

Figure 1: General framework of the application of the transmission model on a dynamic double dike system.

Firstly, a simplified case study was performed based on conditions in the Western Scheldt. Opening the existing dike in the current hydraulic conditions necessitates the construction of a second dike that is only 1.7 meter lower than the single dike system. A sea level rise (SLR) of 0.4 meter in 2070 and 1.0 meter in 2120 was implemented. In addition, morphology scenarios were applied, ranging from no accretion to maximum accretion. In the scenario with maximum accretion, rapid accretion to Mean High water takes place, after which the bed level accretion follows SLR.

Comparing systems based on equal failure probability, a single dike should be raised identically to the SLR. In the case of a double dike system and 1.0 meter SLR, this increase in height of the second dike should be approximately 1.15 meter to maintain equal failure probability. Sedimentation in the interdike area has a negligible impact on failure probabilities due to the dominant influence of water depth, meaning the water depth is too high for waves to be affected by the bottom of the interdike area.

However, this comparison changes when based on equal LIR. With 1.0 meter SLR, the additional required height of a single dike increases to 1.7 meters. Applying this approach to a double dike system, the effect of the height of bed level of the interdike area on the breach flow does have significant influence. Analysing the effectiveness of a double dike system in comparison to a single dike system based on volume increase, these differences are magnified. However, generally, it can be noted that the extreme storm surge in the Western Scheldt is dominant and a second dike with substantial dimensions is needed to comply to its retaining function.

Secondly, a sensitivity analysis was performed on four different parameters and system configurations: 1) height of the first dike in combination with the length of the interdike area, 2) hydraulic conditions with lower water levels, 3) varying area size of the hinterland and 4) implementation of vegetation.

The effect of the first dike on the failure probability is not dominant, since the required increase of the height

of the second dike is not proportional to the applied decrease in height of the first dike, increasing its effectiveness in terms of dike volume. This effectiveness increases also for hydraulic conditions with lower extreme water levels. In addition, there is a positive relation between the effectiveness and the area size of the flooded hinterland. Vegetation does not have any influence on the dike height due to the high water depths under design conditions.

In conclusion, the following three location specific circumstances are important for an open DDS to be an effective alternative to a regular single dike reinforcement:

- Sufficient sediments present to allow for a higher rate of sediment accretion compared to sea level rise.
- Hydraulic conditions in which waves are more important than storm surge.
- Large hinterland area.

It is more advantageous to employ the local individual risk approach in comparative studies assessing the effectiveness of double dike systems. The significant positive impact of bed level accretion on flood impact is disregarded when only considering failure probabilities.

It is recommended to improve the flood model, implementing a 2D model and considering the effect of the foreshore on breach growth, to gain a more comprehensive understanding of the potential of an elevated bed level of the interdike area on the flood impact, so it can be effectively incorporated into the Dutch flood risk approach. In addition, it is recommended to consider the implementation of an open dynamic DDS in coastal areas with high sediment concentrations and suitable hydraulic conditions (sufficient tidal range and mild storm surge).

Furthermore, the wave damping function of the first dike is not critical for interdike areas with sufficient length and reduced depth. It is more efficient to prioritize the flood safety of the second dike. This allows for more effective design and management decisions concerning the height and safety requirements of the first dike.

Finally, it is advisable for areas with high water levels during extreme conditions to consider a closable system. This entails the ability to close the gaps in the first dike under specific conditions, such as utilizing tidal culverts, limiting the hydraulic loads on the second dike. However, implementing a closable system necessitates larger investments in modifications to the first dike.

Additionally, the maintenance of the first dike becomes more crucial due to its retaining function first. Therefore, it is recommended to conduct a comprehensive cost-benefit analysis to compare the open dynamic double dike system with the closable double dike system.

Contents

List of Figures

List of Tables

1

Introduction

This chapter provides an introduction to the research subject. Section 1.1 contains the context of the subject. The problem description is stated in section 1.2, which forms the basis of the formulated research questions in section 1.3. At last, the general approach and structure is introduced in section 1.4.

1.1. Context

Coastal areas are experiencing an increase of flood risk due to sea-level rise, land subsidence and higher risk of extreme storm conditions (Mal et al., 2018). In addition, many people live in the coastal areas and this fraction is only growing, thereby increasing the impact of extreme coastal events (Neumann et al., 2015). This reflects the social and economic importance of having flood defences that meet predefined safety standards. The Netherlands faces a major task in complying with their own flood safety guidelines as well. However, upgrading their coastal defences will likely be at higher costs than previously expected (Hinkel et al., 2014; S. N. Jonkman et al., 2013).

Therefore, coastal protection strategies based on solutions that are robust, sustainable, adaptable and cost-effective for future changes are more and more considered (Slobbe et al., 2013). These so-called nature-based solutions often use hydro-morphological processes and ecological processes to adapt to changes in climate. Instead of focusing mainly on flood protection, these solutions often involve systems with multiple uses with the accompanying challenges and opportunities (Marijnissen, 2021). Several studies show the value of salt marshes as an additional safety buffer in front of sea dikes (Gedan et al., 2011; Möller et al., 2014; Vuik et al., 2016). However, the right hydraulic conditions are not always encountered. The same holds for the space to create these outer dike salt marshes. To solve this, the concept of double dikes as a nature based coastal protection systems is currently being considered (Van Belzen et al., 2021).

A double dike system consists of two dikes with an interdike area (former polder) in between. The first, most seaward dike, has an opening which creates hydraulic interaction (ebb and flood) between the sea and the interdike area. This provides the needed morphological adjustments and the formation of an adaptable salt marsh. The second or inner dike provides the final barrier between the sea and low-lying hinterland (Marijnissen et al., 2021; Mesel et al., 2013; Van Belzen et al., 2021). An concept example can be found in figure 1.1.

Project: Dynamic Dike Systems

This thesis is part of the project 'Dynamic dike systems, which is a collection of exploratory studies on the application of the concept of dynamic (double) dike systems in the Western Scheldt, Zeeland. This is a collaboration between NIOZ (Royal Netherlands Institute for Sea Research), HKV lijn in het water, Deltares, Delft University of Technology, University of applied sciences Zeeland, water boards, provincial government and multiple other organizations. Topics include water safety, morphological development, salt intrusion and public support. The guiding concept is an open system in which natural dynamics and morphological development are very important. The system must have the potential to grow with sea-level rise, thus creating a higher salt marsh in the interdike area.

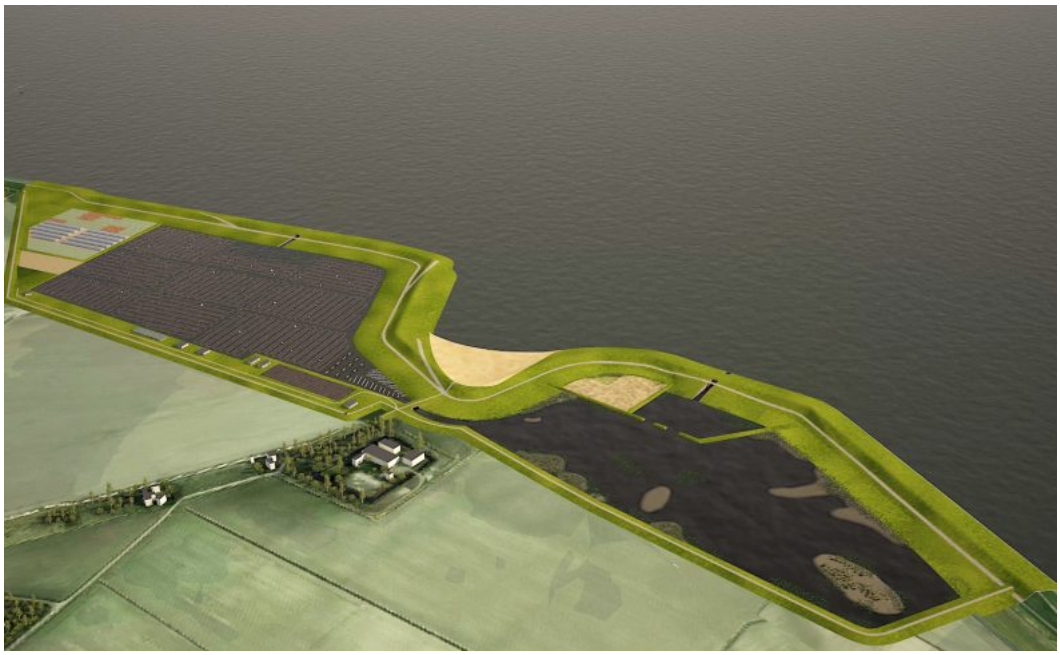

Figure 1.1: Concept art of double dike system (EemsDollard2050, 2018)

1.2. Problem statement

Rising sea level and the salinization and subsidence of Dutch polders result in the consideration of new ways of dike reinforcement, such as a double dike system. It is assumed that there are many advantages to such a system with multiple uses (Marijnissen et al., 2021; Van Belzen et al., 2021). However, it is often difficult to implement these nature-based solutions in the main stream of coastal protections (Vuik et al., 2019a). In order to implement them, a lot of energy must be put into proving the feasibility of the system. A feasibility study by Van Belzen et al., which includes the benefits of the additional potential activities, indicates that there is some potential in the cost-effectiveness of a double dike protection system. However, an in-depth hydraulic engineering substantiation for flood risk reduction is lacking.

Studies into a case study of a pilot double dike system in Eemshaven, Groningen, indicate that implementing two dikes as flood protection does not directly lead to additional flood safety (Marijnissen et al., 2021; Wauben, 2019). Both studies suggest that the second dike does not provide additional protection in case of failure of the

first dike. Wauben even concludes that the system does not meet flood safety standards, despite the potential for lower costs.

An important aspect is the definition of a double dike system. It is not the lack of definition that complicates the concept, but the differences in the various variants. A small change in the system can lead to a completely different functionality. Looking at the flood safety of a case study with a pre-defined system does not necessarily give a good picture of a double dike system in general. An important aspect is the functionality of the first dike and the interaction between the sea and the inter dike area.

Also, the dynamic effect of the system in time, frequently mentioned as one of the biggest opportunities, is often forgotten in the flood risk analysis. Both studies include sea level rise in their research, but lack a morphological analysis. This means that the effect of sedimentation of the inter dike area is not included. In addition, by treating it as a more dynamic system, one may be able to look at a more permissive development of the erosion of the outer dike.

Marijnissen et al. proposed a transmission model that can be used to analyze the dynamic effect and damping of hydraulic loads on the second dike. According to Wauben, a failed dike can still have some protection value by having a damping effect on the hydraulic loads. This is emphasized by Marijnissen et al. with the suggestion that within the framework of dike failure analysis, integration of both erosion and transfer of hydraulic loads is needed.

Finally, the effect of the system on the flood impact is often forgotten in the analysis. Wauben acknowledged that this can have a positive effect on the effectiveness of the system. The height of a foreshore affects the breaching development and amount of water flowing through and therefore affects the probability of death and economic damage (Zhu et al., 2020). If the consequences of a breach are smaller, the probability of failure of the system might be increased in order to keep the same level of flood risk.

1.3. Objective and research questions

The goal of this thesis is to investigate which factors determine the effectiveness of a double dike system as an alternative to a regular dike reinforcement regarding failure probability and flood risk. The influence of the morphological development of the system in time on the safety plays an important role. An important element is the extension and implementation of a transmission model in a probabilistic framework, by which the system can be analyzed according to the current flood risk standards. The results of this thesis could provide valuable insights in the implementation and (cost)effectiveness of a double dike system. This objective is summarized in the following research question:

Under which circumstances can a double dike system be an effective alternative to a regular single dike reinforcement?

To answer the research question in a structured manner, the following sub questions are proposed:

1. *What types of double dike systems can be defined?*
2. *How to assess double dike systems on dike failure and flood risk*
3. *How does the effectiveness of a double dike system compare to that of a single dike system for different morphological scenarios and sea level rise, under conditions present in the Western Scheldt?*
4. *What is the sensitivity of influential system characteristics on the dynamic double dike system?*

1.4. Approach and structure

The comparison between single and double dike systems is conducted using equal failure probabilities and Dutch risk norms. In this study, a transmission model is employed to analyze the failure probabilities and flood risk of a double dike system. The study utilizes a simplified probabilistic case study representative to the Western Scheldt region. The findings obtained from this analysis form the basis for a sensitivity analysis aimed at assessing the system's potential.

The structure of this thesis is as follows. Chapter 2 gives more insight in the different concepts of flood risk, dike failure and functioning of salt marshes in the form of a literature study. Chapter 3 explains the concept of double dike systems and a definition of a dynamic double dike system is formulated. Chapter 4 contains the methodology of this research. This includes the explanation of the different approaches for the comparison of dike systems and the introduction of the used models. In chapter 5, an analysis of simplified case study based on the conditions in the Western Scheldt is performed. Chapter 6 contains a sensitivity analysis in which four different parameter and system variations are analysed. A discussion of the findings can be found in chapter 7. The thesis is finalized with a conclusion an recommendations in chapter 8.

2

State of the art

2.1. Flood risk

This section gives a very brief summary of the principles of flood risk, failure mechanisms and failure probabilities.

2.1.1. Flood risk in the Netherlands

History proves that the Netherlands is vulnerable to flooding and, therefore, nowadays protected by a system of primary flood defences. These flood defences consists of a variety of dikes, dams, dunes and surge barriers. Over the years, safety standards were developed and it was defined as such that flood defences should be able to withstand hydraulic load conditions with a certain probability of exceedance. Since then, substantial advancements have been made over the past decades in the development of methods for analyzing the reliability and risk of the primary flood defences (Jonkman et al., 2021). And as of 2017, the Dutch safety standards are based on a more risk approach (Ministerie van Infrastructuur en Milieu, 2017a). Risk in this research is defined as the probability of an undesired (dike failure) event multiplied by the consequences (S. Jonkman et al., 2020) and can be expressed as:

$$risk = probability \cdot consequences \tag{2.1}$$

All primary flood defence systems have been analysed using this flood risk approach (VNK - Veiligheid Nederland in Kaart, 2014), containing the following steps:

1. Flood hazard analysis: determination of extreme conditions (hydraulic loads)
2. Reliability analysis : determination of probability of failure
3. Breaching analysis and hydrodynamic simulation of flood scenarios
4. Damage and life loss estimation
5. Risk quantification

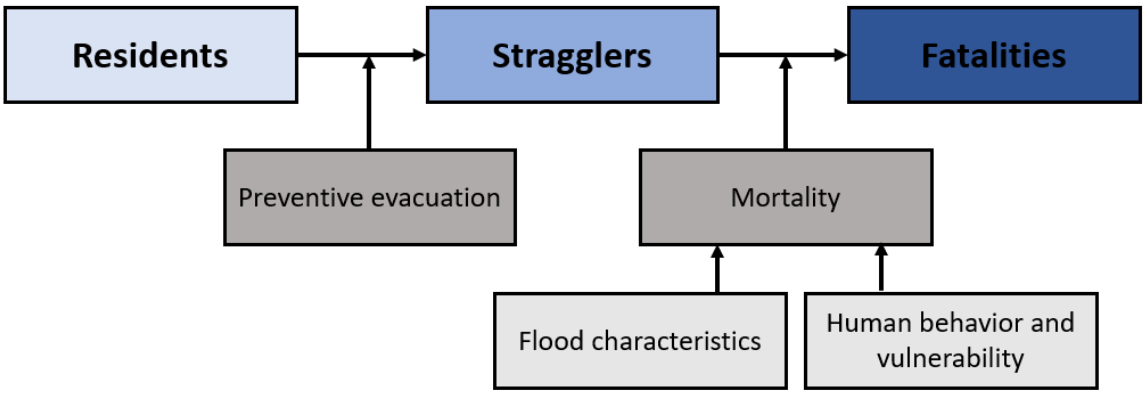

Figure 2.1: Steps for calculating LIR, based on (Beckers & de Bruijn, 2011)

From a practical point of view, the safety of a dike section is often assessed using a safety level or acceptable failure probability per dike cross-section. Thus, after assessing the potential flood impact and risk norms, the calculations are then reconverted into failure probabilities.
Risk quantification is assessed using a societal and economic perspective. From a societal point of view, the probability of an individual dying from a flood and the probability of high number of victims is considered . The economic perspective is based on economic damage in monetary terms.
New acceptable risk standards and modelled flood consequences are used to determine maximum failure probabilities of these dike trajectory, a so-called safety level. In the Netherlands, these risk perspectives are analysed in three practical approaches: **Personal risk**, **societal risk** (dutch: groepsrisico) and **societal cost-benefit analysis**. These are discussed separately below.

2.1.2. Personal risk

To determine individual risk, both location-specific riks (dutch: plaatsgebonden risico or PR) and local individual risk (dutch: local individual risk or LIR) can be used. Both indicators give the probability of a person dying as a result of flooding. However, the LIR is adjusted for preventive evacuation, which makes it better suitable for prediction actual personal risk . In the Netherlands, a so-called LIR-norm of 10^{-5} is maintained, meaning that there is a maximum risk of dying from flooding once every 100000 years (Beckers & de Bruijn, 2011). Determining the LIR consists of three steps:

1. Failure probability of dike section (p_f)
2. Probability of being present or not being evacuated ($1 - f_e$)
3. Probability of becoming a fatality (f_d, mortality)

These steps can be combined in the following equation and schematized in figure 2.1:

$$LIR = p_f(1 - f_e)f_d \tag{2.2}$$

Mortality

The mortality (f_d) is defined as the fraction of fatalities in relation to the residents present. The Mortality of large-scale historic floods is on average around 1% (S. N. Jonkman, 2007). Flood characteristics are often used to get better insight in the spatial distribution of mortality (Jonkman, 2007; Maaskant, 2007):

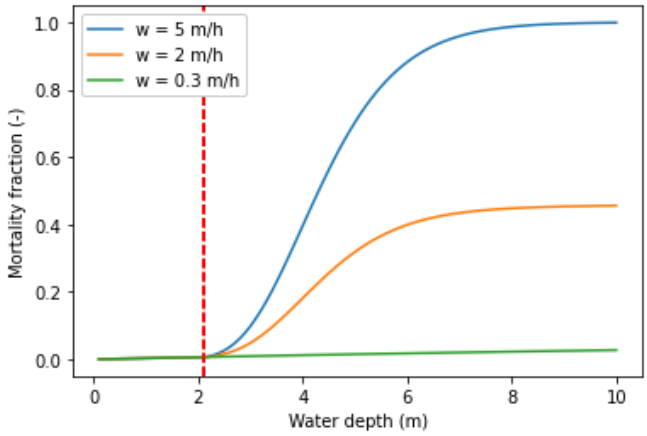

Figure 2.2: Mortality function for different rates of water level rise.

- Water depth of the flooded area (h)
- Rate of rise of the water level (w)
- Flow velocity (in case fast-flowing water)

For dike failure, the situation in which flow velocity is dominant only occurs in the breach zone, for which a mortality fraction of 1 can be assumed (Jonkman, 2007). However, in comparison with total flooded hinterland, this is in the Netherlands almost non-existent and often not included in the calculations (Maaskant et al., 2009). For the significant flood zones, Jonkman derived a mortality function (Eq. 2.3) based on the cumulative normal distribution of a log-normal dose response function which depends on the maximum water depth and rate of rise of the water level. This function is based on data of the 1953 floods in the Netherlands and, therefore, human behaviour and vulnerability is implicitly included.

$$F_d(h) = \Phi(\frac{ln(h) - \mu_N}{\sigma_N}) \tag{2.3}$$

in which h is the maximum water level, Φ the cumulative distribution function of a standard normal distribution and the constants μ_N and σ_N depend on the different hazard flood zones. These zones are defined by the flood characteristics as well: 1) rapdily rising water ($F_{d,rise}$), 2) transition zone ($F_{d,trans}$) and 3) remaining zone ($F_{d,remain}$). Equation 2.3 can be used for zone 1 and 3, but with different corresponding values for μ and σ (Table 2.1). For the transition zone, interpolation between zone 1 and 3 can be used as depicted in Equation 2.4 (Jonkman et al., 2021). Figure 2.2 gives an visual overview of the mortality fraction relative to the maximum water level during a flood for different rates of water level rise.

$$F_{d,trans} = F_{d,remain} + (w - 0.5)\frac{F_{d,rise} - F_{d,remain}}{3.5} \tag{2.4}$$

	zone	max water level (m)	rise of water (m/hr)	μ_N	σ_N
1	Rapidly rising waters	h $\geq$ 2.1 and	w ≥ 4	1.46	0.28
2	Transition zone	h $\geq$ 2.1 and	$0.5 \leq w < 4$	-	-
3	Remaining zone	h $<$ 2.1 **or**	w < 0.5	7.60	2.75

Table 2.1: Defined flood zones with corresponding mortality constants, based on Jonkman (2007).

Evacuation

The number of people present in a hazard zone can be reduced by preventive evacuation. Preventive evacuation can be defined as 'the evacuation before occurrence of the event' (Jonkman, 2007). Therefore, the evacuation fraction (F_e) includes the fraction of people who are not present during the flood due to evacuation. People who get to safety during the disaster, for example by fleeing to local higher areas, are included in the calculation of the mortality fraction. In general, the amount of time available between the first signs of a flood and the actual event is the most important factor determining the evacuation fraction (Jonkman, 2007). This available time depends on the physical behaviour of the flood (slowly building-up vs. sudden) and the quality of the warning system; identifying the upcoming hazard and warning the population.

For this research, an average region dependent fraction is used (Beckers & de Bruijn, 2011; Maaskant et al., 2009). An overview of the different fraction within the Netherlands can be seen in Figure 2.3.

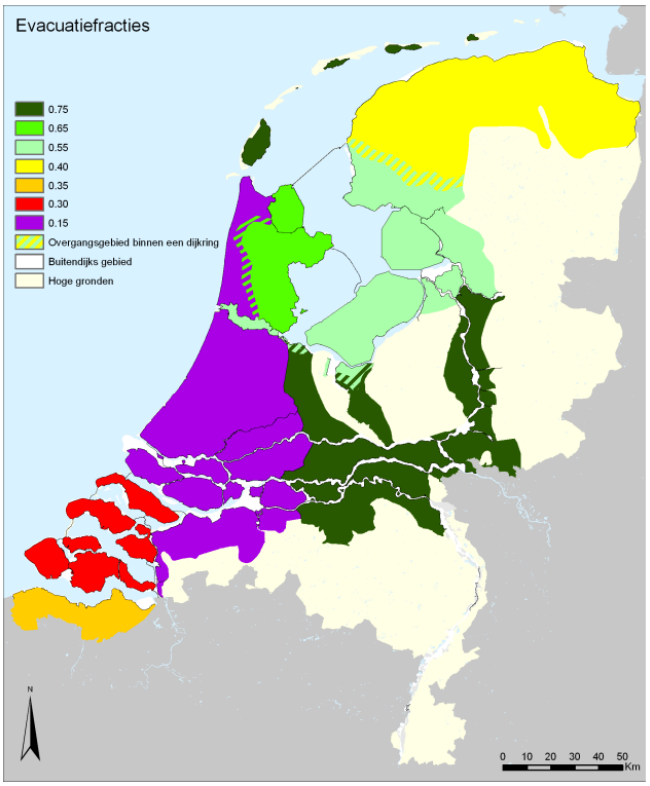

Figure 2.3: Average evacuation fraction for different regions in the Netherlands (Beckers & de Bruijn, 2011)

2.1.3. Societal risk

Societal risk concerns the probability per year that a large number of people will die during a flood event (Jonkman, 2007; Klijn et al., 2013). This analysis follows almost the same approach as that of personal risk. So, it looks at the probability of failure of a dike trajectory, the potential of evacuation and the mortality of those left behind. Only, in the case of societal risk, additional consideration is given to the expected number of victims per trajectory and the dependency between the breaches of different dike trajectories (Beckers & de Bruijn, 2011). Reasoning often start with the concept of social disruption. Hence, societal risk is often analysed on national scale and, therefore, dependency between the failure of dike trajectories is important (Klijn et al., 2013). The Netherlands is divided into sub-regions (Figure 2.4), between which correlation with respect to hydraulic loads is negligible

(Beckers & de Bruijn, 2011). One can think of high river discharges and vulnerability to storms from different directions.

Figure 2.4: Defined sub-regions within the Netherlands regarding societal risk (Beckers & de Bruijn, 2011)

2.1.4. Societal cost-benefit analysis

A societal cost-benefit analysis (Dutch: Maatschappelijke kosten-baten analyse or MKBA) has the purpose of comparing the costs and benefits of flood reduction measures, specifically dike reinforcements. This type of analysis aims to determine the economically optimal failure probability per dike section and the investment costs associated with it.

At the basis of the MKBA model lies an already proven concept or economic analysis method that seeks an optimal, long–term investment strategy for dike reinforcements (Eijgenraam, 2006; van Dantzig, 1956). This means that the total costs of investments in dike heightening and expected damage over a longer period are minimized (Deltares, 2011; Kind, 2014). This economic method can be graphically represented as in Figure 2.5. The investment is profitable if it out-weights the monetary value of further reduction in damage. To conduct a time-based analysis, it is important to consider economic growth, climate change, soil subsidence, and increasing implementation costs (labour, material etc.), which could contribute to a nonlinear increase in costs (Jonkman, 2013).

Sometimes, a decimation height is used to quantize the effect of an investment in dike reinforcement. This refers to the additional required height of the dike to reduce the probability of dike failure by a factor of ten and can be converted into costs per kilometer of dike (Deltares, 2011).

In addition to economic damage, monetary value can also be assigned to flood victims. In the Dutch MKBA method, an average amount of 12.000 euros per victim is used. This number includes all immaterial damage and personal costs for evacuation. For fatalities, an amount increases to 6.7 million euros per victim (Bockarjova et al., 2012; Deltares, 2011).

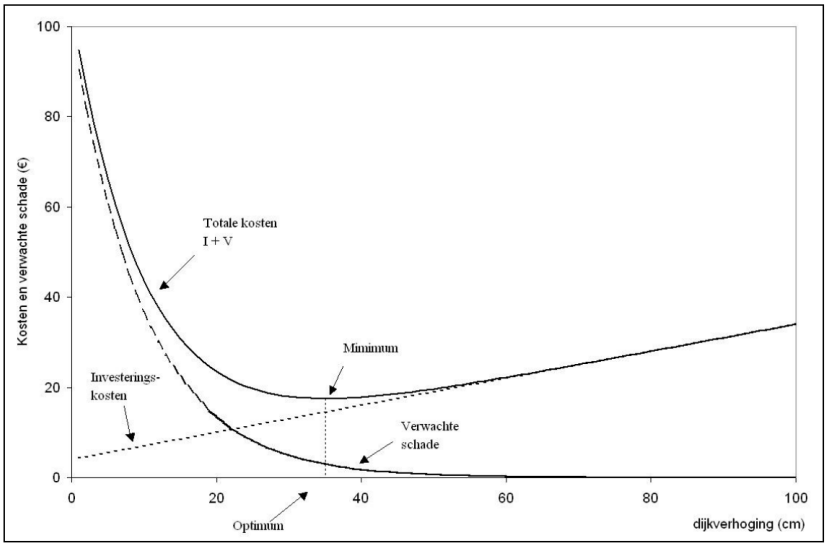

Figure 2.5: General principle MKBA. Example of the expected costs of investment and damage (€) in relation dike heightening (cm) (Deltares, 2011).

2.2. Dike failure

2.2.1. Failure mechanisms

Failure of a dike can occur due to various causes or so-called failure mechanisms. Possible failure mechanisms are visually summarised in Figure 2.6. In the Netherlands, safety of dutch flood defences is assessed using the Statutory Assessment Instruments (Dutch: Wettelijk Beoordelingsinstrumentarium or WBI) (Ministerie van Infrastructuur en Milieu, 2017b). The WBI mainly looks at the geotechnical failure of a dike and the stability of revetments. These are summarized in Table 2.2 and described in more detail below.

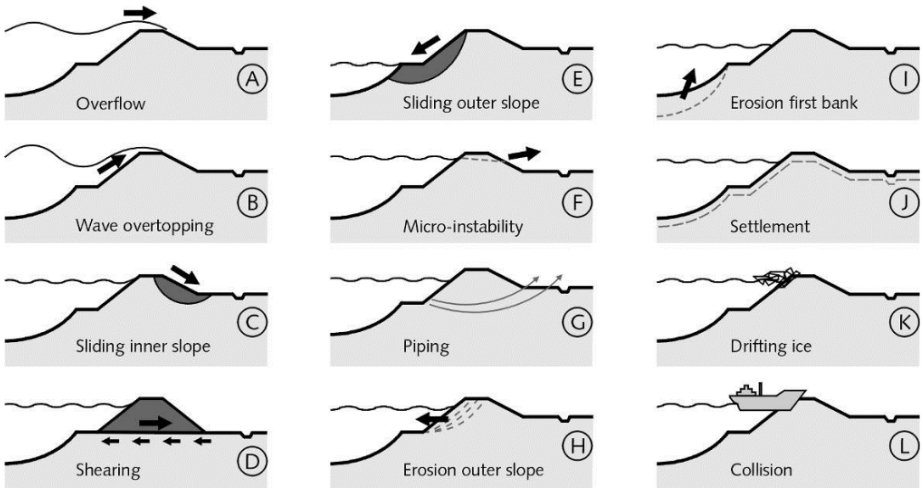

Figure 2.6: Overview of failure mechanisms of a dike (Jonkman et al., 2021)

Macro-instability of the slope

Macro-instability or sliding can occur on both the inner and outer slope. Sliding of the inner slope is caused by high water levels at the outside of the dike. Failure occurs due to a combination of decreased shear strength of the soil caused by increased water pressure, the extra weight of the dike and uplift forces caused by the higher water

Failure mechanisms of a dike (WBI)	Code
Geotechnical	
Macro-instability of the inner slope	STBI
Macro-instability of the outer slope	STBU
Piping	STPH
Micro instability	STMI
Revetment	
Wave impact on asphalt	AGK
Overpressure of water under asphalt	AWO
Grass cover erosion outer slope	GEBU
Grass cover sliding outer slope	GABU
Grass cover erosion crest and inner slope	GEKB
Grass cover sliding inner slope	GABI
Stability of stone revetment	ZST

Table 2.2: Failure mechanisms of a dike classed by WBI (Ministerie van Infrastructuur en Milieu, 2017c).

level. Sliding of the outer slope can occur when the water level at the outer side of the dike declines rapidly. The excessive pore pressure causes a decrease in shear strength of the soil. The slope of the outer dike can become unstable without the counter weight of the higher water level, which leads to sliding. Despite the slightly different hydraulic causes, increased pore pressure leads to instability and sliding of the slope, and total failure of the dike in both cases.

Piping

Piping is caused by a substantial hydraulic gradient within the dike, which is the difference in water level between the outside and inside of the dike. Due to this hydraulic gradient, water can be 'pushed out' at the inside of the dike. This groundwater flow causes underneath a dike and eventually an erosion pipe can occur, which leads to stability problems and, eventually, failure of the dike. This process can be described by two needed conditions:

1. Uplift: uplifting and rupturing of the inside of the dike due to the large hydraulic head and upward pressure, starting a groundwater flow through the soil layer.
2. Heave: sand starts eroding if the pressure gradient exceeds a critical (heave) gradient. This critical gradient depends on the soil characteristics and the seepage length, which is the length between the outside and inside of the dike.

If these two conditions are satisfied, backwards erosion underneath the dike starts, which leads to the formation of pipes.

Micro-instability

Micro-instability considers the stability of individual grains. If the phreatic line increases to the level of the inner slope and the slope layere is permeable, grains are washed out by the excessive water pressure.

Stability of revetments

Different types of revetments are used on dikes. The most common types are: grass, asphalt and stones. Every type has his different failure modes, which also depends on the location of the dike (outer slope, inner slope and

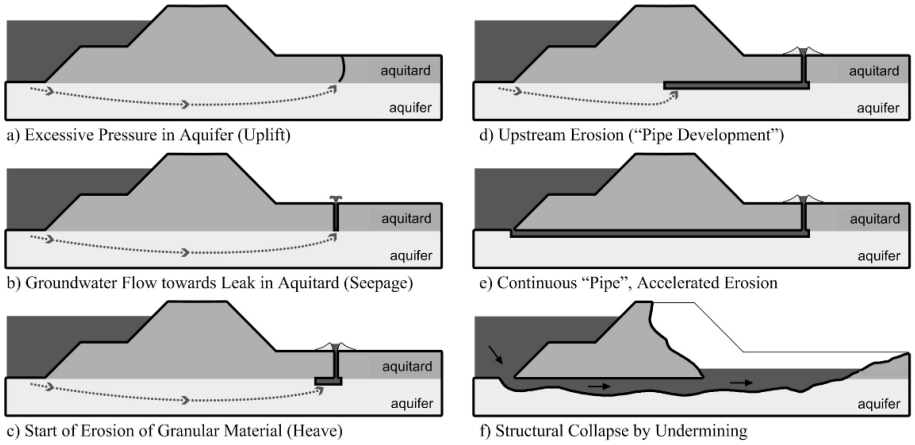

Figure 2.7: The different phases of the piping process (Jonkman et al., 2021)

crest). Grass revetments primarily fail due to erosion caused by wave impact, run-up (outer slope) or when water reaches the crest or inner slope of the dike due to a combination of water level and waves (crest and inner slope). Asphalt is primarily used on the outer slope and fails due to wave impact, causing deformation, and high excess pore pressure due to rapid decline in water level. Stone revetment (outer slope) failure is caused by the same failure mechanisms as asphalt; stones are moved or pushed of by wave impact and/or large pore pressures inside the dike.

Comparing the failure mechanisms of Figure 2.6 and those classed by WBI in Table 2.2, **overtopping** and **overflow** are not classified in the WBI failure mechanisms. Overflow is direct failure of the retaining function of a dike due to the overflow of water due to insufficient crest height. Overtopping is a similar feature, caused by wave run-up. However, both do not always leads to geotechnical failure and breach development. Large quantities of overflowing water (overtopping discharge) can cause erosion to occur on the inner slope, which affects the stability of the dike. The amount of the overtopping discharge a dike can withstand depends on quality of the revetment.

2.2.2. Calculating failure probabilities

During a failure probability assessment of a dike all relevant failure mechanisms must be checked for failure. This can be done using the limit state function:

$$Z = R - S \tag{2.5}$$

in which R is the resistance and S the load. Failure occurs when Z < 0; the load is bigger than the resistance. There are four different kinds of reliability methods.

- level 3: full probabilistic methods. Costs a lot of computational time, but calculates the failure probability exactly.
- level 2: Approximation of full probabilistic methods. The limit state function is linearized in a so-called design point.
- level 1: Semi-probabilistic methods. Safety factors are used to upgrade the load an resistance parameters, leading to design parameters.

- level 0: Full deterministic method.

In the safety assessment it is important to distinguish the difference between failure probability, failure probability of a cross-section and failure probability of a dike trajectory. Within the dutch WBI dike assessment these are defined as follows (Ministerie van Infrastructuur en Milieu, 2017b).

- *Failure probability*: The probability of exceeding ultimate limit state of a dike for a specified failure definition or failure mechanism.
- *Failure probability of a cross-section*: The failure probability of a cross-section for a combination of failure definitions or failure mechanisms.
- *Failure probability of a dike trajectory*: The failure probability of a cross-section projected to a dike trajectory, considering load dependencies and length effect. This definition of failure probability is used for the calculation of the LIR (Eq. 2.2).

The failure probability of a cross-section is a combination of different failure mechanisms. This combination depends on the amount of contribution of each failure mechanism to the total failure probability, which can be expressed as a **contribution factor** (ω). Table 2.3 gives an overview of these factors for the different failure mechanisms. Overtopping and overflow is covered by the *grass cover erosion of the crest and inner slope*.

Expanding the analysis to trajectory level also introduces the impact of the **length-effect**. The probability that a dike breaches somewhere along this trajectory is higher than for a single cross-section (Jongejan, 2016). Therefore, the length-effect increases the failure probability for a certain dike trajectory. The factor of the length-effect (N) is location specific and depends on the failure mechanism, total length of the trajectory and dependency of hydraulic loads.

Equation 2.6 shows how the failure probabilities of a trajectory (P_{req}) can be adjusted to that of a failure mechanism for a specific cross-section ($P_{req,j}$).

$$P_{req,j} = \frac{\omega P_{req}}{N} \tag{2.6}$$

Failure mechanisms of a dike	ω
Grass cover erosion crest and inner slope (GEKB)	0.24
Piping (STPH)	0.24
Macro-stability inner slope (STBI)	0.04
Grass cover erosion outer slope (GEBU)	0.05
Other revetment outer slope	0.05
Piping at structure	0.02
Strength and stability structure (STKWp)	0.02
Other failure mechanisms	0.30

Table 2.3: Different failure mechanisms and their corresponding contribution factor to the failure probability of a cross-section according to WBI (Ministerie van Infrastructuur en Milieu, 2017b).

2.2.3. Breach stages

Predicting the development of a dike breach is a challenging task. This primarily due to its dependency on different mechanisms and conditions, such as hydraulic conditions, dike dimensions, soil characteristics and non-

uniformity, and different failure mechanisms. Breach growth is often described using different phases. Verheij and Van der Knaap 2003 describes the following three phases:

1. Start phase: The formation of an initial gully by either erosion due to overtopping or sliding of the inner slope.
2. Deepening phase: The initial trench deepens to form a breach with a bottom at a certain level, but it does not widen yet.
3. Widening phase: The breach no longer grows vertically, but only in width.

Visser (1998) follows broadly the same steps, but makes additional distinctions in some hydrodynamic processes; critical and sub-critical flow. In addition, he makes an additional distinction within the initial vertical growth of the breach. He describes the process in the following five steps, which are also illustrated in Figure 2.8:

1. Steepening of the slope angle β of the channel in the inner slope from an initial value β_0 at $t = t_0$ up to a critical value β_1 at $t = t_1$.
2. Retrograde erosion of the inner slope at constant angle β_1 for $t_1 < t \leq t_2$, yielding a decrease of the width of the crest of the dike in the breach; this stage ends at t_2 when the crest vanishes and the breach inflow starts to increase.
3. Lowering of the top of the dike in the breach, with constant angle of the breach side-slopes and equal to the critical value γ_1, resulting in an increase of the width of the breach for $t_2 < t \leq t_3$. At $t = t_3$ the dike in the breach is completely washed out down to the base of the dike at polder level.
4. Critical flow stage, in which the breach flow is virtually critical throughout the breach for $t_3 < t \leq t_4$, an the breach continues to grow mainly laterally. the side-slope angles remain at the critical value γ_1. the breach growth in vertical direction depends in this stage on the erodibility of the base of the dike. At t_4 the flow through the breach changes form critical to sub-critical.
5. Sub-critical flow stage, in which the breach continues to grow, mainly laterally due to the sub-critical flow in the breach for $t_4 < t \leq t_5$. At t_5 the flow velocities in the breach become so small (incipient motion) that the breach erosion stops. The side-slope angles remain at the critical value γ_1. The flow through the breach continues and stops when at t_6 the water level in the polder has equalled the outside water level.

Phases 1 and 2 of the formulation of Verheij and Van der Knaap and phases 1, 2, 3 of that of Visser describe the initial formation of the breach and vertical growht. Phase 3 of Verheij and Van der Knaap and phase 4, 5 and 6 of Visser describe the widening process of the breach.

The impact on the flood development of the different phases depends very much on the duration. The deepening phases of the breach is often short; in the order of minutes for sand to max one hour for clay (Verheij & Van der Knaap, 2003). The total inflow of water during these phases is often limited and therefore vertical growth is often simplified in models.

The initiation phase of the breach is often not included in breach modelling (Wahl, 2004), because it focuses on the inflow of water, which does not occur in large quantities during the initiation phase, and the time-frame of the development of the initial trench is often difficult to predict (Verheij & Van der Knaap, 2003). However, this phase can be important regarding available warning and evacuation time (Wahl, 2004).

The last phase described in Figure 2.8 stops when the underlying polder is completely filled, because then the flow through the breach stops. However, this is not the case in a tidal system. A low tide, the water will flow in the opposite direction through the breach, thus following the tidal wave.

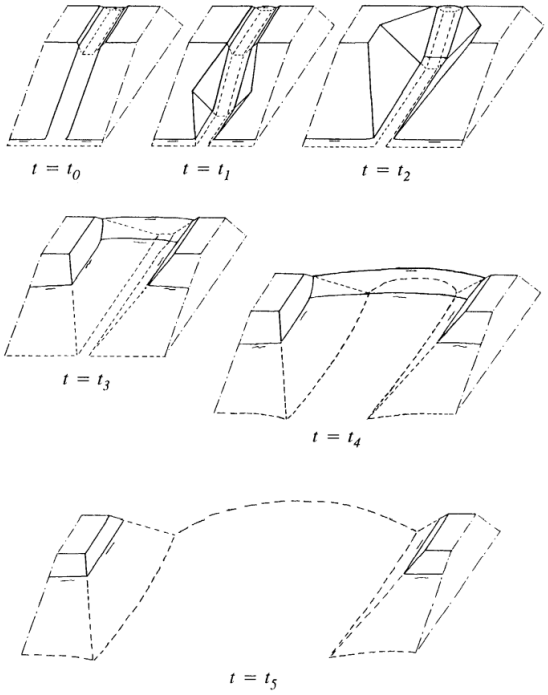

Figure 2.8: Schematic illustration of breach growth phases in a sand dike (Visser, 1998)

2.2.4. Breach growth

Breach dimension in time are determined by breach growth rates. As described above (Section 2.2.3), a distinction is mainly made between vertical and horizontal growth and modelled independently.

Modelling vertical growth is often simplified as a linearized deepening of the breach in time between crest level and the final vertical depth of breach (Verheij & Van der Knaap, 2003). This way, the vertical growth is only dependent on its assumed total duration as can be seen in Equation 2.7 .

$$z(t) = z_{crest} - (z_{crest} - z_{min})\frac{t}{t_0} \tag{2.7}$$

in which $z(t)$ the vertical breach level in time, z_{crest} the height of the dike, z_{min} the minimum breach level and t_0 the total duration of vertical growth.

After the minimum breach level is reached, the breach starts to widen. Two horizontal breach growth formulations are considered: 1) Verheij and van der Knaap (2003) and 2) Van Damme (2020).

The formulation of Verheij and van der Knaap (2003) can be found in Equation 2.8 and its practical application is well used within the dutch flood risk assessments (Beckers & de Bruijn, 2011). It primarily depends on the water level difference across the breach and the soil characteristics (critical flow velocity).

$$B = 1.3\frac{g^{0.5}H^{1.5}}{u_c}log(1 + \frac{0.04g}{u_c}t) \tag{2.8}$$

in which B is the breach width, g the gravitational constant, H the difference in water level on the inside and outside of the dike and u_c the critical flow velocity for soil particles.

Van Damme (2020) formulated the breach growth for dilatant soils based on a process based relation between a displacement rate and shear stress, as depicted in Equation 2.9. Since a breach develops on two sides, the total breach growth is twice the displacement rate ($2c_{fit}$).

$$c_{fit} = m\tau_0^{0.5} + c_1 \tag{2.9}$$

$$\tau_0 = \rho g n^2 u_{breach}^2 (1/R^{(\frac{1}{3})}) \tag{2.10}$$

in which c_{fit} (m/s) is the one-sided displacement rate and τ_0 (Pa) the shear stress. m ($m^2 s/kg$ and c_1 (m/s) are the displacement factor and displacement coefficient respectively and empirical fitted. These empirical fit depends on the hydraulic conductivity (K_s, m/s), initial porosity (n_0) and critical porosity (n_{loose}). Regarding the shear stress; ρ is the density of (salt)water, g the gravitational coefficient, n the Manning's roughness coefficient (often assumed to be 0.020), u_{breach} the velocity (m/s) in the breach and R the hydraulic radius (m).

2.3. Salt marshes

Salt marshes can have multiple functions (e.g. ecosystem service, wave attenuation and sediment trapping) and are often incorporated as a solution in building with nature concepts. This section describes some important elements regarding the functioning of salt marshes with the focus on flood risk mitigation.

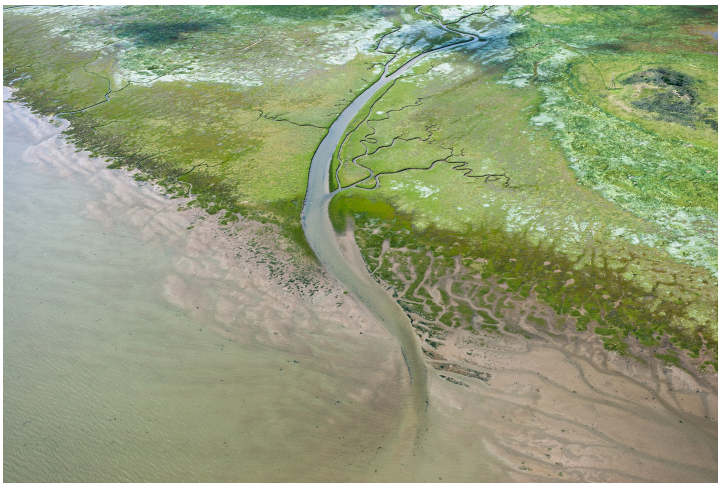

Figure 2.9: Salt marsch Schiermonnikoog (beeldbank.rws.nl)

2.3.1. Morphological development under sea level rise

Salt marshes are often praised for their dynamic morphological behaviour regarding adaptability to sea level rise. Global measurements of bed level changes indicate that salt marshes are generally building with similar rates to historical sea level rise (Kirwan et al., 2016). Vertical growth rates are enhanced by the sediment trapping effect of vegetation which tends to increase vegetation productivity due to mineral sediment disposal (Gedan et al., 2011). So, these factors have a reinforcing effect on each other. In addition, regular inundation makes sure that enough sediments are naturally supplied.

However, there are limits to this adaptability. At faster rates of sea level rise - above a certain threshold - the bed level deepens and can not support vegetation, breaking the reinforcing effect of vegetation on sedimentation (Kirwan et al., 2010). This threshold depends on the suspended sediment concentrations of the system and has a positive relation with the tidal range.

2.3.2. Behaviour under extreme conditions

Several studies highlight the potential effectiveness of salt marshes on the reduction of storm surges and wind waves (Gedan et al., 2011; Möller et al., 2014; Vuik et al., 2016). This can be attributed to three reasons: depth-induced breaking, increased bottom friction due to vegetation and wave propagation through vegetation fields. Wave propogation across a salt-marsch can be best described via a one-dimensional wave energy balance (Vuik et al., 2018):

$$\frac{dEc_g}{dx} = S_{in} - S_{ds,w} - S_{ds,b} - S_{ds,f} - S_{ds,v} \tag{2.11}$$

The different energy source terms are described on the right hand side. They consist of the wind input (S_{in}) and dissipation terms due to whitecapping ($S_{ds,w}$), depth-induced breaking ($S_{ds,b}$), bottem friction ($S_{ds,f}$) and vegetation ($S_{ds,v}$). The wave energy on the left hand side can be expressed as follows:

$$E = \frac{1}{8}\rho g H_{rms}^2 \tag{2.12}$$

where H_rms is the root mean squared wave height (m), ρ the density of water (kg/m^3), g gravitational acceleration (m^2/s), c_g the group velocity (m/s).

It can be concluded that the state of the vegetation is important for the effectiveness regarding wave energy dissipation. Vegetation characteristics as stem height, drag coefficient and flexibility contribute to the stability of the vegetation.

A dynamic salt marsh typically has a large spatial variation in vegetation and bed level height. Often seen as a good feature for the natural system, this creates more uncertainty regarding the probability of failure of the system (Vuik et al., 2018). According to Vuik et al. the effect of the vegetated foreshore on the probability of failure is as follows:

- Increases with foreshore width
- Decreases with overtopping resistance of the dike
- Increases with vegetation strength
- Increases with increasing dependence between wind, water level and wave height
- Increases with offshore wave height
- Decreases with sea level rise, without change in foreshore elevation

2.3.3. Impact on dike breaching

This subsection is based on a study by Zhu et al.(2020). This study shows a connection between flood impact an coastal wetlands via the breach characteristics of a dike. With historical flood maps a comparison can be made between the quantity and size of breaches of different dike sections during the an extreme events. Zhu et al. concludes that a healthy salt marsh foreshore not only reduces the likelihood of dyke failure (see previous subsection), but lowers the impact of the flood by limiting breach dimensions as well. Mainly the height of the foreshore is an important positive factor. The breach dimension has a direct impact on the inflow volume and discharge of the flood, slowing down water level rise and decreasing inundation depth of the hinterland (S. Jonkman et al., 2008).

2.3.4. Implementing salt marshes in flood risk strategies

This subsection considers implementation strategies of salt marshes as foreshore regarding flood risk reduction described by Vuik et al.:

1. Traditional dike heightening.
2. Vegetated foreshore via sediment nourishment.
3. Using detached structures (e.g. breakwaters) to enable salt marsh formation.
4. Construction of a wave breaking high zone in combination of lowering the seaward section of the salt marsh.
5. Construction of a system with brushwood dams and drainage ditches to facilitate sedimentation and prevent lateral erosion.

The first strategy is the most common response but will for this study be used more as a benchmark for different strategies involving salt marshes. Combinations of dike reinforcement en salt marsh implementations are possible. Sediment nourishment is an proven and effective strategy to construct foreshores. However, successful implementation depends on available sediments and the wave energy (bron). The establishment of vegetation requires sheltered areas. Structures with the function to trap sediments can enhance marsh accretion. During extreme events the wave loads are reduced by both the structures as the elevated foreshore. The construction of a higher zone in front of the dike increases the needed effort by moving the sediments to a high which is not achievable by natural accretion. An additional benefit is the lowering and renewal of the foreshore in other places, which creates a more diverse natural system (bron). Using brushwood dams is relatively similar to the third strategy. This is an old method which is historically proven to be effective (bron).

Figure 2.10: Vegetated foreshore, Friesland (beeldbank.rws.nl)

Regarding the effectiveness of the implementation of these strategies, Vuik et al. concludes that the construction of salt marshes is generally cheaper. However, their effectiveness regarding failure probabilities is uncertain because of their dependency on the sediment accretion. The combination with the construction of a high zone in the foreshore improves the probability of failure substantially. Sheltering structures do have an positive effect on the flood risk, but do need continuous maintenance, making them less attractive. Generally, salt marsh construction is only more cost-effective if the economic impact is small in case of breaching.

2.3.5. Application on a double dike system

So far, the applicability of a salt marsh is mainly discussed as a vegetated foreshore. Implementing a salt marsh as a dynamic system between two dike gives as an advantage by the fact that the area is more sheltered for high wave energies and erosion is less likely to occur. This also makes sedimentation of suspended sediments in this area easier.

However, care must be taken to assure that, despite the dike, there is sufficient interaction between the sea and interdike area. The is because the supply of sediments is positively correlated with the tidal range and quantity of inundation.

In addition, the smaller chance of occurring erosion and the two dike as boundaries of the marsh system tends to reduce the vertical and horizontal variation, which negative for a diversified ecological system.

In Chapter 3, this application is further discussed.

3

Double dike systems

A double dike system is, by definition, a type of flood protection that contains two parallel dikes with an interdike area in between. The first dike or outer dike is closest to the sea, river or estuary. The second dike or inner dike is closest to the hinterland and can be seen as the last line of defence. This chapter describes different functions and applications of a double dike systems. In addition, some examples of already existing systems are described and analyses. This chapter concludes with a definition of the double dike system used in this research.

3.1. Parallel dikes

A simple approach for a double dik system is starting to define the system as two parallel dikes, each with its own function. These double dike systems can be classified using the probability of a flood (P_f) for the two dikes separately (Marijnissen et al., 2021). This classification can be seen in Figure 3.1 and focuses on the flood protection function of the system. This is not direclty about the geotechnical failure of the dike, but more about the retaining function regarding water levels. The outer dike is indicated with (1) and the inner dike with (2). Five types of dike configurations can be distinguished. Type I is a system in which the outer dike is stronger than the inner dike. For type II, both dikes have the same probability of flood. Type III and IV describe an system in which the outer dike is smaller. Type V is a system with a breached outer dike.

One can understand that these different configurations of dike elements serve different functions and in particular, the function of the outer dike should by examined. Although the entire system is seen as the flood defence system, one dike is often designated as the primary flood defence. This is the outer dike in the first and second type. The second dike functions primary as back-up or mitigation measure after failure of the outer dike or the provide for some containment in case of overtopping. The inner dike is the primary flood defence for the third, fourth and fifth type. The last two types are different by not providing any flood safety for the inter dike area and only providing some load reduction (primarily waves) on the inner dike. For the third type this depends on the severity of the extreme hydraulic event. All things considered, the function of the outer dike can vary from water retaining to permeable, with only a damping effect on incoming waves.

Systems may also change type as a result of erosion, breaching of the outer dike of changes in hydraulic conditions (e.g. climate change). For example, type II system changes to a type V system after breaching of the outer dike. This changes the functioning of the system and this can be seen as function failure of the outer dike.

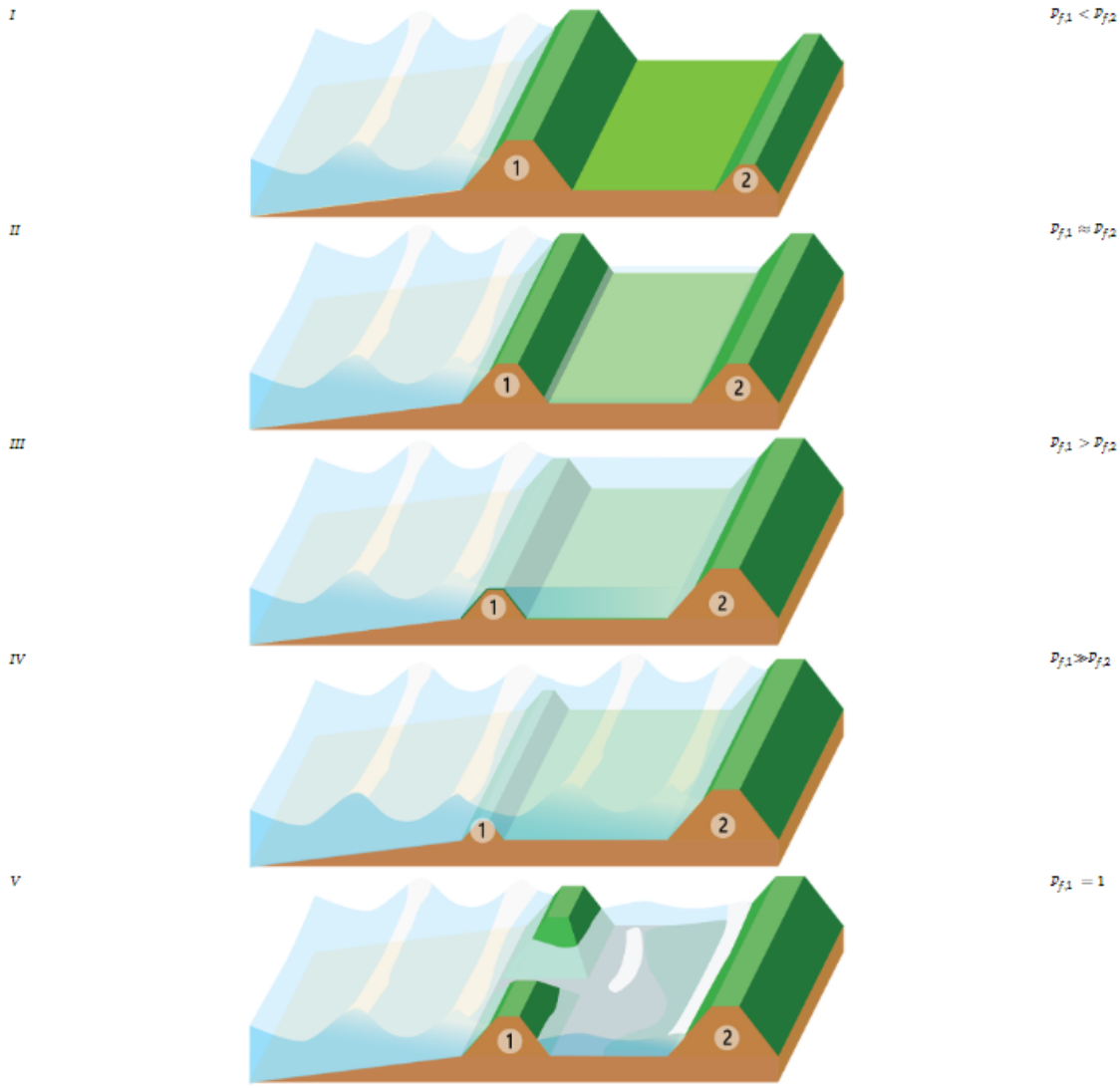

Figure 3.1: Classification of double dike systems (Marijnissen et al., 2021)

However, one can only speak of system failure when the second dike has also breached which causes flooding of the hinterland.

3.2. Interdike area

In the classification of the system above, only parallel dikes are considered. However, double dike systems are often considered because of the potential added value that the interdike area can offer in terms of flood safety, nature development, recreation, clay mining and new forms of agriculture. The way the interdike area is used has influence on the functioning of the system and, possibly, the choice of a particular parallel dike configuration.

If purely considered in terms of flood safety, the intermediate dike area mainly affects wave damping. As described in Section 2.3.2, bed level height and roughness play an important role in this. The effect of the latter is enhanced by the possible presence of vegetation. If we then include the concept of flood risk and impact, vegetation and a higher foreshore also affect breach stability and inflow. In addition, in some special cases, the extra space for water created in the interdike area may also have an effect on the water level outside the system.

A popular concept is the so-called 'wissel polder' (Van Belzen et al., 2021; Zhu et al., 2020), which can be implemented in silt-rich coastal areas. This is explained in figure 3.2. The function of the interdike area can be often traced back to the interaction with the sea, river or estuary. In this concept, different functions (nature, agriculture, recreation and safety) are combined over time. Modifying the function of the interdike area often means adjusting the retaining function of the outer dike. For example, to successfully form, less to no salt water will be allowed in the system. In both flood safety and the concept of 'wissel polder', the growth of the bed level plays and important role in the success of the system. This depends on the inflow of sediments which in turn depends on the inflow of water. More inflow means more potential bed level growth. So, the trade-off has to be made to what extent the first dike maintains its retaining function.

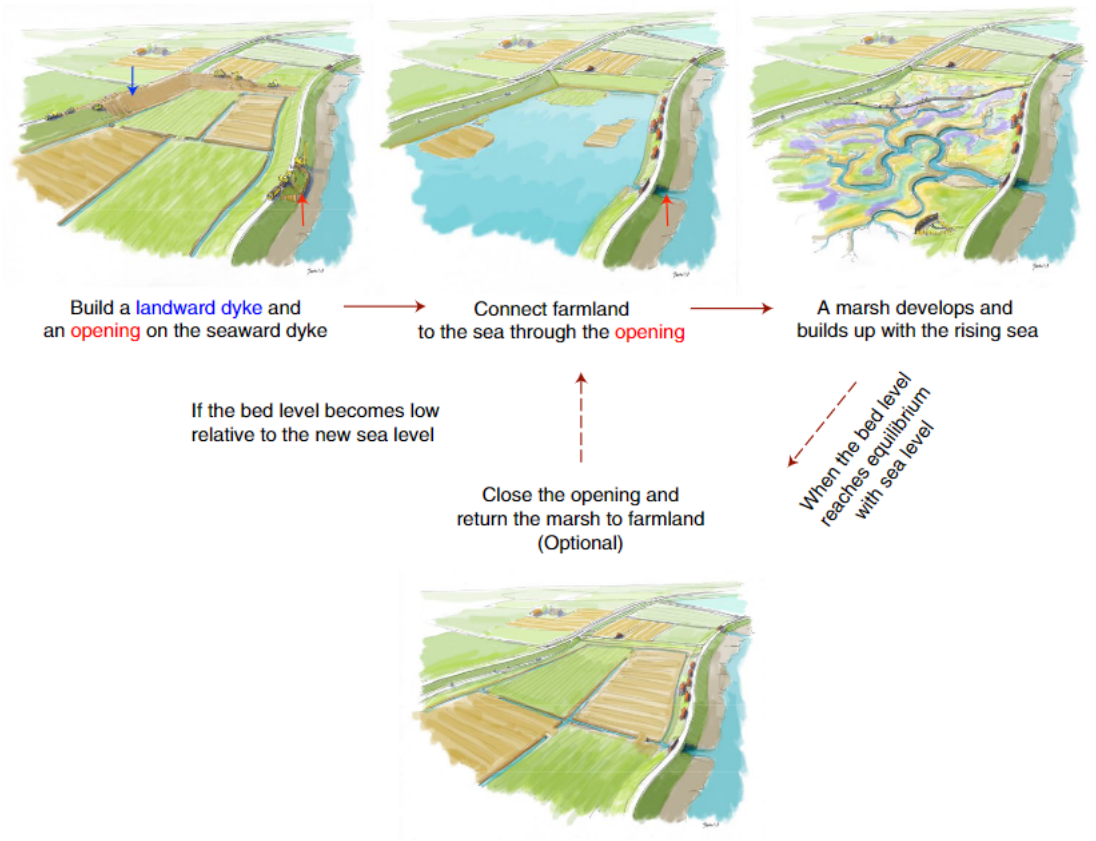

Figure 3.2: The function of a wisselpolder within a double dike system (Zhu et al., 2020)

3.3. Existing multiple lines of defence

Double dike systems or systems with multiple physical lines of flood defence are not uncommon. These have been implemented in different places and described by multiple studies. A few examples ware described below. Each example will be described according to the classification of figure 3.1 and linked to the different functions and objectives of the system.

Double dike system - Ems-Dollard

In the province of Groningen in the north of the Netherlands, a double dike system has been constructed as part of a pilot-project (EemsDollard2050, 2018). Because a sea-dike at the east-side of Eemshaven did not meet the

safety standards, it provided for the opportunity to combine the reinforcement project with the creation of multi-functional interdike area with a ecological objective in the form of a natural wetland. The existing sea-dike will become the outer dike of the system and a smaller existing inner dike will be upgraded - but remains smaller in size - for the containment of the water in the inter dike area. Water can also flow into the inter dike area by means of a constructed culvert (Marijnissen et al., 2021; Wauben, 2019). Figure 1.1 is an illustration of this project.

This system can be identified as type I system with an stronger outer dike than inner dike. During extreme storm conditions, the culvert can be closed, making the outer dike the primary flood defence. Water that may spill over the first dike is retained by the second dike. Using a culvert makes the retaining function of the outer dike adaptable to the hydraulic boundary conditions. It allows for interaction during normal conditions,

However, safety assessments performed by both Wauben and Marijnissen et al. question the added value of this pilot project in terms of flood risk reduction. The probability of non-closure of the culvert, which leads to possible high water levels in the interdike area, in combination with a lower second dike creates an additional risk.

The innerdike area is meant to become a nature area with tides and the deposit of sediments. This gives space for salt marsh vegetation and experiments will be carried out with salt agriculture. However, a culvert limits free inflow and therefore limits the potential natural sedimentation and bed level growth.

Waterdunen - Zeeland

The Waterdunen is a created brakisch/salt water system in West Vlaanderen near Breskens. It is developed as an integral project to improve flood safety of a weak spot in the coastal defences and environmental quality, improving nature, recreation and proving for a economic boost (Boudewijn et al., 2008; Provincie-Zeeland, 2010). Considering the system, there are many similarities to the system of the Ems-Dollard (type I). The primary flood defence is the first 'dike' (partly natural dunes), which contains a single tidal culvert to provide for the necessary tidal interaction and can be closed during extreme conditions. The function of the double dike system focuses on creating a new natural and recreational tidal area, since the second dike does not provide for much extra safety during failure of the primary flood defence.

As stated above, the function of the innerdike area is solely natural an recreational in nature. The dampened tidal interaction due to the culvert is sufficient to make this happen (Stark et al., 2006).

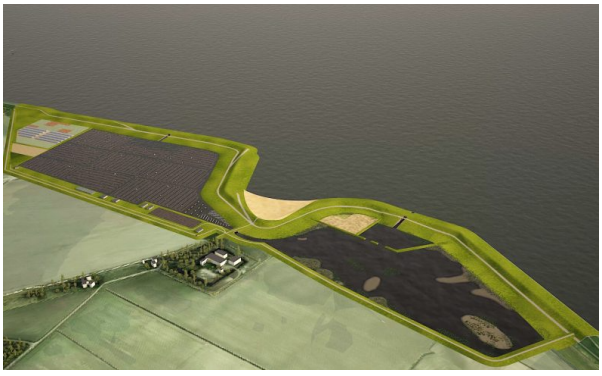

Figure 3.3: Concept art of double dike system Eems-Dollard, Groningen (EemsDollard2050, n.d.)

Figure 3.4: Aerial view of the Waterdunen (Provincie-Zeeland, n.d.)

Red River Delta - Vietnam

In the Red River Delta in Vietnam there are places with continues substantial coastal erosion (Fan et al., 2019; Nguyen & Takewaka, 2020), which weakens the coastal protection and causing dike failure during extreme events.This is a continuous process, losing dike sections frequently (Vinh et al., 1996). A second line of dikes has been built as local response to this hazard. This can be seen as a type II system, having a back-up dike ready in case of dike failure. Both dikes have similar functions. In this case, this system can be seen as a flood risk mitigation or management strategy (managed coastal retreat), reducing the impact of flooding. In case of failure of the first dike, it can be seen as a type V system. The interdike area does not have any function in this system.

Room for the river - Netherlands

Implementing a double dike system can also be an effective flood protection strategy for rivers. After extreme river water levels in 1995, the Netherlands started with a project called 'Room for the River' which was completed in 2015 (Rijke et al., 2012). This river management project gives, where possible, more space for the rivers to make the whole river delta more flood resistance and improves spatial quality. This has been done by creating river floodplains in between dikes which are flooded during peak discharge. This directly reduces the peak discharge and water levels down stream (Bornschein & Pohl, 2018). The dikes can be categorized as a summer- (lower) and winter dike (higher). Which can be classified as a type III in which the interdike area inundates during peak river discharge. Both dikes have a retaining function, however for different river discharges. The interdike area or flood plain functions as temporary water storage. This is different in comparison with a sea-dike system. The volume of water that can be that can be 'stored' in this interdike area is very small relative to the volume of the sea, making water level reduction negligible. Figure 3.5 gives a schematic depiction of the concept.

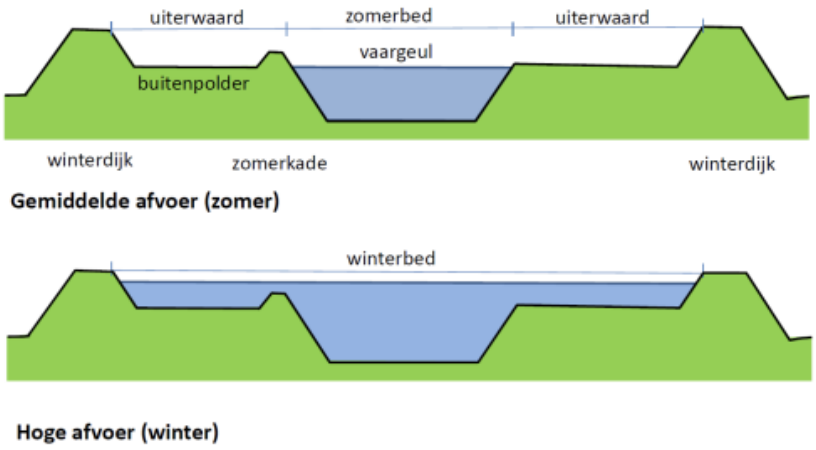

Figure 3.5: Schematic depiction of Room for the River (Rivierenland, n.d.)

Compartment flooding

Pasche et al. introduces the idea for a concept using compartments for adaptive flood response in which Hamburg is used as example. Multiple dikes are arranged such that these will function as cascading flood compartments. This idea emphasises on the fact that for every next compartment the probability of flooding will be lower. Adjusting the impact of a flood on the failure rate of a compartment provides a shared and overall smaller flood risk. These different compartments can be best described by type I system. Smaller secondary compartment dikes provide for impact reduction. Depending on the system, this is better referred to as a multi-dike system, although compartments can take other forms. The (multiple) interdike areas do not have an immediate function, but can be

taken account in the flood risk adaptation strategies; giving functions based on probability of flooding to mitigate the impact.

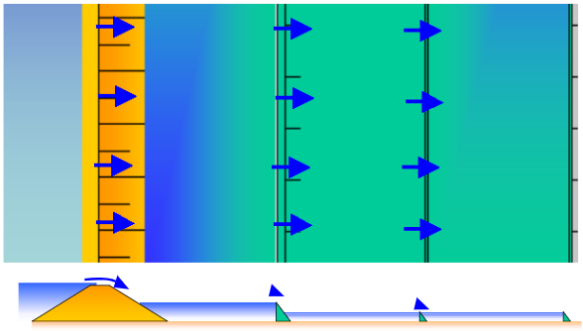

(a) Principle of compartment flooding

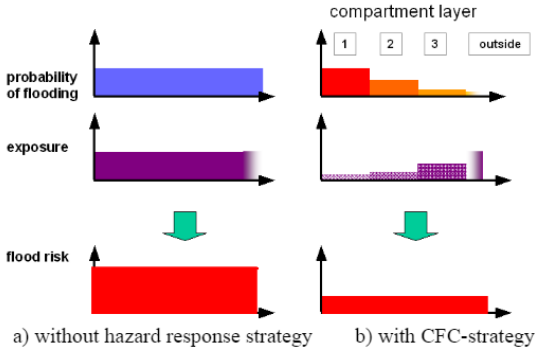

(b) Flood risk reduction

Figure 3.6: Concept of flood risk reduction due to compartment flooding (Pasche et al., 2008)

The examples above show that there are often two reasons for deciding to implement a double dike system: 1) creating additional safety or 2) improving the natural and/or recreational value of the area. In the first two examples from the Netherlands (tidal systems) this is both integrated in the solution. However, it should be added that in both examples the interdike area has no extra safety function in terms of load reduction and flood probability, but mainly mainly the function of creating a new natural tidal system. Still, different examples show the potential in the flood risk reduction due to impact mitigation. Reviewing these different concepts and ideas show the importance of context and functionality in definition of such system. The systems definition is decisive for determining the failure modes and different failure paths, but also to what extent this system can develop naturally.

3.4. Assessing double dike systems

Marijnissen et al. (2021) introduced a transmission model to include the the influence of the first dike and interdike area on the safety assessment. The model makes a distinction between hydraulic loads (S) and transmitted hydraulic loads (T(S)). The framework of the the transmission model is shown in figure 3.7. The failure of the second dike depends on the portion of loads transmitted by the first dike and interdike area. This framework consists of the following steps:

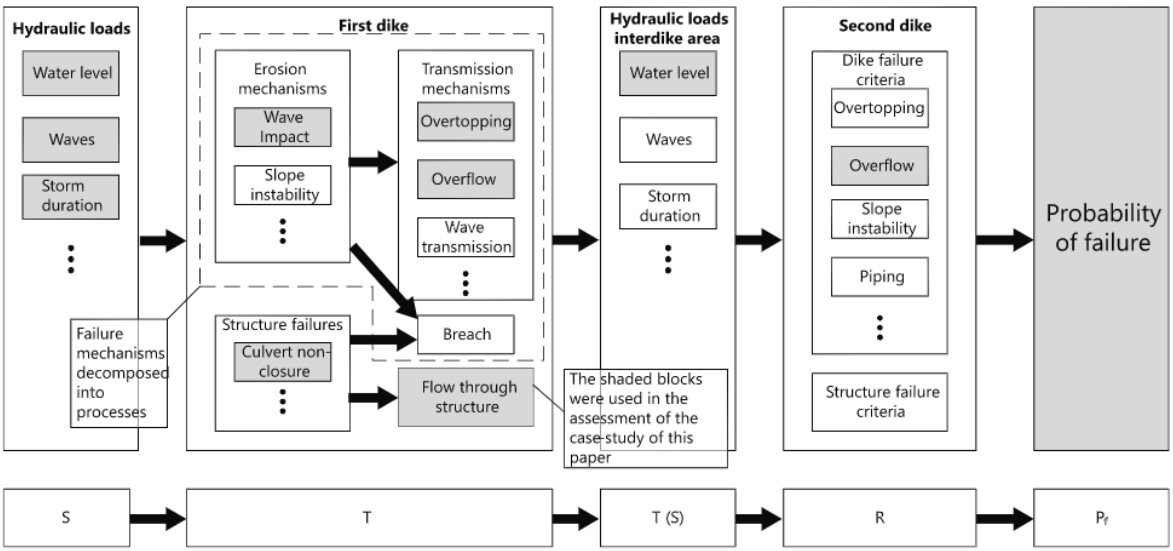

Figure 3.7: General framework of the transmission model (Marijnissen et al., 2021)

1. Retrieval of the hydraulic boundary conditions.
2. Identify and model the failure mechanisms of the outer dike.
3. Link the models of step two to calculate the transmitted hydraulic loads.
4. Determine the resistance of the inter dike regarding the normal failure mechanisms.
5. Use a probabilistic method to compute the probability of failure.

The failure probability (P_f) can be expressed as follows:

$$P_f = P(T(S) > R) \tag{3.1}$$

3.5. Dynamic double dike systems - a system definition

This system analysis focuses on the concept of dynamic double dike systems in the context of the the project 'Dynamic Dike Systems' (see 1.1). As stated, the guiding concept is an open system in which natural dynamics and morphological development are very important. There can be concluded that the function of a dynamic system primarily focuses on the creation of a valuable inter dike area while improving or maintaining flood safety according safety standards. This can be formulated in the following two requirements regarding the implementation of such system in a coastal area:

1. **Safety:** The flood safety of the hinterland must be guaranteed.
2. **Interaction:** There must be sufficient interaction regarding sediments between the estuary and the inner dike area leading to sedimentation of the inner dike area.

As a basis for this research, an open system is chosen to facilitate maximum potential morphological growth of the bed level in the interdike area (verwijzing naar salt marsh morphology). Foremost, creating a natural high foreshore in front of the second dike. This open system does not contain culverts, but the first dike has been breached, allowing water to flow more freely. Figure 3.8 gives an 1D cross-section of this concept. Figure 3.9 shows an open system without any structures (e.q. tidal culverts) which may constrict the inflow. Other

concepts are possible, most important is the unconstricted inflow during normal and extreme conditions. From this perspective, the following system characteristics and functions can be distinguished:

- **The first dike** acts as a breakwater and does not retain any water.
- **The innerdike area** develops naturally. Water levels are the same as outside the system.
- **The second dike** functions as the primary flood defence. In case of its failure, the system fails.

Linking this chosen system to the classification of Marijnissen (Figure 3.1), it can be seen that this can be classified as a type V system; the first dike is intentionally breached and is already failed regarding its retaining purpose. In the further course of this research, the focus will from now on be on the failure probability of the retaining function of the second dike.

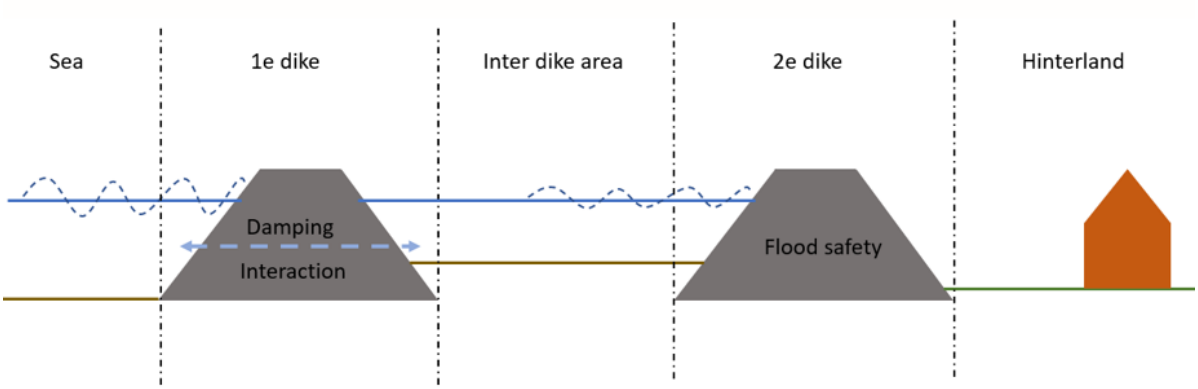

Figure 3.8: 1D display of the dynamic dike system

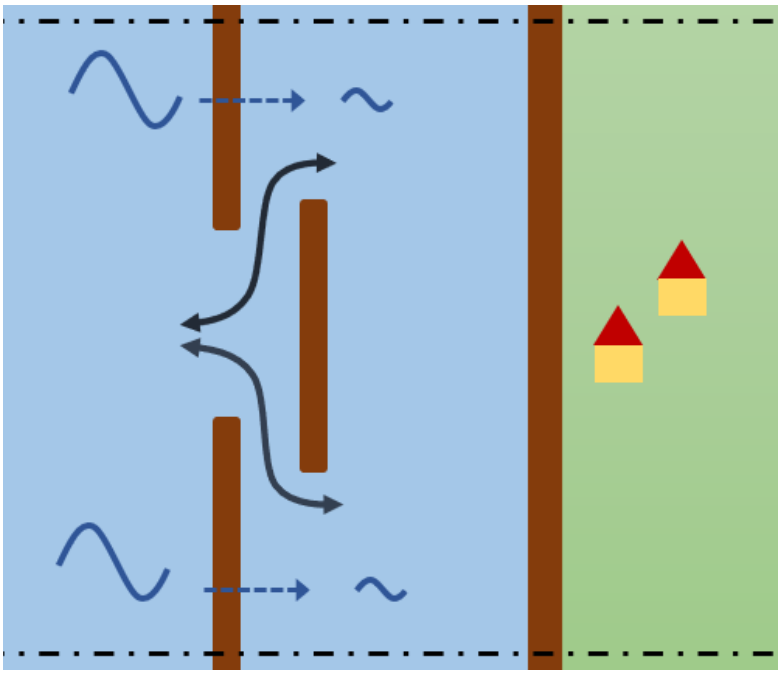

Figure 3.9: Concept aerial view of the system

4

Methodology

This chapter explains the research methodology. This research follows two approaches based on 1) failure probability and 2) Local Individual Risk (LIR). The first approach uses the transmission model of Marijnissen introduced in section 3.4, which is customised for the application on dynamic double dike systems. For the second approach, a flood model is added focusing on the effect of the height of the foreshore. Flood characteristics determine the mortality and this allows to calculate the probability of death by flooding (LIR). The outline of the methodology can be found in Figure 4.1. First, the failure probability approach is introduced section 4.1, followed by an explanation of the Local Individual Risk approach in section 4.2. Sections 4.3 and 4.4 explain the implementation of the transmission and flood model respectively. At last, Section 4.5 describes the approach for the comparison of different systems.

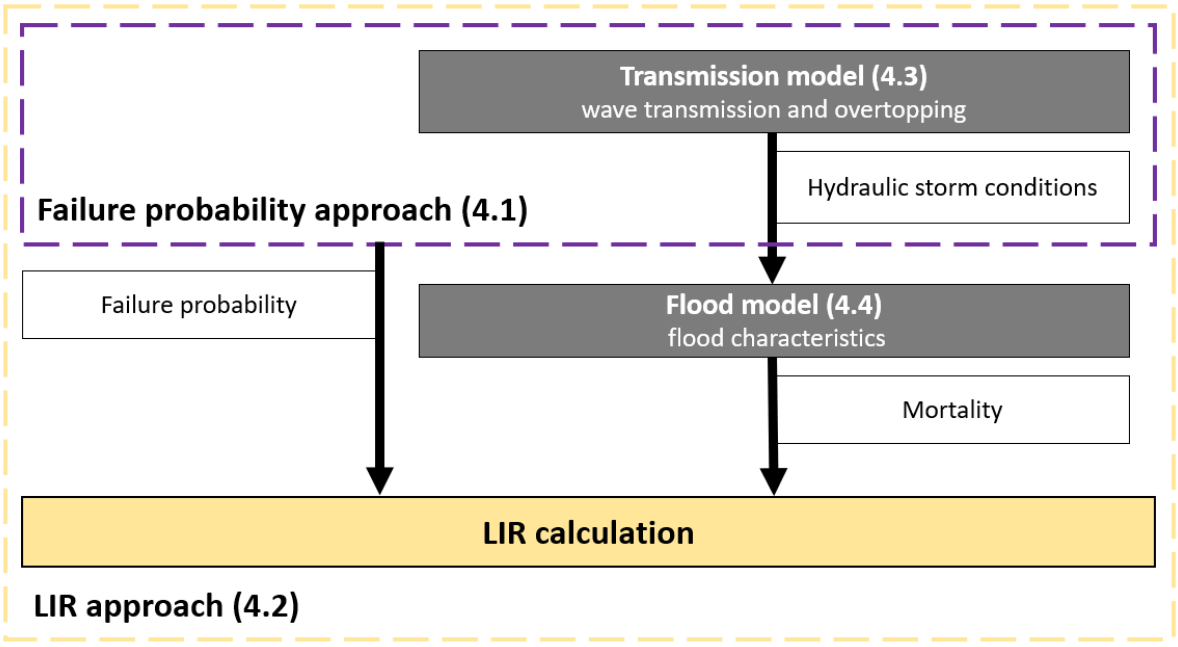

Figure 4.1: Outline of the methodology

4.1. Failure probability approach

The transmission model of Marijnissen et al. (2021) works towards a failure probability of a cross-section of the second dike. The same is also done in this study. A FORM analysis of the transmission model was included to calculate the probability of failure of the second dike. Applying this probabilistic analysis on Equation 2.5, the failure load (S) is the overtopping discharge calculated by the transmission model and the resistance (R) is the max overtopping discharge allowed for this dike section. In a FORM analysis, important parameters can be implemented as stochastic rather than deterministic values. FORM is a level 2 probabilistic analysis (Section 2.2.2). This means, by implementing different distributions, FORM allows to find the design point. This is the point on the limit state function for which the probability density is at its maximum and the combination of conditions are most likely to cause failure. This design point can be used as the starting boundary conditions for the flood model and risk approach.

4.2. Local Individual Risk approach

The local individual risk approach (LIR, Section 2.1.2) focuses on the calculation of the personal probability of death due to flooding . Figure 4.2 gives a general overview of the approach.

The mortality is determined using the flood characteristics calculated by the flood model. The mortality curves of Jonkman (2007) are used for this purpose (Section 2.1.2). For this research, the maximum inundation in the first 24 hours and the average rate of rise over the first 1.5 metres are used. The evacuation fraction is constant and assumed to be 0.35 (Zeeuws-Vlaanderen, Figure 2.3). The failure probability of the system as calculated by FORM is corrected for the different failure mechanisms and length effect (Section 2.2.2).

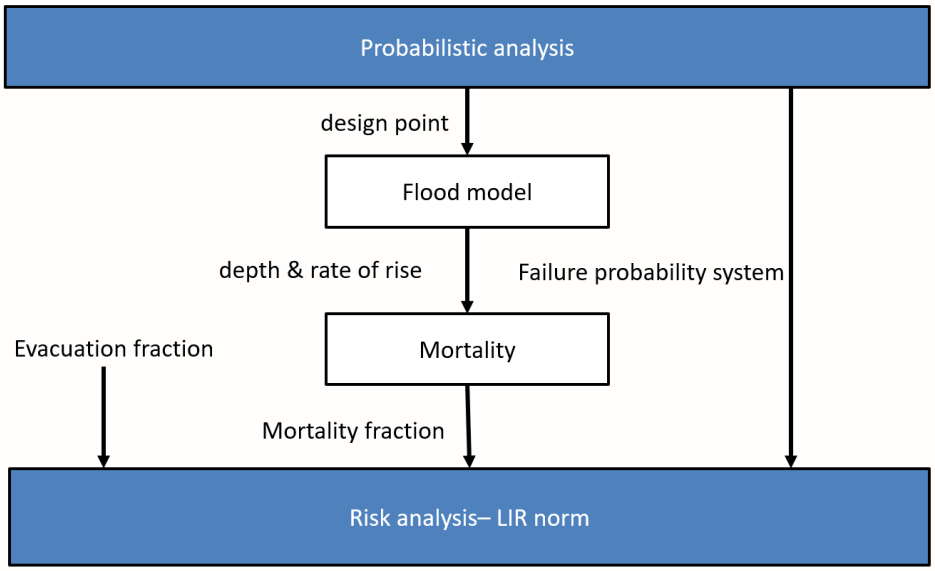

Figure 4.2: General overview of the risk approach

4.3. Implementation of the transmission model

4.3.1. General framework of implemented transmission model

For the application of the transmission model Marijnissen et al. (2021) on a dynamic double dike system, the model is adjusted for the assumptions and simplifications made. Section 3.5 provides more explanation about the choices and assumptions made for the functioning of a dynamic double dike system. In summary, the first dike only functions as breakwater and there is open a connection between the interdike area and sea or inlet. Thus, the water level in the interdike area is the same as outside the first dike.

For this research, the failure mechanisms are limited to overtopping and overflow. The transmission model primary describes the wave progression through the system and determines the overtopping discharge of the second dike. The model can be divided in three different modules, which division is physical based.

- **Module 1:** description of wave transmission over the first dike. Dike functions as breakwater.
- **Module 2:** description of wave growth and dissipation in the interdike area. Water level stays uniform.
- **Module 3**: determination of overtopping discharge over the second dike.

More in-depth descriptions of these modules can be found below. These modules address the physical processes related to the transmission of hydraulic loads within the system. The probabilistic approach for this model can be found in Section 4.1. A visual overview of the transmission model can be found in Figure 4.3.

Note that this model is used to assess the failure probability and risk of a double dike system at a certain state or point in time. Long-term processes such as bed level accretion and sea level rise determine this certain state of the double dike system in time, but are discussed in Chapter 5.

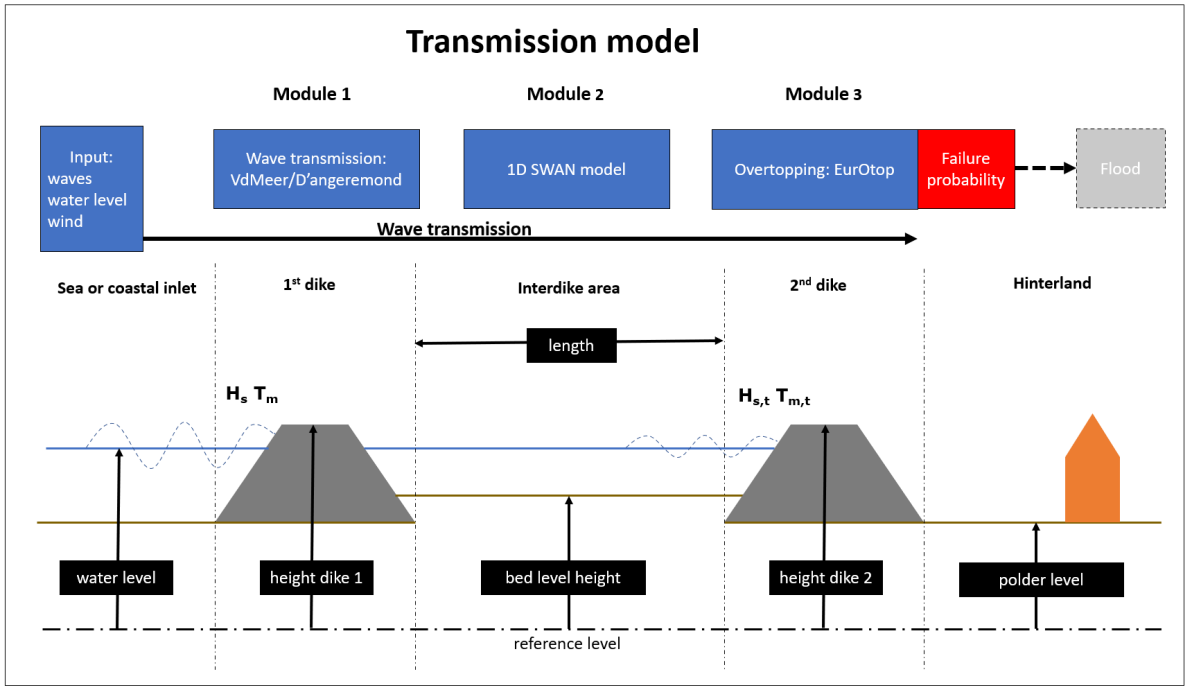

Figure 4.3: General framework of the application of the transmission model on a dynamic double dike system.

4.3.2. Model set-up

Module 1: First dike

The first module describes the transmission of hydraulic loads over the first dike. Since, the first dike functions as breakwater, water level stays the same. The mean wave period (T_m) is transmitted as a pulse and, therefore, also does not change. The significant wave height is is transmitted using a transmission using a transmission coefficient (Eq. 4.1).

$$H_{m0,t} = K_t * H_{m0,i} \tag{4.1}$$

in which $H_{m0,t}$ is the transmitted wave height, K_t the transmission coefficient and $H_{m0,i}$ the height of the incoming significant wave. Figure 4.4 gives a simple overview of the module.

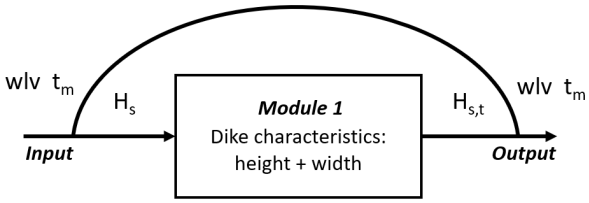

Figure 4.4: Simple overview of the functioning module 1 regarding input and output.

Both d'Angremond et al. (1996) as well as van der Meer et al. (2005) derived quite similar empirical expressions for this transmission coefficient. For a permeable breakwater, the expression by d'Angremond is as follows:

$$K_t = -0.40\frac{R_c}{H_{m0,i}} + 0.64 * \frac{B}{H_{m0,i}}^{-0.31} * (1 - e^{-0.50\xi}) \tag{4.2}$$

and for impermeable structures:

$$K_t = -0.4\frac{R_c}{H_{m0,i}} + 0.80 * \frac{B}{H_{m0,i}}^{-0.31} * (1 - e^{-0.5\xi}) \tag{4.3}$$

The expression by Van der Meer is slightly different and reads as follows:

$$K_t = -0.35\frac{R_c}{H_{m0,i}} + 0.51 * \frac{B}{H_{m0,i}}^{-0.65} * (1 - e^{-0.41\xi}) \tag{4.4}$$

Both d'Angremond as Van der Meer make use of the same input parameters. Important are the freeboard (R_c), incoming significant wave height ($H_{m0,i}$), width of the dike at the crest (B) and the Irribaren parameter (ξ). For this research, the method of d'Angremond is applied.

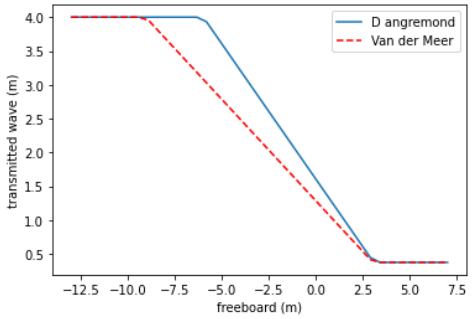

Figure 4.5: Example of transmitted wave height with an incoming wave of 5 meter and a variable freeboard using the expressions by d'Angremond (1996) and Van der Meer (2005).

Logically, the transmission coefficient will be 0 for very large free-boards and almost 1 for very small structures. However, these functions have the property to make the transmission coefficient become infinitely positive or negative. Both D'Angremond and Van der Meer proposed the following practical limits: K_t: $0.075 < K_t < 0.80$. For practical application's, Van der Meer stated that the expression of d'Angremond can be best used for a small dike width in comparison to the incoming wave height (B/H_i < 8). As example, the transmitted wave height under the same conditions ($H_{m0,i}$ = 5 m, water level = 4 m) with a variable free-board is plotted in Figure 4.5.

Module 2: Interdike area

This model utilizes the 1D numerical wave model SWAN (Booij et al., 1996) to simulate wave propagation in the interdike area. Its primary focus is on wave growth due to wind, and wave dissipation resulting from depth-induced breaking, bottom roughness, and vegetation. Figure 4.6 provides and overview of the model's input and output. The water level remains consistent throughout the length of the interdike area and is the same as the outside water level. Additionally, to simplify the model, it assumes that there is no variation in bed level along the length of the interdike area since it is difficult to simplify the natural behaviour of creeks to a 1D line model.

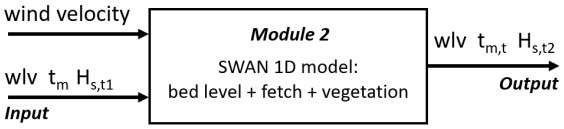

Figure 4.6: Simple overview of the functioning of module 2

A variety of mechanisms is incorporated to account for wave dissipation and bottom friction. For depth-induced wave breaking, a breaker parameter is applied following the method of Battjes en Jansen 1978. This parameter is the ratio of maximum individual wave height over depth and, for this research, assumed to have a value of 0.65. Bottom friction is considered using the method of Madsen and Rosengaus (1988) with an equivalent roughness length scale of 0.02 m. In addition, Quadruplet wave-wave interaction and white capping are accounted for in the model as well.

Vegetation can be implemented in SWAN according to the method by Suzuki et al. (2012). This method describes the impact of a vegetation field on the wave dissipation over the full spectrum of SWAN and is proportionate to the wave energy over all wave frequencies. The numerical model is proven to be well capable of describing the wave dissipation due to vegetation (Vuik et al., 2016). The input of model depends on the size of the plants (height and diameter), vegetation density, and a bulk drag coefficient (Cd). This coefficient is often used as calibration coefficient. Vuik et al. (2016) calibrated a value of Cd = 0.5 for Hellegat, Western Scheldt (plant: *Spartina anglica*), which will be used as constant parameter in this analysis.

The SWAN model input file with some extra explanation can be found in **??**.

Module 3: Second dike

This module aims to determine the overtopping or overflow over the second dike. The specific overtopping discharge (q $[m^3/s/m]$) is calculated using the Eurotop formulas (Eurotop, 2018) stated in Equations 4.5 until 4.8. These are the design formulas. Figure 4.7 gives a simple overview of the input and output of the module.

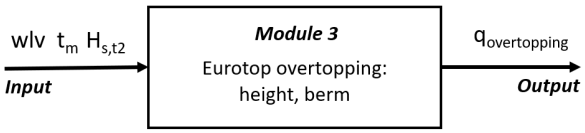

Figure 4.7: Simple overview of the functioning of module 3

$$q_1 = 0.54 * \sqrt{g * |Rc_2|^3} \tag{4.5}$$

$$q_2 = \frac{0.026}{\sqrt{\tan\alpha}} * \sqrt{g * H_{m0}^3} * \gamma_b * \xi_{m-1,0} * \exp -(2.5 * \frac{Rc}{\xi_{m-1,0} * H_{m0} * \gamma_b * \gamma_f * \gamma_\beta * \gamma_v}^{1.3}) \tag{4.6}$$

$$q_3 = 0.01035 * \sqrt{g * H_{m0}^3} * \exp -(1.35 * \frac{Rc}{H_{m0} * \gamma_f * \gamma_\beta * \gamma_v}^{1.3}) \tag{4.7}$$

$$q_4 = 10^{-0.50} * \sqrt{g * H_{m0}^3} * \exp -\frac{Rc}{H_{m0} * \gamma_f * \gamma_\beta * (0.33 + 0.022 * \xi_{m-1,0})} \tag{4.8}$$

The primary input includes the significant wave height (H_{m0}), freeboard (R_c), Iribarren number (ξ) and geometry of the dike. The wave period is implicitly used in the Iribarren number, which describes the type of breaking waves or run-up on dikes and depends on the slope, wave height and wave period.

The first formula (Eq. 4.5) is used for overflow when the freeboard is negative. The second formula (Eq. 4.6) is the general overtopping discharge formula and is used if the Irribaren parameter $\xi < 5$, with the third formula as the maximum value (Eq. 4.7). The last formula (Eq. 4.8) is used for large values of the Irribaren parameter ($\xi > 7$). In-between, linear interpolation can be used to calculate the overtopping discharge.

An overview of the different reduction influence factors (γ) can be found in table 4.1. For this research, only the reduction factor for the berm is used as a variable and depends on the berm characteristics.

factor	**symbol**	**value**
reduction for the berm	γ_b	variable
reduction for roughness of the slope	γ_f	1
reduction for oblique wave attack	γ_β	1
reduction factor for effect of wave wall	γ_v	1

Table 4.1: Reduction factors Eurotop formulas (2018)

4.4. Implementation of a flood model

This section explains the implementation of a flood model. Firstly, the general framework of the model is explained. Secondly, the flow through the breach or breach hydrodynamics is described, form which the inflow discharge is determined. Lastly, it is explained how the breach growth is modelled, which plays a major role in the breach hydrodynamics.

4.4.1. General framework of the flood model

The main goal of the flood model is to describe the development of inundation of the hinterland after the dike is breached. Based on the inundation per time step, flood characteristics (rate of inundation and maximum inundation) can be determined, which provide the necessary link to the risk calculations. Inundation is the depth of the flooded hinterland with respect to the polder level.

The main body of the flood model are the breach hydrodynamics. This part describes the discharge of water through the breach and depends on the width of the breach, inundation depth of the polder and water level outside of the dike. The first two again depend on the breach hydrodynamics; breach flow determines the breach growth and the discharge determines the inundation level. An overview of the framework of the flood model is given in Figure 4.8.

For simplicity, the inundation per time step is modelled using the so-called 'bucket' approach. The inflow of water is equally distributed over the hinterland. The discharge (m^3/s) subdivided over the flooded area (m^2) gives a rate of inundation (m/s). In addition, the simplification is made that the outside water level does not change during flood modulation and depends on the hydraulic conditions in the design point.

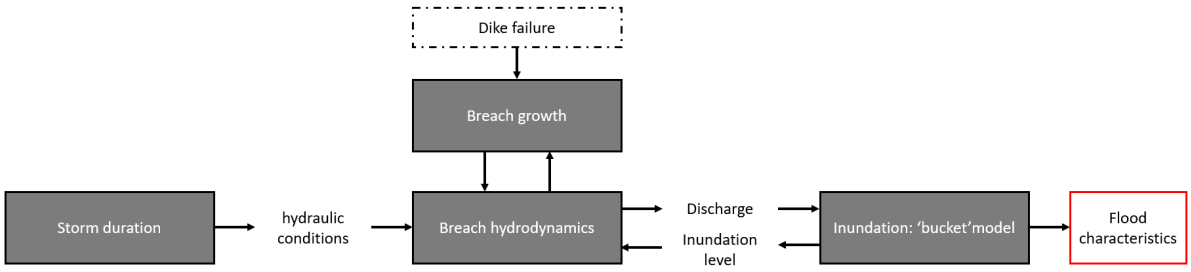

Figure 4.8: General framework of the flood model

4.4.2. Breach hydrodynamics

The goal of modelling the breach hydrodynamics is to determine the discharge through the breach taking into account the effect of the foreshore. In order to do so, the general weir equations are applied, which determine the discharge over a rectangular weir and are commonly used for modelling breach flow. The weir equations can be found below, and distinguishes the difference between free (Eq. 4.9) and submerged weir flow (Eq.4.10).

$$Q = m * \frac{2}{3} * B * h_1 * \sqrt{\frac{2}{3} * g * h_1} \tag{4.9}$$

$$Q = m * B * h_2 * \sqrt{2 * g * (h_1 - h_2)} \tag{4.10}$$

in which Q is the discharge (m^3/s), B the width of the breach, h_1 the outside water level, h_2 the inside water level, g the gravitational constant and m a flow constriction coefficient. The latter is assumed to be 1.

To apply these weir equations on a situation with a breach with foreshore, three different situations are defined: 1) free breach flow, 2) sub-critical breach flow and 3) submerged breach flow. These are described in more detail below and can be seen in Figure 4.9. A physical distinction is made between breach conditions and polder inundations, so that flow velocities in the breach can be determined in combination with a elevated foreshore.

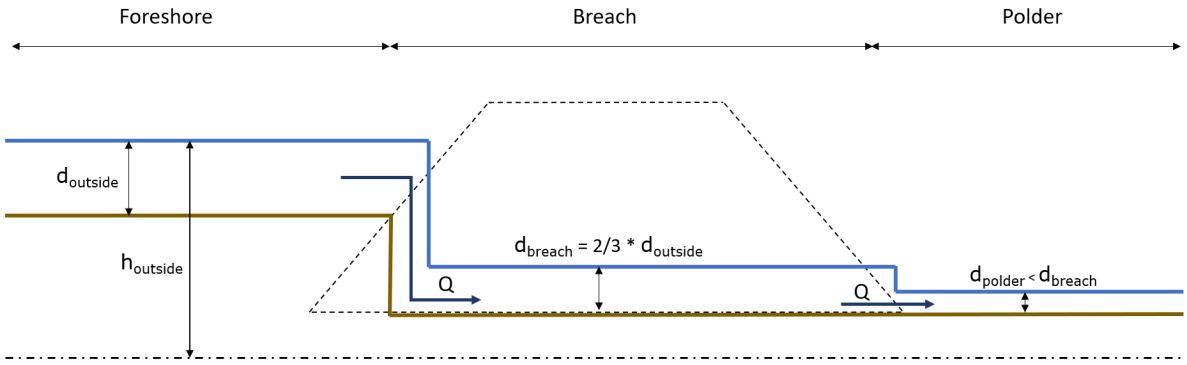

(a) Free breach flow

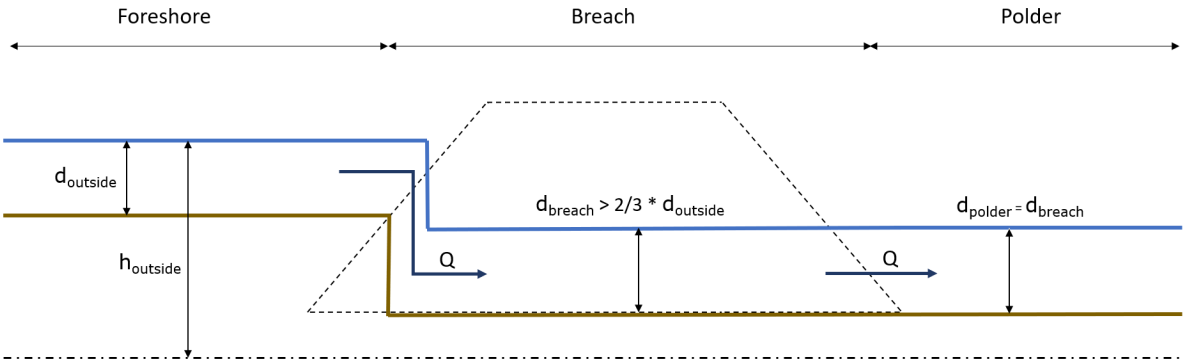

(b) Sub-critical breach flow

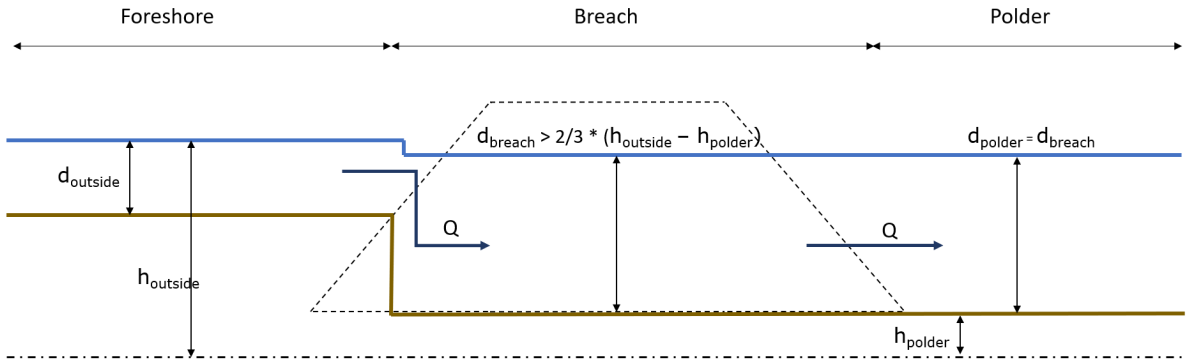

(c) Submerged breach flow

Figure 4.9: Implementation of the weir approach on breach hydrodynamics with foreshore.

1. *Free breach flow*

   The inundation depth (d_{polder}) is smaller than the depth in the breach. Therefore, the breach flow is not limited by the polder inundation depth. The flow is critical and only depends on the outside water level. Critical flow relations give:

$$d_{breach} = \frac{2}{3} d_{outside} \tag{4.11}$$

$$u_{breach} = \sqrt{\frac{2}{3} g d_{outside}} \tag{4.12}$$

   The discharge can be modelled as free weir flow, since the depth in the breach is smaller than 2/3 the height

of the outside water level ($h_{outside}$)

2. *Sub-critical breach flow*

   The inundation depth has reached the same depth as that of the breach and will rise above the critical depth of the breach flow. Therefore, the breach flow is limited by the water level in the polder and becomes sub-critical. The following relations apply:

$$d_{breach} = d_{polder} > \frac{2}{3} d_{outside} \tag{4.13}$$

$$u_{breach} = \frac{Q}{B_{breach} d_{breach}} \tag{4.14}$$

   As can be seen, the flow velocity in the breach depends on the discharge, and the width and depth of the breach. The discharge can be modelled as free weir flow, since the condition $d_{breach} < 2/3 h_{outside}$ still applies.

3. *Submerged breach flow*

   The inundation (and breach) depth has become bigger than 2/3 times the outside water level. Therefore, both the discharge as the breach flow depends on the inundation depth and sub-critical flow. The following relations apply:

$$d_{breach} = d_{polder} > \frac{2}{3} h_{outside} \tag{4.15}$$

$$u_{breach} = \frac{Q}{B_{breach} d_{breach}} \tag{4.16}$$

   The discharge can be modelled as submerged weir flow.

4.4.3. Breach growth

The goal of modelling the breach growth is to get a plausible breach size over time. Breach phases introduces in Section 2.2.3 are simplified to vertical and horizontal growth. These happen one after the other in time: first vertical growth, second horizontal growth. The different formulations for breach growth used in this section are introduces in Section 2.2.4.

Equation 2.7 can be used for vertical growth, since it is assumed that the duration of the vertical growth phases is very short (Verheij & Van der Knaap, 2003; Visser, 1998). For this research, a duration of 10 minutes after the start of the initial breach is assumed.

Both the method of Verheij and Van der Knaap (2003) (Eq. 2.8) and Van Damme (2020) (Eq. 2.9) can be applied for the horizontal growth. For the application in the flood model per time step, Verheij and Van der Knaap (2003) suggested the following equations:

$$B(t_i) = B(t_{i-1}) + \frac{\delta B}{\delta t} \Delta t \tag{4.17}$$

$$(\frac{\delta B}{\delta t})_{t_i} = \frac{f_1 f_2}{ln(10)} \frac{(g(h_{up} - h_{down}))^{1.5}}{u_c^2} \frac{1}{1 + \frac{f_2 g}{u_c}(t_i - t_0)} \tag{4.18}$$

in which h_{up} is the upstream water level, h_{down} the downstream water level, t_i the time, t_0 the duration of vertical growth and f_1 and f_2 are fitting coefficients for a sand dike (respectively 1.3 and 0.04).

The method of Van Damme can be easily applied using the breach velocities of the flood hydrodynamics module to calculate the shear stress per time step. Equation 2.9 (Section 2.2.4) makes use of two empirical

fitted parameters (m and c_1), which are assumed to be 0.0003253 m^2s/kg and 0.00625 m/s respectively (Van Damme, 2020). Since the parameter c_1 gives an initial growth for situations without shear stress, calculation of the breachgrowth via this method is only applied for situations with flow and zero for situations without flow.

The main difference between the two methods is that method of Verheij and Van der Knaap utilizes the difference in water level and the method of Van Damme makes use of the shear stress and thus flow velocity. A raised foreshore creates a larger hurdle and thus a smaller water depth in front of the breach. Following theory of the weir equations, this limits inflow and, therefore, flow velocities. Less inflow means the inundation level does not rise as fast and, therefore, the difference in water level remains larger. Following this reasoning, the method of Verheij and Van der Knaap gives higher breach growth rates and wider breaches over time. This does not replicate the positive stabilising effect that foreshores have on breach growth according to literature (Zhu et al., 2020). The method of Van Damme indirectly does reflect this, as it makes uses of the reduced flow velocities due to a raised foreshore.

Both methods are applied using a variable boundary water level as introduced in Section 7.2.4 with a maximum water level of 7 meter and a tidal amplitude of 2.5 meter, and the breach hydrodynamic model introduced in Section 4.4.2. This is done for a dike with a height of 9 meter and a hinterland area of 20 km^2. The results for inundation in time and breach growth for different raised foreshores can be found in Figure 4.10.

First , the impact of the raised foreshore on the inundation levels is clearly visible. The peak of the inundation can be found in the second tidal wave. Second, The breach for the method of Verheij and Van der Knaap stabilizes around a width of 200 meter. The breach for the method of Van Damme continues to grow to large widths. This primarily due to the impact of the fitted parameter c_1 (Section 2.2.4), which has a large share in the growth rate. At last, the effect of the raised foreshore on the breach growth is not noticeable for the method of Verheij and Van der Knaap. This is the case with Van Damme's method, but this is mainly due to stopping inflow due to higher foreshore. If flow occurs, breach growth rates are similar for different heights.

Despite the fact that in theory Van Damme's method better simulates the breach growth in combination with a raised foreshore, the fit parameter c_1 provides for an unrealistically rapid growth even for very low flow velocities. This creates very large breach widths. Therefore, it was chosen to apply Verheij and Van der Knaap's method for the remainder of this study.

4.5. System comparison

For this study, different systems, both single and double dike, are compared using the failure probability approach and LIR approach. The current situation with a single dike is used as reference system.

The failure probability approach compares systems based equal failure probability. Every system should have the same failure probability as the current single dike system.

For the LIR approach, the system must meet the LIR-norm of an individual probability of death of 1/100000 year. It is assumed that the current situation, with a single dike and a known failure probability, exactly meets this standard. This can be achieved by calibrating the model to a specific area-size of the hinterland for the 'bucket' model. This specific area-size is used for the compared double dike systems.

The practical application of the model for both approaches is similar. The failure probability and LIR are calculated for a variety of heights of the primary flood defence (second dike for double dike systems). Interpolation is used to determine the specific dike height corresponding to the reference failure probability and LIR norm. The different systems can be compared with each other using dike heights and dike volumes. The dike volumes depend on the dike height and can be determined as described in Appendix E.

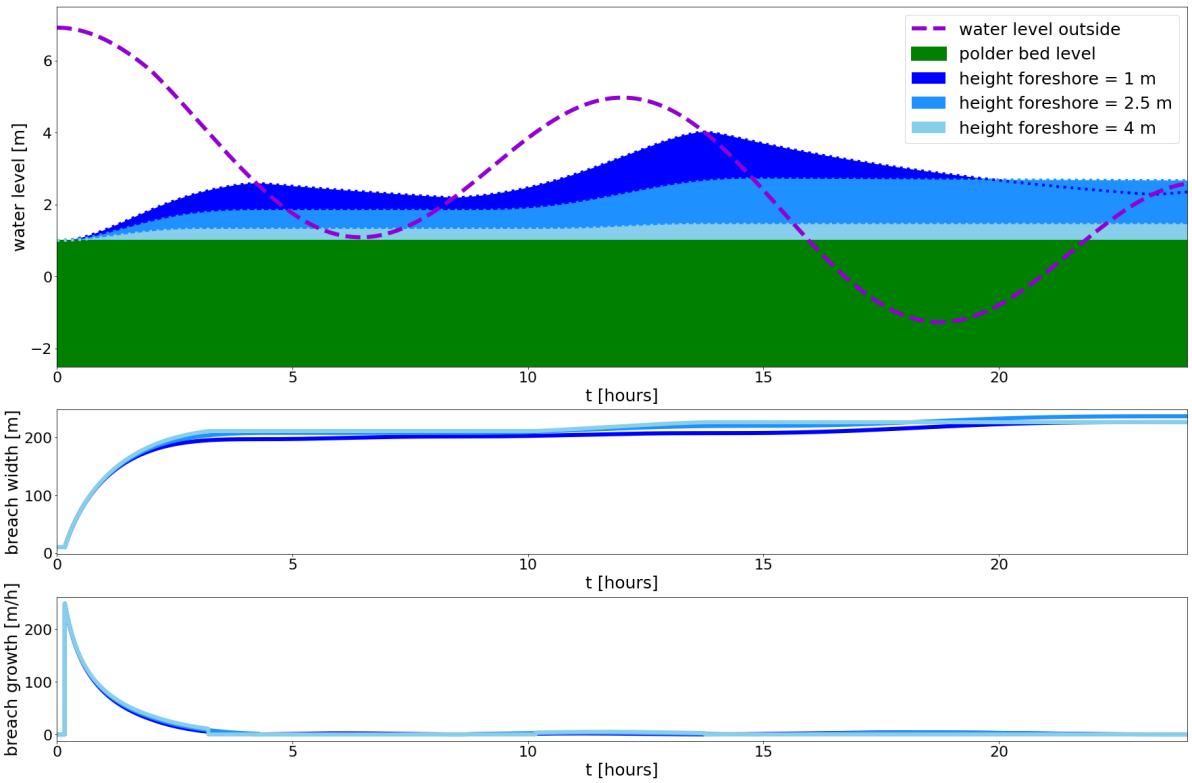

(a) Method of Verheij and Van der Knaap (2003)

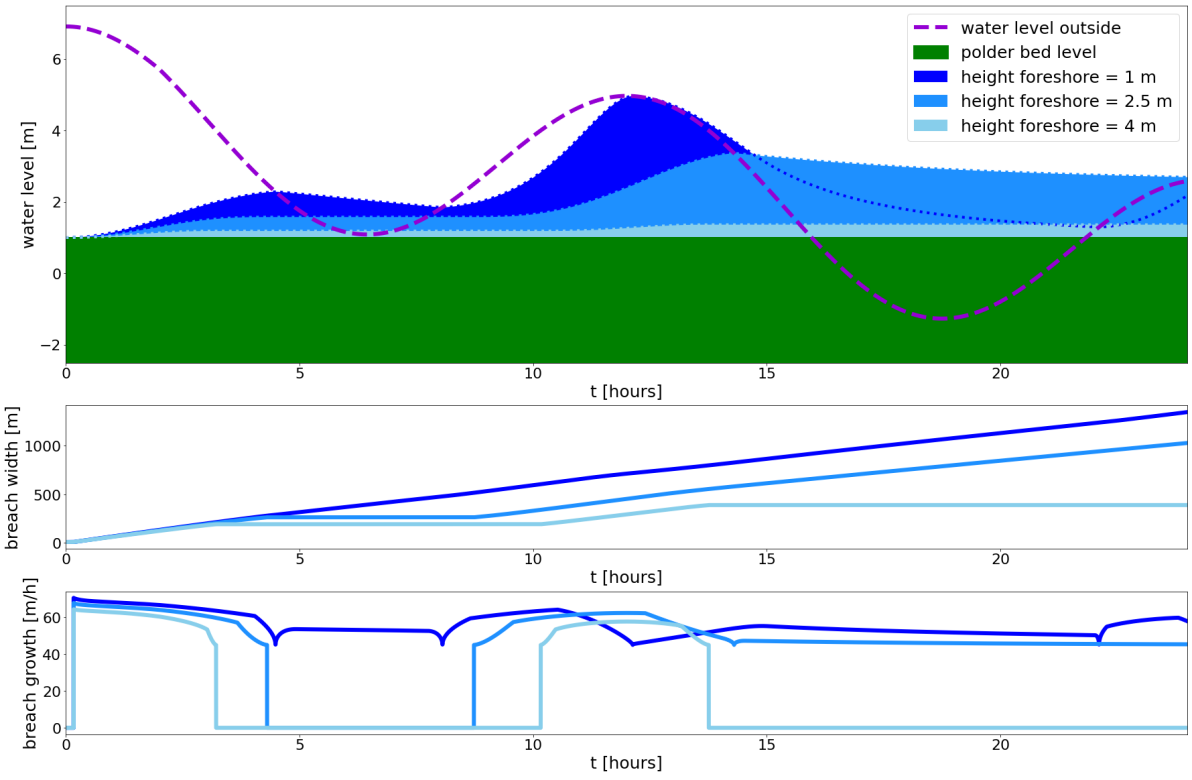

(b) Method of Van Damme (2020)

Figure 4.10: Application of two different breach growth methods: a) Verheij and Van der Knaap and b) Van Damme. Each figure gives the inundation development, breach width and breach growth in time.

5

Case study - Western Scheldt

5.1. Introduction to the Western Scheldt and area of interest

The Western Scheldt is the estuary of the Scheldt River, situated between the North Sea and the Port of Antwerp, and is important for shipping. Unlike the Eastern Scheldt, which has been closed off as part of the Dutch Delta Works, the Western Scheldt remains open. This makes the dikes in this area more vulnerable to extreme hydraulic conditions. Moreover, the Western Scheldt contains more sediments due to this fully open connection (Van Belzen et al., 2021).

This research focuses on a specific area of interest: the stretch of dike between the Griete and Knuitershoek, particularly around the Eendragtspolder. This dike section is part of dike trajectory 32-4 with a safety norm of 1/3000 years. Figure 5.1 provides an overview of the Western Scheldt and highlights this area. This particular location was selected because, during storm conditions, prevailing winds typically come from the Northwest, making this part of the Western Scheldt more vulnerable to high waves. The dynamic double dike system mainly serves a wave-damping functions, making it a suitable area for its application.

Figure 5.1: Overview of the Westernscheldt and indicated area of interest ("Google Maps", n.d.)

5.2. Model application to the Western Scheldt

5.2.1. System cross-section

For this case study, a simplified 1D system based on the area of interest (Section 5.1) is applied. To capture this area in a 1D situation, a typical dike cross-section, polder height and fetch length (interdike area) are considered. The current single dike height is 8.9 meter. A cross-section of this dike can be found in Figure 5.2. Transforming this into a double dike system, the length of the interdike area is assumed to be 1000 meter. The current height of the bed level in the polder is 1.5 m NAP (Appendix D) and vegetation is not yet applied. Figure 5.3 gives an overview of the chosen dimensions.

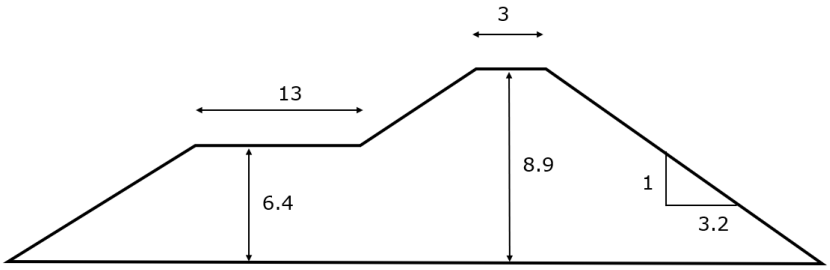

Figure 5.2: Cross-section of the current single dike. All dimensions are in meter.

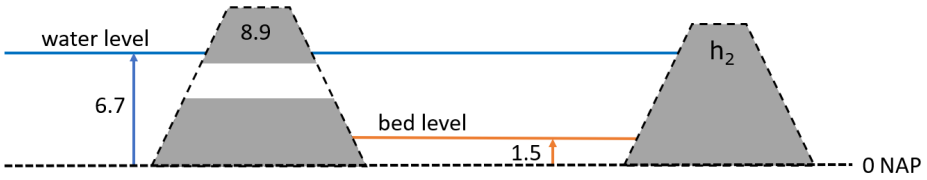

Figure 5.3: Cross-section of simplified 1D system based on Western Scheldt conditions. All dimensions are in meter.

5.2.2. Hydraulic boundary conditions

HydraNL is used for the data during extreme hydraulic boundary conditions. These can be found Appendix B. The data consists of wind velocities, water levels, significant wave heights and wave periods corresponding to a given return period. The output of HydraNL contains the design conditions for multiple wind directions. For this research, only the data of the dominant wind direction is used, which is 300° North.

5.2.3. Probabilistic implementation

It is assumed that the water level and wave characteristics are fully correlated to the wind velocity. For this location of the Western Scheldt, design conditions are mainly governed by a normative wind direction of 300° North, since this normative wind direction causes most of the surge of water from the North Sea. In addition, wave conditions in the Western Scheldt tend to be locally wind driven. The wind data is fitted to an exponential distribution. The exponential fit and distribution can be found in Figure 5.4.

This allows for the probabilistic FORM analysis to be simplified to a single stochast on the load side, which is the wind velocity. The wind velocity is linked to the wave height and water level via interpolation in a look-up table, which means a deterministic relationship. On the resistance side (R), the FORM analysis is done with a

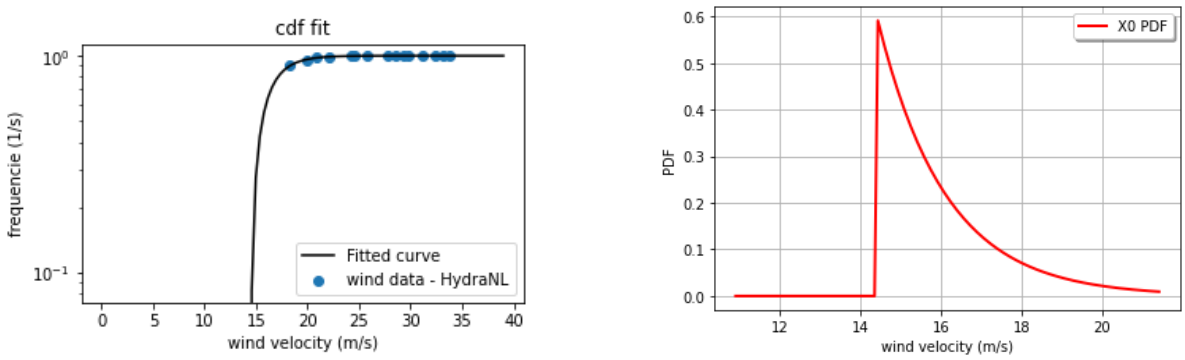

(a) Exponential fit

(b) Exponential PDF

Figure 5.4: Exponential fit and probability density function of the wind data (HydraNL).

deterministic maximum overtopping value of 10 l/s, which is the maximum of a reasonably well-maintained grass embankment (Eurotop, 2018). This simplification enables for faster and clearer comparisons on system level.

Whether this approach is a reasonable simplification is validated with a comparison calculation between HydraNL and the FORM analysis. HydraNL calculates the required dike height based on omni-directional water level statistics and a wave database combined with a return period. The same conditions are used in the simplified FORM analysis (one-directional) for a single dike situation. Figure 5.5 shows good resemblance despite major simplification.

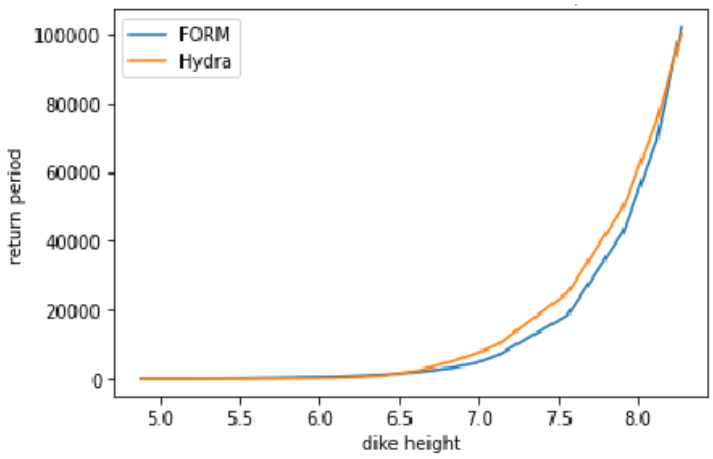

Figure 5.5: Model validation for the simplification of the FORM analysis.

5.3. Double dike system scenarios

This section aims to develop simple realistic scenarios in different points in time. These scenarios are developed for the current situation and in 50 and 100 years time. The scenarios consist of two factors; 1) Sea level rise and 2) morphological development. The latter depends on the sea level rise.

For this case study, it is assumed that a dynamic double dike system consists of a breached first dike and an upgraded second dike for retaining the water. The height of the first dike remains 8.9 meter and does not change for the different scenarios. The height of the second dike is adjusted to meet the safety requirements (failure probability and LIR norm).

5.3.1. Sea level rise

IPCC (2013) considers different sea level rise scenarios, which can be found in Appendix C. For this analysis, it is chosen to use the RCP8.5 scenario. Sea level rise over 50 and 100 years will be applied, for 2070 and 2120 respectively. Expected sea level rise data in IPCC (2013) stops at the year 2100. Therefore, the data is extrapolated with the use of an exponential smoothing (ETS) algorithm. This is done for the median, lower and upper bound of the RCP8.5 scenario. The expected sea level rise for this scenario can be found in Figure 5.6. It is chosen to use a sea level rise of **0.4 meter** for the year 2070 and **1.0 meter** for the year 2120.

In addition, it is assumed that the wave conditions do not change due to sea level rise. This is justifiable because the wave conditions in the Western Scheldt are predominantly limited by the wind velocity and fetch, and not by the depth.

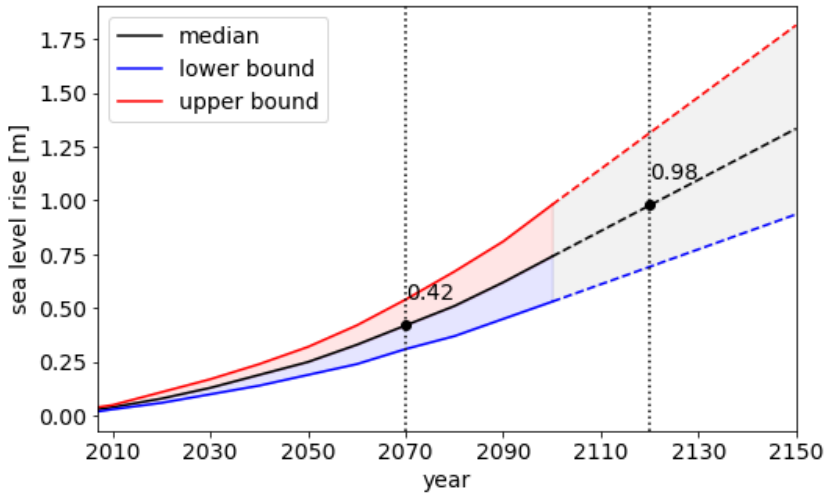

Figure 5.6: Sea level rise according to the IPCC scenario RCP8.5

5.3.2. Morphological development

Using sea level rise as starting point, several scenarios are developed for sedimentation of the bed level of the interdike area. It is assumed that the accretion of the bed level is a certain percentage with respect to sea level rise. The percentages used for the scenarios are 0, 50, 100 and 150. Furthermore, a maximum bed level accretion scenario is introduced. In this scenario, the bed level grows to Mean High Water Level (MHWL) within 50 years, which depends on the tidal amplitude and is assumed to be 2.5 meter. After reaching MHWL, the bed level follows sea level rise. Table 5.1 gives an overview of bed level growth in 2070 and 2120 for the scenarios applied.

	% of Mean SLR	**2070**	**2120**
SLR [m]	-	0.4	1
bed level growth			
scenario 1	0	0	0
scenario 2	50	0.2	0.5
scenario 3	100	0.4	1.0
scenario 4	150	0.6	1.5
scenario 5	max MHWL	1.4	2

Table 5.1: bed level growth (m) scenarios for a fixed sea level rise for the years 2070 and 2120.

5.4. Case study - results

The results of this case study are divided into three parts: 1) Probabilistic analysis, 2) Risk analysis and 3) Volume comparison of single and double dike systems. The first analysis considers only the failure probabilities of the system, which gives the opportunity to analyse the effect of the bed level on waves. The second analysis considers the flood impact as well and is based on equal LIR. These two approaches use dike heights as method of comparison. The last part uses dike volumes to compare double dike systems and single dike systems for both the failure probability approach as the LIR approach. All results can be found in Appendix F.

5.4.1. Probabilistic analysis

This probabilistic analysis compares the dike heights calculated following the failure probability approach (Section 4.1). The basis of this approach is a comparison based on the same failure probability. For this purpose, the failure probability of the current single dike (2020) is used. This means that all new analysed systems must comply to the failure probability of the current situation. Using the FORM probabilistic method for a single dike situation under the current hydraulic conditions in the Western Scheldt (Section 5.2.2), the failure probability of a single dike system with a height of 8.9 meter is $3.55 \cdot 10^{-5}$ per year. The wind velocity in the design point (point of failure) is 31.7 m/s. This corresponds to a water level of 6.7 meter, a significant wave height of 2.8 meter and a mean wave period of 5.0 seconds.

The next step is to see what dikes are needed if a double dike system is applied for the current conditions. The first dike does not change in height for this case study and remains the current dike of 8.9 meter (Section 5.2.1). The height of the second dike is chosen such that it complies exactly to the failure probability requirement. Figure 5.7 shows the failure probability for different heights of the second dike. Linear interpolation is used to find the correct dike height for this specific failure probability. In this case, the crest level of the second dike should be 7.2 meter. Figure 5.8 gives a schematic depiction of this double dike system with the accompanying design or failure conditions.

It can be seen that the water level in this design point is the same as for the single dike situation. This follows expectations, since the probabilistic method is simplified to a single stochast for wind velocity; the failure probability follows directly from the wind statistics (Section 5.2.3). This means that the same wind velocity is linked directly to this specific failure probability. The double dike system does not affect the water level, thus, the

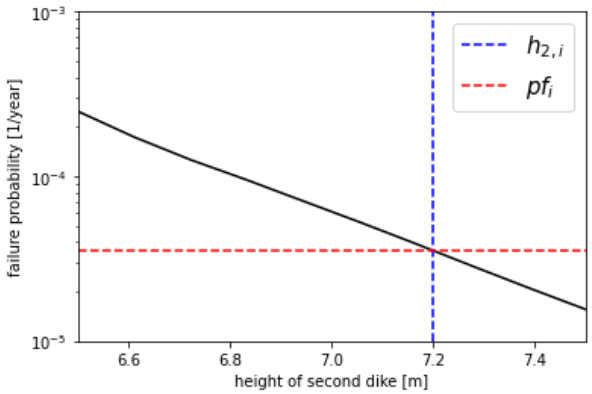

Figure 5.7: Calculation of the second dike of the double dike system ($h_{2,i}$) with the same specific failure probability of a single dike system ($Pf_i = 3.55 \cdot 10^{-5}$ per year) using the current hydraulic boundary conditions. The failure probability for a range of dike heights is calculated, which is indicated by the black line. Interpolation is used to link the specific failure probability to the dike height.

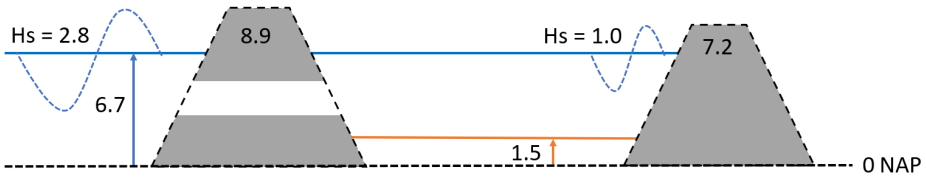

Figure 5.8: Schematic depiction of a double dike system for the current conditions (2020) with design water level and wave height. All values are in meter.

water level is equal is equal for every scenario apart from sea level rise. Therefore, the difference in dike height between the double dike systems is only affected by the difference in wave characteristics at the second dike.

Applying sea level rise

Sea level rise of 0.4 meter (2070) and 1.0 meter (2120) is applied to both the single as the double dike systems (Section 5.3.1). This simulates the reaction of the systems in terms of required dike height to accommodate the development of hydraulic boundary conditions in time without any morphological development. The first dike of the double dike system remains the same. The same interpolation method is used as explained above and shown in Figure 5.7 and the calculated dike heights can be found in Table 5.2. In addition to the dike heights, Table 5.2 also shows the difference between the dike heights in time and the current situation for both the single dike system (Δh_1) and double dike system (Δh_2). This is the additional dike height required to comply to the failure probability requirement and shows the effectiveness of the systems in relation to sea level rise.

		single dike		**double dike**		
year	**SLR**	$\mathbf{h_{1,sd}}$	$\mathbf{\Delta h_1}$	$\mathbf{h_{1,dd}}$	$\mathbf{h_{2,dd}}$	$\mathbf{\Delta h_2}$
2020	0	8.9	0	8.9	7.2	0
2070	0.4	9.3	0.4	8.9	7.62	0.42
2120	1	9.9	1	8.9	8.36	1.16

Table 5.2: Dike heights (m) for a single dike system and a double dike system without accretion subject to sea level rise (SLR) in time following the probabilistic approach; $h_{1,sd}$ is the single dike height, Δh_1 is the difference between the height of a dike in time and its height in 2020 for a single dike system, $h_{1,dd}$ the height of the first dike in the double dike system, $h_{2,dd}$ is the height of the second dike in the double dike system and Δh_2 is the difference between the second dike of the double dike system and its height in 2020.

First, the response of a single dike system to sea level rise is analysed. It can be observed that the required increase in height (Δh_1) matches the amount of sea level rise. This is consistent with the approach of adding sea level rise to the model, without altering wave conditions. Consequently, the only extra hydraulic load on the dike is due to sea level rise.

Second, the response of the double dike to sea level rise is analysed. This follows roughly the same trend as the single dike system. It can be seen that for a sea level rise of 0.4 meter (2070), the additional dike height required is almost the same as sea level rise (0.42 meter). For the year 2120, the additional dike height is 1.16 meter, which is more than the 1 meter sea level rise.

It can be assumed that 0.4 meter sea level rise does not affect the wave conditions in the interdike area. However, this does not apply for the situation in 2120, which shows an additional negative effect of 16% on the dike height due to sea level rise. There are two possible explanations:

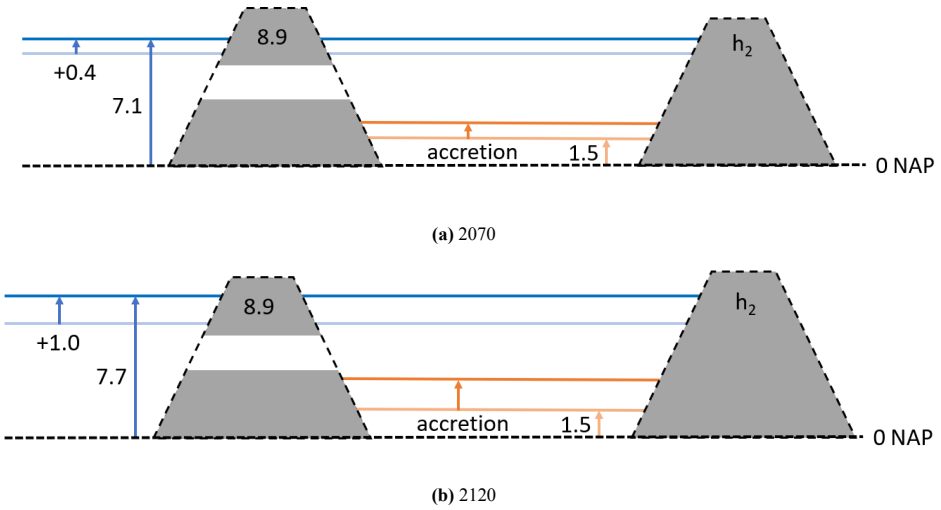

Figure 5.9: Schematic depiction of the double dike system for the years 2070 and 2120, with a sea level rise of 0.4 and 1.0 meter respectively. The different morphology scenarios determine the amount of accretion.

1. The effect of wave breaking and bottom friction is reduced due to a larger water depth.
2. Wave damping by the first dike is reduced due to a smaller freeboard.

Applying morphology scenarios

In order to analyse the effect of bed level accretion on the failure probability of a double dike system and, thus, wave characteristics at the second dike, the different morphology scenarios introduced in Section 5.3.2 are applied. A graphical overview of the situation can found in Figure 5.9. The calculated dike heights can be found in Table 5.3, for the situation in 2070 en 2120 respectively. Additionally, these also show the additional required dike height compared to the current situation (Δh_2) and the design wave height at the second dike (H_s). Note that for all scenarios, the double dike system in 2020 is exactly the same and shown in Figure 5.8, because no morphological development has yet occurred.

For both 2070 and 2120, no significant differences can be seen between the different scenarios. All scenarios with accretion (scenario 2 t/m 5) follow the same trend as the scenario without any accretion (scenario 1). The accretion of the bed level in combination with a large water level of 6.7 meter plus sea level rise in the interdike area is to small to have any significant increased influence on depth induced wave damping. This can be seen in the difference in design significant wave height (H_s). This varies most for 2120, but the difference is only 6 centimeter between no accretion (scenario 1) and maximum accretion (scenario 5). Summarized; the waves do not 'feel' the bottom.

For a sea level rise of 0.4 meter, the effectiveness in terms of additional dike height required is similar for both single as double dike systems and follows the same trend as sea level rise. For a sea level rise of 1.0 meter, the effectiveness of a double dike system declines since wave damping is reduced. Because depth induced damping of the interdike area does not have significant influence, this can be explained by reduced wave damping of the first dike due to sea level rise.

Generally, it can be noted that the large water level is dominant in this case study due to the application of an open double dike system and unrestricted inflow, which means that the second dike needs to have substantial dimensions compared to the single dike situation to obtain an identical probability of failure.

2070	accretion (m)	h_2 (m)	Δh_2	H_s (m)
Scenario 1	0	7.62	0.42	1.01
Scenario 2	0.2	7.62	0.42	0.99
Scenario 3	0.4	7.62	0.42	0.98
Scenario 4	0.6	7.62	0.42	0.98
Scenario 5	1.4	7.56	0.36	0.98

(a) 2070

2120	accretion (m)	h_2 (m)	Δh_2	H_s (m)
Scenario 1	0	8.36	1.16	1.16
Scenario 2	0.5	8.36	1.16	1.16
Scenario 3	1	8.34	1.14	1.14
Scenario 4	1.5	8.33	1.13	1.12
Scenario 5	2.0	8.32	1.12	1.10

(b) 2120

Table 5.3: Calculated heights of the second dike (h_2) in 2070 and 2120 for the different morphology scenarios using the probabilistic approach. Δh_2 is the difference between the second dike of the double dike system and its height in 2020 and H_s is the significant wave height in the design point of the second dike.

5.4.2. Risk analysis

This risk analysis compares dike heights calculated following the risk approach (Section 4.2). The basis of this approach is the comparison based on equal probability of death due to flooding or local individual risk. An acceptable risk level of 10^{-5} per year (LIR, Section 2.1.2) is used for this purpose, for which all systems must comply. As a start, it is assumed that the current situation with a single dike of 8.9 meter exactly meets this risk norm. This assumption is used to find the corresponding area size of the flooded hinterland, acting as a kind of calibration factor. The method of calibration is similar to the calculation of dike heights using the probabilistic approach. However, the calculation is extended with the addition of the flood model and risk calculation. The LIR is calculated for a range of area sizes and linear interpolation is used to find the correct area size corresponding to the combination of the current single dike height and risk norm. This calibration is shown in Figure 5.10, which also shows the calculated mortality rate as the main outcome of the impact calculation. It can be seen that the rate of water level rise increases for smaller polder areas, corresponding to a higher mortality fraction. For this situation, the corresponding area size is 8.38 km^2, which is used as area size implemented in the flood model. Considering the area upon which this case study is based, this represents only a limited portion of the hinterland. Consequently, it becomes evident that within more detailed flood calculations, this flooded area does not fully behave as a 1D 'bucket' model characterized by uniform water levels.

As for the probabilistic approach, it is calculated which dikes are needed if a double dike system is applied for the current condition (2020). Again, the method of interpolation is used. It follows that the double dike system should be exactly the same as calculated by the probabilistic approach shown in Figure 5.8. This is to be expected, since the no accretion has yet occurred and all other important factors determining flood impact are considered the same. Furthermore, this double dike system has the same failure probability as the single dike system, which was the main assumption of the probabilistic approach. Also, this shows once again that dike height and vertical breach growth have almost no influence on the flood characteristics.

Subsequently, the same sea level rise for 2070 and 2120 is applied to both the single as the double dike

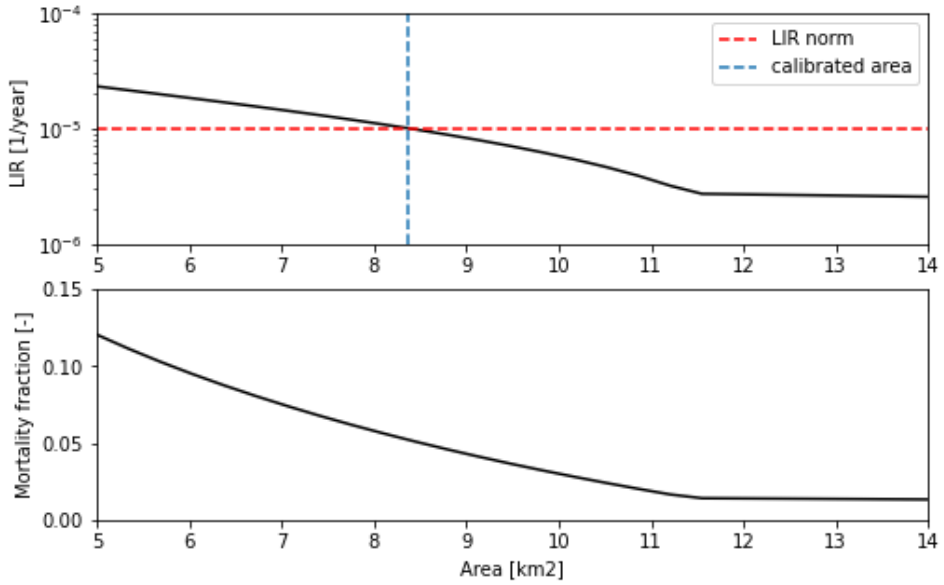

Figure 5.10: Calibration of the area size of the flooded hinterland for a single dike system with a height of 8.9 meter and accompanying mortality fraction. The LIR is calculated for different area sizes. Linear interpolation is used to find the area size linked to the risk norm of 10^{-5}. The calibrated area size is 8.38 km^2

systems (Section 5.3.1). No morphological development does occur yet and the first dike of the double dike system remains the same. The calculated dike heights can be found in Table 5.4. This table also shows the additional dike height required to comply to the risk norm for both the single dike system (Δh_1) and double dike system (Δh_2).

		single dike		**double dike**		
year	**SLR**	$\mathbf{h_{1,sd}}$	$\mathbf{\Delta h_1}$	$\mathbf{h_{1,dd}}$	$\mathbf{h_{2,dd}}$	$\mathbf{\Delta h_2}$
2020	0	8.9	0	8.9	7.2	0
2070	0.4	9.69	0.79	8.9	7.98	0.78
2120	1	10.57	1.67	8.9	8.96	1.76

Table 5.4: Dike heights (m) for a single dike system and a double dike system without accretion (scenario 1) subject to sea level rise (SLR) in time following the risk approach; $h_{1,sd}$ is the single dike height, Δh_1 is the difference between the height of a dike in time and its height in 2020 for a single dike system, $h_{1,dd}$ the height of the first dike in the double dike system, $h_{2,dd}$ is the height of the second dike in the double dike system and Δh_2 is the difference between the second dike of the double dike system in time and its height in 2020.

First, the response of a single dike system to sea level rise is analysed. It can be observed that the required increase in height (Δh_1) is much larger than the imposed sea level rise for both 2070 and 2120, namely 0.78 and 1.76 meter respectively. This is an additional height of around 100% and 70% respectively to sea level rise. Increased water levels have a negative effect on the impact calculation. This can be explained by the fact that higher water levels cause a higher breach discharge following the breach flow equations in Section 4.4.2. Putting this in the perspective of the risk calculation; the increased mortality rate due to an increased water level must be compensated by an decreased failure probability to comply to the same risk norm. In other words, a higher dike is needed than for the failure probability approach.

Second, the response of the double dike system to sea level rise is analysed. As can be seen, this follows roughly the same trend as the single dike system. An additional height of around 100% and 75% is needed. This

similar increase in required dike height is to be expected, since morphology scenarios are not yet applied.

Next, the effect of bed level accretion of the interdike area on the risk approach considered by applying the same morphology scenarios (Section 5.3.2). It can be assumed that all differences in dike height are caused by the positive effect of the height of the bed level on the breach flow and flood impact, because the results of the probabilistic approach show that the bed level accretion does not have a significant impact on the failure probability due to a dominant water level during extreme conditions. The calculated heights for both 2070 and 2120 can be found in Table 5.5. Furthermore, these show the additional dike height required (Δh_2), and the design water level and wave height at the second dike (H_s).

2070	accretion (m)	h_2 (m)	Δh_2	water level (m)	H_s (m)
Scenario 1	0	7.98	0.78	7.36	1.15
Scenario 2	0.2	7.93	0.73	7.32	1.13
Scenario 3	0.4	7.85	0.65	7.28	1.10
Scenario 4	0.6	7.76	0.56	7.22	1.08
Scenario 5	1.4	7.02	-0.18	6.63	0.89

(a) 2070

2070	accretion (m)	h_2 (m)	Δh_2	water level (m)	H_s (m)
Scenario 1	0	8.96	1.76	8.07	1.38
Scenario 2	0.2	8.89	1.69	8.06	1.34
Scenario 3	0.4	8.8	1.6	7.99	1.29
Scenario 4	0.6	8.63	1.43	7.9	1.22
Scenario 5	1.4	7.71	0.51	7.3	0.91

(b) 2120

Table 5.5: Calculated heights of the second dike (h_2) in 2070 and 2120 for the different morphology scenarios following the LIR approach. Δh_2 is the difference between the second dike of the double dike system in time and its height in 2020 and H_s is the significant wave height in the design point of the second dike.

Before comparing dike heights of different morphology scenarios, it must be touched upon that the water level does change for the different scenarios. The design point (water level) depends on the failure probability, which is variable for the LIR approach. For example, a lower failure probability corresponds to a higher water level with an longer return period, for which higher dikes are needed to comply to the failure conditions of overtopping (Section 5.2.3). So, the same graphical depiction of the situation as the probabilistic approach can be used (Figure 5.9), but the water level (not sea level rise) is variable. The specific matching design conditions for each scenario can be found in Appendix F.

It can be seen that morphology does have an impact on the dike height using the risk approach. This difference is noticeable for more moderate scenarios of accretion (scenario 1 to 4). Although, the additional dike height still exceeds sea level rise and is larger than that of the probabilistic approach. The decrease for scenario 5 (maximum accretion) is much larger. In fact, it is so substantial that the required dike height of 7.02 meter is lower than for no sea level rise. The required dike height in 2120 of 7.71 meter is smaller than sea level rise as well. This can be only explained by the reduced breach discharge due to smaller water depths in front of the dike, since stability of the breach is not implemented in the model and wave energy dissipation was not dominant for these extreme water levels.

Therefore, by using the LIR approach, the reducing effect of a raised foreshore on the breach discharge is

noticeable in the dike height calculation. A tipping point between 150 % bed level growth (scenario 4) and maximum growth (scenario 5) can be found, in which this effect is amplified and surpasses the effect of sea level rise.

5.4.3. Dike volume comparison

In the sections above, the effectiveness of the systems by looking at total dike heights and additional dike height required for a given sea level rise. This section considers the additional needed volume with respect to a reference situation, which is the single dike situation of the same year. This is done for both the dike heights calculated by the probabilistic as risk approach (Sections 5.4.1 and 5.4.2) By comparing volumes, a more realistic image is created of the effectiveness of a double dike system with an possible relation from the cost perspective. This allows for a better comparison in effectiveness between the single and double dike situations.

Firstly, the single dike situation is analysed. Figure 5.11 gives the percentage of additional volume needed relative to the current single dike situation. As is shown in the probabilistic analysis (Section 5.4.1), the additional height required matches sea level rise. This additional height increased by following the risk approach (Section 5.4.2). As can be seen, the effect of sea level rise on the volume is relatively larger. Differences are magnified by the quadratic relation between height and volume (Appendix E). As an example, the situation in 2120 for the probabilistic approach is picked. For sea level rise of 1.0 meter the same additional height is required. Considering the current dike of 8.9 meter, this is increase of just more than 10 %. This is contrasted by a volume increase of more than 25 %.

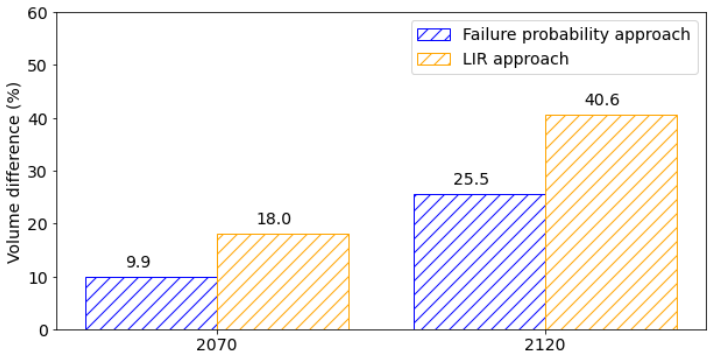

Figure 5.11: The difference in volume (%) between current single dike reference situation (8.9 m) and the volume needed for a single dike system in 2070 and 2120 prone to sea level rise.

Secondly, the volumes of the double dike systems are considered. This includes the 8.9 meter first dike and the variable second dike. The volume of a double dike system for both the probabilistic as risk approach is the same and has an increase of 70.8 % compared to a single dike of 8.9 meter. This increase can be fully attributed to the second dike, since the current single dike of becomes the first dike in the double dike system. Figure 5.12 gives the percentage of additional volume needed for 2070 and 2120 considering all morphology scenarios. The double dike systems are compared to the single dike system required in the time conditional to the chosen approach.

Analysing the effectiveness in time, it can be seen that for the scenario without accretion (Scenario 1) there is an decrease in additional needed volume relative to the single dike situation. This decrease between 2020 en 2120 for both the probabilistic as risk approach of 70.8% to 55.3% and 70.8% to 46.6% respectively, means the increase of effectiveness a double dike system due to sea level rise. Additionally, it can be noted that double dike systems are considered to be more effective using the risk approach, since relatively less volume is needed

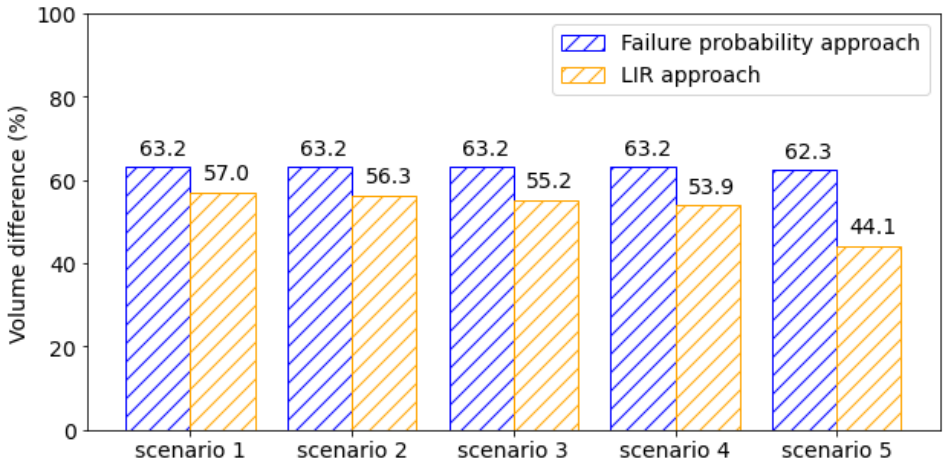

(a) 2070, sea level rise of 0.4 meter

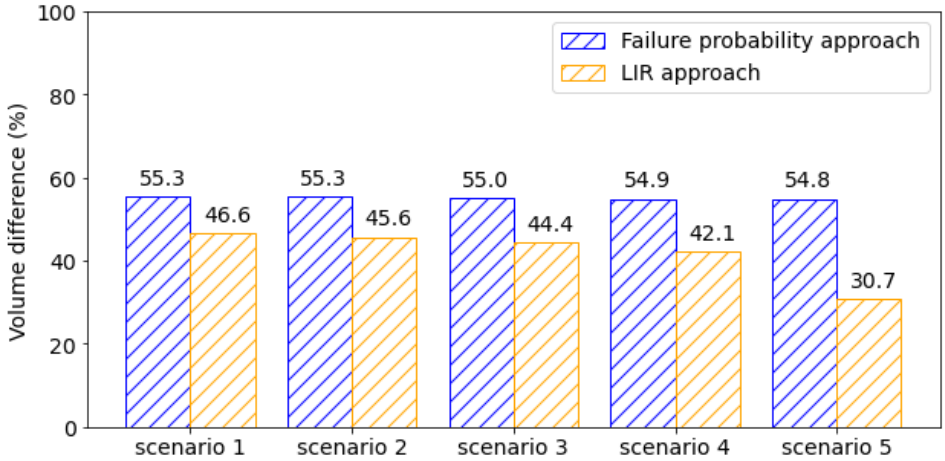

(b) 2120, sea level rise of 1.0 meter

Figure 5.12: The difference in volume (%) of a double dike system compared to a single dike for 2070 and 2120. This is done for both the failure probability approach as LIR approach and all five morphology scenarios.

compared to the probabilistic approach. This can be primarily explained by the fact that the increase of single dike heights following the risk approach is much larger and this effect is amplified in this volume comparison.

Considering the morphology scenarios, there is no significant change for the probabilistic approach. This follows the same trend as the probabilistic analysis (Section 5.4.1), since morphology has no influence on the failure probability. As already shown in Section 4.2, bed level accretion does has an positive effect on the efficient of the double dike system following the risk approach. A difference of 16 % point between no accretion and maximum accretion can be found for 2120.

Comparing volumes for this most favourable scenarios with maximum accretion gives a somewhat different impression of the efficiency of a double dike system than by looking only at dike heights. A 30% volume increase gives a more friendlier image compared to the additional substantial second dike needed as calculated in the previous sections.

All calculated volumes per meter of dike section can found in Appendix F.

5.5. Conclusion

This analysis investigated the effectiveness of a dynamic double dike system in the Western Scheldt with a simplified model based on the Eendragtspolder region. Various scenarios encompassing sea level rise (SLR) and morphology were examined. In the present situation, opening the existing dike necessitates the construction of a second dike that is only 1.7 meters lower than the single dike system.

When comparing the system based on equal failure probability, a single dike should be raised identically to the SLR that takes place. In the case of a double dike system and 1 meter SLR , this increase in height of the second dike should be approximately 1.15 meters to maintain the same failure probability. Sedimentation in the interdike area has a negligible impact on failure probabilities due to the dominant influence of water depth.

However, this comparison changes when based on equal flood risk. With 1 meter SLR, the additionally required height of a single dike increases to 1.7 meters to prevent an increase in local individual risk. Applying this approach to a double dike system, the effect of the height of bed level of the interdike area on the breach flow does have an influence. For instance, when combining 1 meter SLR with rapid bed level increase, raising the second dike by just 0.5 meters would be sufficient to maintain an equal level of LIR for the hinterland polder.

Examining the effectiveness of single and double dike systems in terms of total dike volumes strengthens the conclusions drawn above. The risk approach shows a more positive picture regarding the effectiveness of a dynamic double dike system in comparison to a single dike. In addition to the reducing effect of the bed level on breach flow, the increased height necessary of a single dike to meet the LIR norm due to sea level rise in the context of dike volumes can not be overlooked. For example, in the scenario involving a 1 meter sea level rise and rapid bed level increase, the failure probability approach necessitates 55% more dike volume for the implementation of a double dike system compared to a raised single dike, whereas the risk approach requires only an additional 31% in volume.

6

Sensitivity analysis

In this chapter, various influential parameters and system configurations are analysed. Firstly, important parameters are identified and ranged based on influence on failure probability and impact. Secondly, with the help of earlier gained hypotheses, four variables and system configurations are chosen for further analysis. This is done in the same manner as the case study of the previous chapter.

6.1. Implementation of sensitivity analysis

6.1.1. Identifying system characteristics

Table 6.1 gives an overview of the important variables in the risk analysis. For all variables it is indicated whether they influence the probability of dike failure and/or flood impact. Vegetation is not yet implemented in previous analyses. The sensitivity analysis is divided into four different analyses:

1. **Configuration of the first dike and interdike area**

   The actual impact of the first dike compared to that of the interdike area during extreme wave conditions is analyzed. The hypothesis is that with an infinitely long interdike area (infinite fetch length), an equilibrium wave height develops depending on water depth and wind velocity. In that case, the effect of wave damping of the first dike is negligible.

2. **Varying hydraulic boundary conditions**

   Different boundary conditions are examined. The case study (Chapter 5) shows that the influence of the water depth can be quite dominant on the failure probability calculations. The positive effect of a double dike on the dike failure is primarily based on wave damping, which should increase with a decrease in water level. Also, this analysis reviews the extent to which risk is affected by different water levels.

3. **Area size flooded hinterland**

   The effect of the flooded hinterland on the risk analysis is considered. The LIR-norm primarily depends on the flood characteristics, which are very much influenced by the size of the flooded area. This analysis examines the relative influence of the total flooded area.

4. **Vegetation**

   Vegetation is implemented in the model. As introduced in Section 2.3, vegetation in the interdike area has an impact on wave dissipation during storm conditions. This impact depends on vegetation characteristics and water depth. Wave dissipation increases with the size and amount of plants and decreases with water depth.

Parameter	Unit	Failure probability	Impact
Bed level interdike	m	X	X
Length interdike	m	X	-
Height dike 1 (h1)	m	X	-
Height dike 2 (h2)	m	X	X
Area hinterland (flood)	m^2	-	X
Bed level hinterland (flooded)	m	-	X
Wave height	m	X	-
Water level	m	X	X
Vegetation height	m	X	-
Vegetation density	Stems/m^2	X	-
Storm duration	h	-	X
Storm surge	m	X	X
Tidal amplitude	m	-	X
Breach growth	m/h	-	X
Breach width	m	-	X

Table 6.1: List of important variables in the risk analysis.

6.1.2. Implementation of parameter variation

Each analysis will use the same probabilistic and risk approach as done for the case study (Chapter 5. Therefore, the same failure probability and risk norm is used.. The effectiveness of the different parameters is expressed in height and dike volume compared to a single dike situation. This is done for 0 (2020) and 1.0 meter (2120) sea level rise. In addition, maximum bed level accretion (scenario 5, Section 5.3.2) is applied for all four analyses. Generally, the hydraulic boundary conditions as for the case study are used.

The single dike situation depends on the hydraulic conditions (failure probability approach) and area size hinterland (LIR approach). Since both are varied in analysis 2 (varying hydraulic boundary conditions) and analysis 3 (area size flooded hinterland), new single dike height must be calculated to comply to the failure probability and risk norm. In that case, these new single dike heights are also used as new reference situation. All variations are graphical shown in Figure 6.1.

1. Configuration of the first dike and interdike area

This analysis considers the degree of dominance of the height of the first dike relative to the length and bed level of the interdike area. The first dike is varied between 8.9 and 4.5 meter, nothing else changes. Therefore, the single dike reference situations remain the same as for the case study.

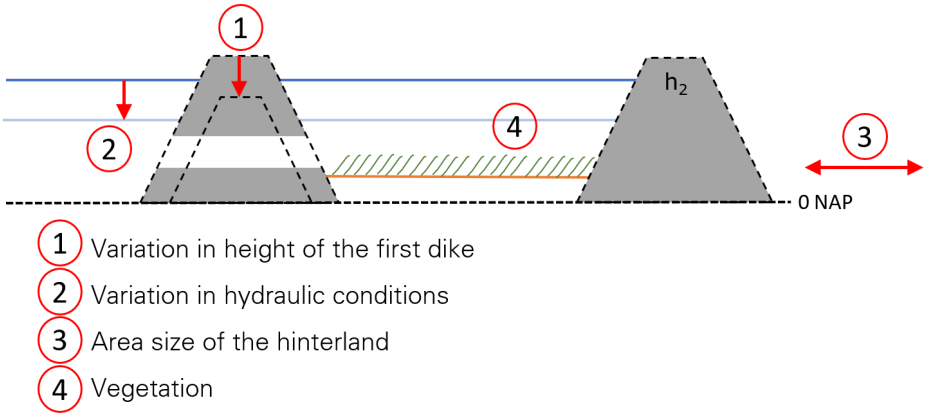

Figure 6.1: Graphical depiction of the application of the different parameter variations.

2. Varying Hydraulic boundary conditions

This analysis considers situations with a less dominant water level. Therefore, two new variations in hydraulic conditions area applied (Table 6.2):

1. The effect of a 50% smaller tidal amplitude
2. The effect of a 50% smaller storm surge

The water level during extreme conditions is made up of tidal amplitude + storm surge. The tidal amplitude for this region is a constant 2.5 meter NAP, the remaining water level is caused by the storm surge. The hydraulic conditions are still assumed to be fully correlated to the wind velocity, but water level is adjusted. The boundary wave characteristics remain the same.

	tide %	**surge %**
Conditions 0	100	100
Conditions 1	50	100
Conditions 2	100	50

Table 6.2: Applied variation of hydraulic conditions. Only the water level changes.

3. Area size of the flooded hinterland

For this analysis, the area size of the hinterland is varied as a percentage of the area size of the case study (8.37 km^2). The corresponding area sizes can be found in Table 6.3. Varation in area size only affects the flood impact and, therefore, this analysis is done for only the risk approach.

% of reference area	**km^2**
150%	12.57
100%	8.37
50%	4.19
25%	2.09

Table 6.3: Applied variation of area sizes

4. Vegetation impact

For this analysis, vegetation is implemented as a variable in the numerical SWAN wave model. Explanation of how to implement vegetation in SWAN can be found in Section 4.3.2. Using SWAN, the influence of the vegetation in this model is only considered in terms of wave dissipation and thus overtopping. The positive impact on salt marsh stability is not accounted for.

The vegetation is varied in height (m) and density (stems/m^2). Vuik et al. (2016) calibrated a drag coefficient with a value of Cd = 0.5 for Hellegat, Westerscheldt. This coefficient remains unaltered. A vegetation diameter of 3 milimeter is used.

	h (m)	**N (stems/m^2)**
vegetation 0	0	0
vegetation 1	0.15	500
vegetation 2	0.15	1500
vegetation 3	0.30	500
vegetation 4	0.30	1500

Table 6.4: Different variations of vegetation using mean stem height (m) and amount of stems per square meter (stems/m^2).

6.2. Sensitivity - Results

This section shows the results for four different variations as described in Section 6.1 . All variations are analysed in time (2020 and 2120) for maximum bed level accretion only (scenario 5). Dike heights and volumes are calculated and compared in the same manner as done for the more specific case study of Chapter 5 following the probabilistic and risk approach.

6.2.1. Configuration of the first dike and interdike area

For this analysis, the height of the first dike is varied between 4.5 and the current 8.9 meter. The single dike situation in time remains the same. The results for the calculated height of the second dike can be found in Table 6.5. The situation with a height of the first dike of 8.9 meter is the same as that of the case study.

Firstly, just considering the probabilistic approach, it can be seen that in 2020 for an decrease in first dike height from 8.9 to 4.5 meter (Δh = 4.4 meter),the required height of the second dike increases by 0.74 meter. This is a difference of almost a factor 6. For 2120, this increase has even dropped to 0.4 meter, which is almost a factor 10 less of the decrease in height of the first dike. The additional height required for the second dike is caused by an increase in significant design wave characteristics. For example, the design wave height of the double dike system in 2020 is around 1.0 meter. Decreasing the first dike to a height of 4.5 meter, this wave height increases to 1.7 meter. This is on par with the required increase in dike height. The wave height in 2120 follows the same trend.

Secondly, analysing the risk approach, the situation in 2020 does not change, since the no morphology has not yet occurred. For 2120, a decrease in height of the first dike to 4.5 meter causes an increase in height of 0.48 meter. This follows the same trend as the probabilistic approach. This can be explained by the fact that this variation primarily affects wave height and not breach discharge, which depends primarily on the depth in front of the breach. Hydraulic conditions in the design point can be found in Appendix G.

height dike 1 [m]	height dike 2 [m]			
	Failure		LIR	
	2020	2120	2020	2120
8.9	7.2	8.32	7.2	7.71
7.5	7.46	8.63	7.46	8.04
6	7.83	8.69	7.84	8.15
4.5	7,94	8,72	7,94	8,19

Table 6.5: Heights of the second dike for double dike system with a decreased height of the first dike for both the failure probability as LIR approach.

Next, the effectiveness of the system considering volumes is analysed. Figure 6.2 shows the relative volume increase in percentage relatively to the single dike situation. It must be noted that the berm of the second dike is not included in the volume calculation of the first dike of the double dike, since this was hard to incorporate for a dike decreasing in height this much. This gives a slightly more positive image of its effectiveness compared to that of the case study. However, It still give an good overview when comparing the different situation and it does not has any affect on its wave damping function in the model.

There is an significant increase in effectiveness for a system with a lower first dike, since the first dike decreases much more in height than the second dike must be increased. This trend is noticeable for 2020 and 2120 for both the probabilistic as risk approach. It can be seen that for systems with a lower first dike, the effectiveness of the double dike system becomes even greater than the single dike in terms of total volume. This can be seen by the negative values in the Figure 6.2. Following the risk approach, total system volume can be reduced by almost 25% in 2120 in comparison to the single dike system.

In addition, it can be seen that that the effectiveness increases following the risk approach. This can be similarly explained as done in Section 5.4.3. The height of a single dike calculated by the risk approach must increase more for a certain sea level rise, which in turn increases the relative effectiveness of a double dike system.

To go more in depth on the influence of the first dike on the waves, Figure 6.5 shows the propagation of the significant wave height at an extended interdike area corresponding to a wind velocity of 31.7 m/s for 2020 and 2120. It can be seen that for all variations in dike height, eventually the wave conditions become the same. This is indicated as the equilibrium wave height (black dotted line). This equilibrium wave height depends on the water depth and wind velocity. Less depth means and wind means smaller waves and vice versa. The equilibrium wave height for 2120 is smaller, since the depth decreases in time by applying the maximum accretion.

Moreover, two distinctive areas can be seen in the figures; the area above the line of equilibrium depth and the area below the line of equilibrium depth. In the first area, the damping function of the first dike (for lower dikes) is to small and the transmitted wave is larger than the equilibrium wave height. Therefore, depth induced wave damping is dominant in the first area. In the second area, the transmitted wave height is smaller than the equilibrium wave height. There is wave growth due to wind forcing. In terms of effectiveness, starting at in the first area, the length of the interdike area works positively on the failure probability. The opposite is true for the second area.

When the equilibrium wave height is reached, the influence of the first dike on the failure probability of the second dike is negligible. Furthermore, it can be seen that for smaller water depths, this equilibrium wave height is reached quicker. For an net decrease in depth due to bed level accretion in time, the influence of the first dike becomes less and less.

These results show that knowing the effect of the first dike on the failure probability gives room for optimiza-

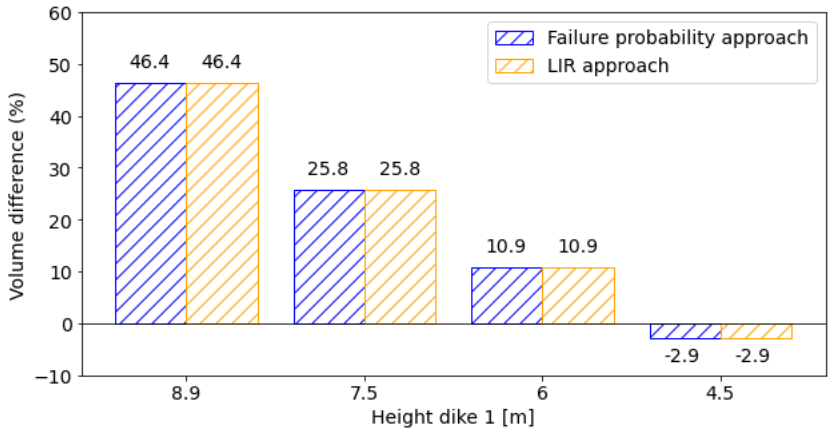

(a) 2020, sea level rise of 0 meter

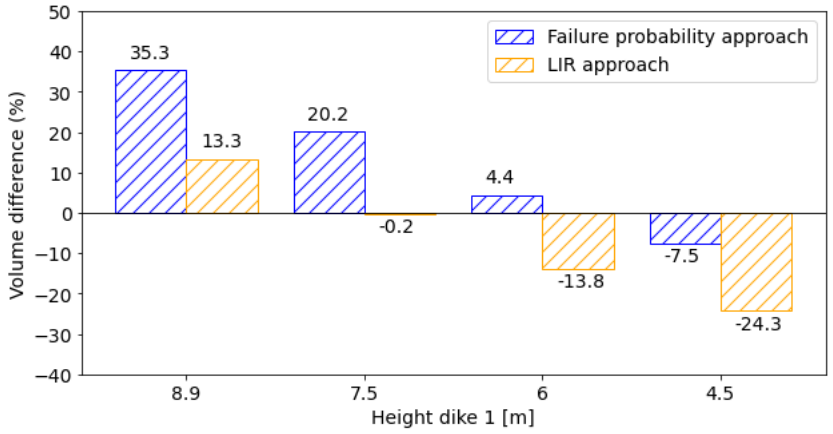

(b) 2120, sea level rise of 1.0 meter

Figure 6.2: The difference in volume (%) between a double dike system in comparison to a single dike system for a variation in height of the first dike. This is done for both the failure probability as LIR approach and for all five morphology scenarios. Note that the berm of the first dike in the double dike system is not included in the volume calculations.

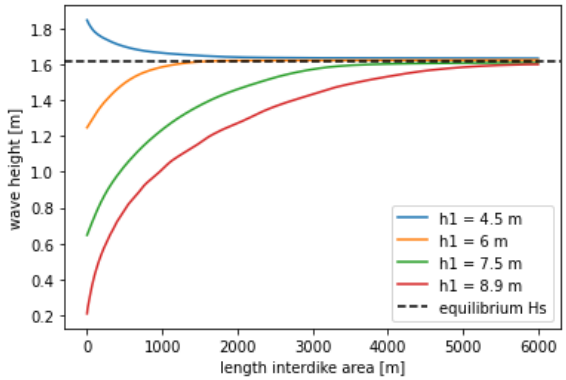

Figure 6.3: 2020, sea level rise of 0 meter

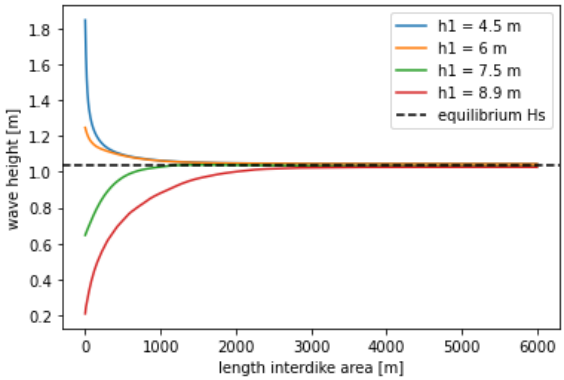

Figure 6.4: 2120, sea level rise of 1.0 meter

Figure 6.5: The propagation of the significant wave height in long interdike area for different heights of the first dike. The black dotted line represents the equilibrium significant wave height. The length of the interdike area is extended in this figure to show the adaptation length for the different dike heights. This is the length it takes for the system to adjust to its equilibrium wave height. The hydraulic conditions used correspond to a wind velocity of 31.7 m/s.

tion of the double dike system. Using smaller first dikes can be more effectively. Optimization can take the form of smart management; focusing on the second dike, allowing for natural erosion of the second dike. Or it can be the re-use of dike volume; using parts of the first dike (for example the berm) for upgrading the second dike.

6.2.2. Varying Hydraulic boundary conditions

This analysis considers three different variations in hydraulic conditions: 1) normal Western Scheldt conditions, 2) 50% tidal conditions and 3) 50% storm surge conditions. This primarily affects the water levels, not the wave characteristics. Varying in water level means the height of the single dike reference situation will also change. In order to comply to the same failure probability, lower dikes are sufficient for lower water levels. Water levels do affect the flood impact as well. New inundation areas must be calculated for the different variations to directly link these situations to the risk norm of 10^{-5}. Table 6.6 shows the calculated single dike heights for the corresponding hydraulic conditions for 2020 and 2120 and both probabilistic as risk approach.

As can be seen, for lower water levels, the breach flow and the flood impact reduces significant. In order to comply to the risk norm exactly, the inundation area decreases to compensate for the reduced breach flow. As expected, the storm surge reduction has most effect, since this gives most reduction in water level. As reaction to sea level rise, the additional heights required follow the same trend as the situation with normal conditions. Following the probabilistic approach, the required height matches sea level rise of 1.0 meter. Following the risk approach, this increases to a additional height of 1.7-1.8 meter.

		Single dike height [m]		
			Failure probability	**LIR**
Hydraulic conditions	**Area (km^2)**	**2020**	**2120**	**2120**
normal conditions	8.37	8.9	9.9	10.57
50 % tidal conditions	2.61	7.65	8.65	9.47
50 % storm surge conditions	0.42	6.8	7.8	8.54

Table 6.6: Dike heights of a single dike system for the different hydraulic conditions: normal conditions and decreased tidal and storm surge conditions.

The results for the application of double dike systems can be found in Table 6.7. For consistency, the single dike calculated for the different variations is used as first dike in the double dike system. Δh_2 is the difference in height between 2020 and 2120 and gives an good indication of effectiveness in reaction to sea level rise. First, considering the probabilistic approach, both a reduction in tidal conditions as storm surge conditions show an increase smaller than 1.0 meter sea level rise, namely 0.73 and 0.95 respectively. The reduction in water level means that waves reduce in height in comparison to the 2020 situation, implying that bed level accretion does has effect on the waves. Second, considering the risk approach, the effect of bed level accretion on the breach flow reduction is still noticeable, but seems smaller. This is primarily evident for the reduction in storm surge, for which the additional height is still larger than sea level rise. This can be explained by the fact that the smaller inundation area is relatively more sensitive to sea level rise. Design conditions for all variations in time can be found in Appendix G.

Hydraulic conditions	Height dike 1 [m]	Height dike 2 [m]					
		Failure probability			LIR		
		2020	2120	Δh_2	2020	2120	Δh_2
normal conditions	8.9	7.2	8.32	1.12	7.2	7.71	0.51
50% tidal conditions	7.65	5.88	6.61	0.73	5.88	6.54	0.66
50% storm surge conditions	6.8	5	5.95	0.95	5	6.2	1.2

Table 6.7: Height of the second dike of a double dike system for different combinations of hydraulic conditions applied. Δh_2 is the difference between 2020 and 2120.

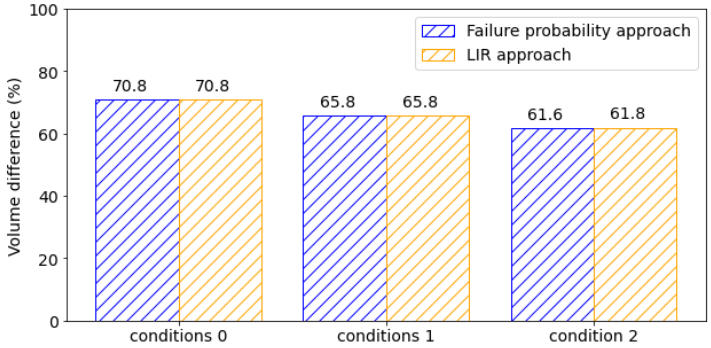

(a) 2020, sea level rise of 0 meter

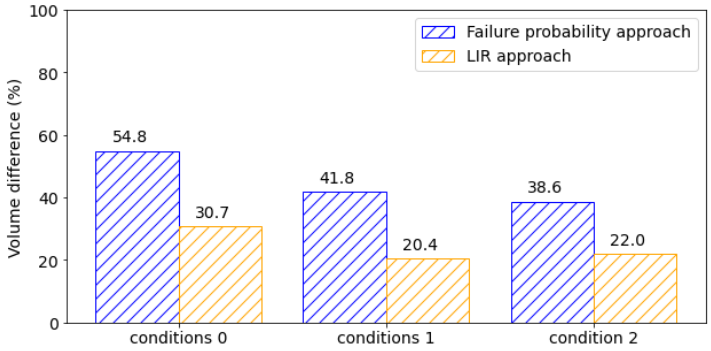

(b) 2120, sea level rise of 1.0 meter

Figure 6.6: The difference in volume (%) between a double dike system in comparison to a single dike system for different hydraulic conditions: 1) normal conditions, 2) 50% tidal conditions and 3) 50% storm conditions. This is done for both the failure probability as LIR approach. Be aware that the single dike heights and, thus, volumes differ for the applied hydraulic variations.

Figure 6.6 shows the additional required volume in comparison to a single dike situation. It can be seen that both reduction in tidal as storm surge conditions are more effective following both approaches in this volume comparison than the normal Western Scheldt conditions. Both variations show similar effectiveness. In contrast to the case study, the reduction in risk is due to a combination of reduction in wave height and reduction in flood impact, since the depth induced wave damping does occur.

It must be noted that the bed level accretion depends on the tidal amplitude. A smaller tidal amplitude gives a reduction in bed level growth of the interdike area. Since all variations are compared using the same maximum morphology scenario, this is not accounted for.

6.2.3. Size of the Flooded hinterland

This analysis considers different sizes of the inundated hinterland for the same hydraulic conditions. This only affects the impact calculations and thus risk approach. Table 6.8 shows the calculated single dike heights corresponding to the different area sizes and their response to sea level rise (2120). A reduction in area size means that, for the same hydraulic conditions, the flood impact increases and, therefore, bigger dikes with a lower failure probability are required.

The difference in height between 2020 and 2120 shows that the larger areas are more affected by sea level rise. The additional height required reduces from 2.08 to 1.23 meter for 150 % and 25% area size respectively.

Table 6.9 shows the dike heights of the applied double dike systems. As already mentioned, there is no difference noticeable following the probabilistic approach. The additional height required following the risk approach is a bit inconsistent and gives no visible trend or relation between area size and dike height, with an area size of 100% having the smallest increase (0.51 meter) due to sea level rise.

		Single dike height [m]		
		LIR		
Area variation	**area (km^2)**	**2020**	**2120**	**Δh_2**
150% area	12.57	8.15	10.23	2.08
100% area	8.37	8.9	10.57	1.67
50% area	4.19	9.56	10.89	1.33
25% area	2.09	9.92	11.15	1.23

Table 6.8: Height of single dike systems for different variations in area size of the hinterland. Δh_2 is the difference between 2020 and 2120.

Area size hinterland	**height dike 1 [m]**	**height dike 2 [m]**					
		Failure			**LIR**		
		2020	**2120**	**Δh_2**	**2020**	**2120**	**Δh_2**
area 150%	8.15	7,2	8,32	1.12	6,63	7,63	1.0
area 100%	8.9	7.2	8.32	1.12	7.2	7.71	0.51
area 50%	9.56	7.2	8.32	1.12	7.69	8,97	1.28
area 25%	9.92	7.2	8.32	1.12	7.99	9.27	1.28

Table 6.9: Dike heights of double dike system for different variations in area size of the hinterland. Δh_2 is the difference between 2020 and 2120.

Figure 6.7 shows the increase in volume for double dike systems in comparison to the single dike system for the risk approach only. For the situation in 2020, there are no significant differences in effectiveness regarding volumes. For the situation in 2120 this is not the case. There is a noticeable decrease in effectiveness for smaller area sizes, although all are more effective than the situation in 2020. This decrease in effectiveness can be partly explained by the differences additional height required for the single dike systems (Table 6.8). There was a stronger increase for the larger area sizes, which causes this relative increase in effectiveness for double dike systems for larger hinterland areas in comparison to the single dike system

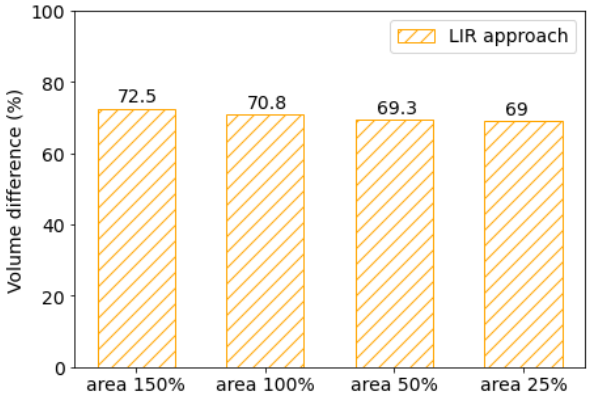

(a) 2020, sea level rise of 0 meter

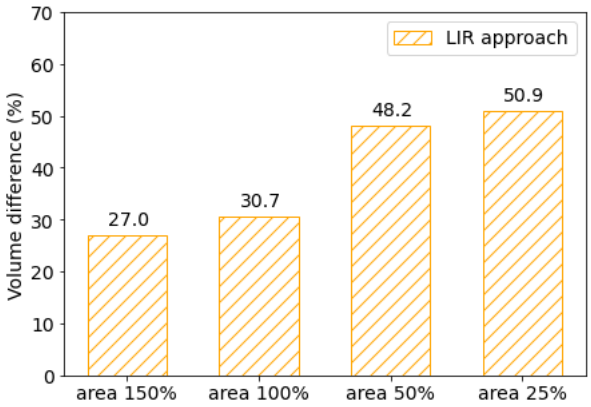

(b) 2120, sea level rise of 1.0 meter

Figure 6.7: The difference in volume (%) between a double dike system and single dike system when for 2020 and 2120, and different area sizes of the hinterland. This is only done for the LIR approach. Be aware that the single dike heights and, thus, volumes differ for the different area sizes.

6.2.4. Vegetation impact

Different combinations of vegetation (Table 6.4) are applied. Table 6.10 gives all heights of the second dike for these combinations for both the probabilistic as risk approach in 2020 and 2120. It can be seen that there is almost no significant difference in height between the different combinations for both approaches.

Vegetation scenarios	**height dike 2**			
	Failure		**LIR**	
	2020	**2120**	**2020**	**2120**
vegetation 0	7.2	8.32	7.2	7.71
vegetation 1	7.2	8.3	7.2	7.71
vegetation 2	7.2	8.27	7.2	7.71
vegetation 3	7.2	8.28	7.2	7.71
vegetation 4	7.2	8.23	7.2	7.69

Table 6.10: Height of the second dike for different combinations of vegetation (height and density) applied.

There is a small difference of less than 0.1 meter between no vegetation and combination with the most vegetation (combination vegetation 4) in 2120 following the probabilistic approach. This is also were most effect

is expected, since the vegetation does not affect breach flow in the model. This small difference in height is completely gone by applying risk calculations. For this storm surge dominant scenario with a large depth during design conditions, the effect of vegetation is negligible.

6.3. Conclusion

Four influential parameters can be identified: dike height of the first dike, interdike area length and accretion, hydraulic boundary conditions, and size of the inundated hinterland. Additionally, vegetation has been incorporated into the model.

The impact of the first dike on failure probability is not dominant, as the required increase in height for the second dike is not proportional to a reduction in height of the first dike. In addition, a significant interdike area with adequate bed level accretion gradually reduces the influence of the first dike in time.

In situations with smaller storm surges or tidal conditions, the effectiveness of the double dike system is higher, both in terms of failure probability and local individual risk approaches. Accretion of the bed level influences wave heights due to decreased water levels. Both reductions in storm surge and tidal amplitude have a similar effect. However, it should be noted that interdike area accretion is directly related to tidal amplitude (sediment inflow), which makes these accretion scenarios in combination with a smaller tidal amplitude less likely.

A larger hinterland area size positively affects the effectiveness of a double dike system. The larger the area size, the longer the duration of the effect of the heightened foreshore on breach flow.

Vegetation does not have a significant effect on the system's failure probability. The increased dissipation of wave energy is not yet noticeable under these hydraulic conditions, where storm surge dominates.

7

Discussion

In this study, certain assumptions were used and simplifications were made regarding the system definition, model approach and case study implementation. This discussion reflects on the choices made and how other choices could lead to different results. The discussion primarily follows the report chronologically. First, Section 7.1 covers the consequence of implementing tidal culverts and how best to do so. Thereafter, various model limitations are addressed in Section 7.2. The choices regarding the implementation of the case study are discussed in Section 7.3. At last, Section 7.4 touches upon some first thoughts on the financial feasibility of dynamic double dike systems.

7.1. System definition: the implementation of tidal culverts

This research has been limited by applying an open dynamic double dike system with the focus on free in- and outflow and morphological development. The case study in the Western Scheldt, Netherlands, shows that the water level is dominant with respect to the bed level accretion in the determination of the failure probabilities of the second dike.

To limit the water level at the interdike area during extreme conditions, a special closable structure such as a tidal culvert can be considered. Applying a closable variant does bring some changes to calculating the probability of failure of the second dike. The probability of non-closure of the tidal culvert as the probability of failure of the first dike should be included, since those have a retaining function now. A new failure scheme can be formulated, which is shown in Figure 7.1. The eventual failure of the system can be calculated as follows:

$$P_{f,syst} = P_{f,closure} \cdot P_{f,2|nonclosure} + (1 - P_{f,closure}) \cdot P_{f,2|closure} \tag{7.1}$$

$\mathrm{P}_{f,closure}$ is the probability of failure of the system, $\mathrm{P}_{f,closure}$ is the probability that the culvert does not close and/or the first dike fails, and $\mathrm{P}_{f,2|nonclosure}$ and $\mathrm{P}_{f,closure}$ are the conditional failure probabilities of the second dike. This works similarly for failure of the first dike, which also can be seen as a non-closure. For this simplification, it can be assumed that the failure probability of the second dike becomes almost 0 if the ($P_{f,2|closure} = 0$), which means that Equation 7.1 becomes:

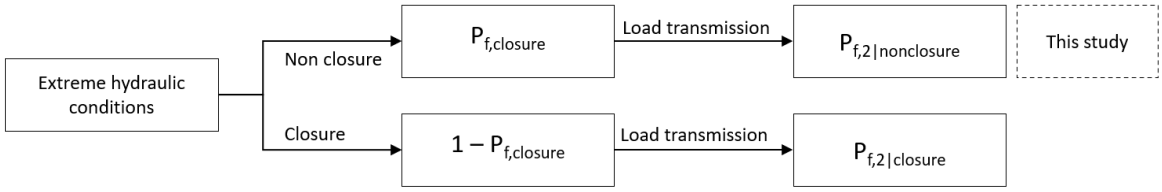

Figure 7.1: Failure scheme of a system with a culvert. $P_{f,closure}$ is the probability that the culvert does not close and/or the first dike fails. $P_{f,2|nonclosure}$ and $P_{f,2|closure}$ are the conditional failure probabilities of the second dike.

$$P_f = P_{f,closure} \cdot P_{f,2|nonclosure} \tag{7.2}$$

As a lower bound, the inflow is not restricted in case of non-closure. This should give similar results as done in this study. However, it can be assumed that the inflow is restricted by the size of the failed culvert and that this reduces the hydraulic loads at the second dike. In addition, this has the potential to reduce the flood impact. The non-closed culvert can be seen as a extra breach, which discharge restricts the inflow through the breach in the second dike.

However, it should no be forgotten that restricted inflow during normal conditions also influences the potential morphological development of the interdike area. Also, investment and maintaining costs are likely to be higher, since the first dike has a more important function than in the dynamic double dike system.

7.2. Model limitations

7.2.1. Wave period and wave spectrum

The wave period and accompanying wave length have a big influence on the overtopping discharge calculated by the EurOtop formulas. Longer waves cause larger overtopping volumes. The lower frequencies in the wave spectrum are dominant in the overtopping calculations. The wave period is transmitted by the first dike as a pulse. This can cause for interesting behaviour of the wave spectrum under certain conditions in combination with high wave velocities.

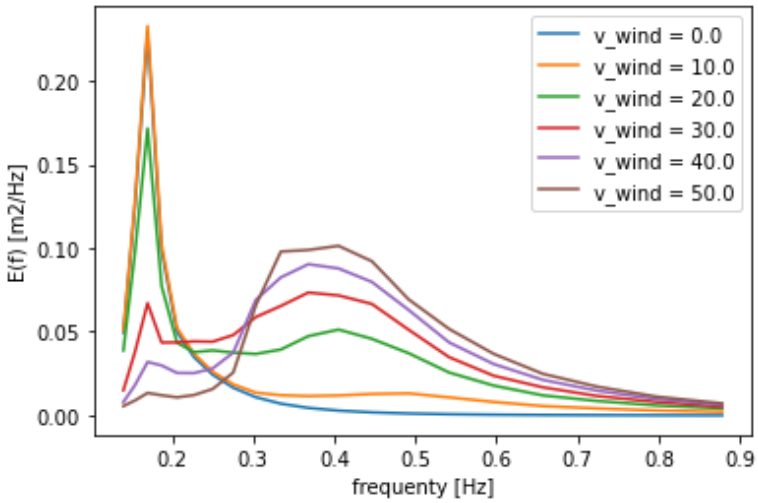

Figure 7.2: Wave spectrum development under high wind velocities (m/s)

Generally, local wind conditions causes shorter waves to develop. For very large wind velocities, much energy is added to the higher frequencies in the spectrum. However, Shorter, steeper waves are more prone to wave breaking. The 1D SWAN model distributes the wave breaking evenly over all frequencies, which has a strong decreasing impact on the energy for the lower frequencies. This creates the situation that the overtopping discharge reduces for very high wind velocities. This reducing effect of high wind velocities on the wave energy in the lower frequencies can be seen in Figure 7.2. This effect is primarily relevant for the combination of long waves from the sea and locally driven wind waves for high wind velocities.

7.2.2. Breach growth

This research shows that it is not easy to implement the effect of a raised foreshore on the breach development. The Verheij and van der Knaap method proofs to be reliable, but does not account for higher foreshore. However, this effect is noticeable in historic flood events (Zhu et al., 2020). Compared to the results shown, this would provide for a smaller breach width and, thus, a smaller flood impact. The effectiveness of a double dike system following the risk approach would increase. The effect can be simulated by introducing an reduction coefficient (C_r) dependent on the height of the foreshore. This coefficient can be calibrated to historic breach data. For example, Equation 4.18 can be modified to Equation 7.3, in which this reduction coefficient (C_r) is applied. As a reduction facor, C_r should have value smaller than 1.

$$(\frac{\delta B}{\delta t})_{t_i} = \mathbf{C_r} \frac{f_1 f_2}{ln(10)} \frac{(g(h_{up} - h_{down}))^{1.5}}{u_c^2} \frac{1}{1 + \frac{f_2 g}{u_c}(t_i - t_0)} \tag{7.3}$$

7.2.3. Flood model

Flood simulations for most areas in the Netherlands can not be simplified to a 1D 'bucket' model. Flood risk assessment in the Netherlands is often done with 2D flood models such as SOBEK2D (Beckers & de Bruijn, 2011). For this simplified case study, applying an 1D flood model made comparing systems and different scenarios faster and more effective. The calculated area size of around 8 km^2, used for the model calibration, is not representative for the area of interest for this case study, which is much larger. However, this calculated area size is within the range of area sizes of dike rings in the Netherlands to which the 'bucket' model is applied, ranging from 0.91 to 13.0 km^2 (Beckers & de Bruijn, 2011). But, this applies to very few dike rings and most area sizes of certain dike rings and for more specific case study's to the area of interest, a more comprehensive 2d model should be implemented.

7.2.4. Hydraulic boundary conditions during a dike breach

The simplification is made to calculate with a constant water level as hydraulic boundary condition in the flood simulation. However, in reality, the water level during storm conditions is variable and can be assumed to increase as the intensity of the storm increases and vice versa.

The irregular course of a storm can be simplified to the shape of triangle or trapezium (Tijssen & Diermandse, 2010). For practical implementation, the evolution of the storm surge can be simplified into a symmetrical trapezium as depicted in Figure 7.3 and considered equal to the course of the storm (wind velocity) over time. The course of the storm depends on the total storm duration, which can be divided into a peak duration (t_{peak}) and storm growth (t_{up}) and decline (t_{down}) . For the region of the Western Scheldt and the North Sea, it is recommended to implement a storm duration of around 2 days (48 hours), with a peak duration of 2 hours.

For simplification, one can assume that the failure of the dike occurs when the peak of the storm is reached.

The water level during failure (probabilistic design point) can be used as starting point and peak water level for the flood model. This means that both tide and storm surge are maximum at failure.

The effect of a variable water level on the results in terms of effectiveness in terms of local individual risk of a dynamic double dike system compared to a single dike reinforcement can be reviewed in two different ways. It can be reasoned this has a positive effect on the effectiveness of a dynamic double dike system. The higher interdike area in front of the second dike provides for an increased inflow hurdle in the breach, which is exceeded by the variable water level for a smaller period of time in comparison to the single dike system without this additional hurdle.

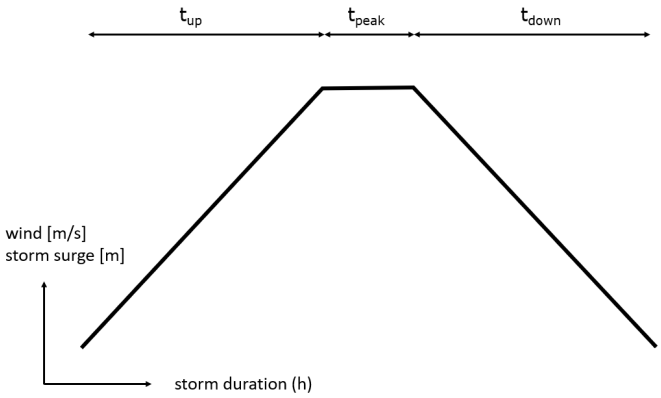

Figure 7.3: symmetrical trapezium as a simple approach of to model storm surge

7.3. Case study implementation

7.3.1. Correlation of hydraulic boundary conditions

For this research, it is assumed that the hydraulic boundary conditions are fully correlated to wind velocity. It is validated that this a correctly applied simplification. This creates the outermost situation in which waves and water levels are maximum in the design conditions. If those are not fully correlated, combinations are possible in which water level and waves are maximum. The hydraulic loads become less compared to the current assumption. The following other extreme combinations are possible:

- Big, long waves in combination with low wind velocities and a low water level.
- High wind velocities, local wave conditions and limited storm surge.
- High water levels in combinations with almost no wind and waves.

Anticipating the discussion of model uncertainties; allowing for a different correlation, means that the stochasts of the water level and wave characteristics must be included separately.

7.3.2. Morphological scenarios

For this research, different morphological scenarios are applied, ranging from no accretion to maximum accretion. Most are expressed as a percentage with respect to sea level rise. Maximum accretion also includes the potential for the bed level to grow to MHWL.

van Belzen and Bouma (n.d.) conducted a research to the morphological development of interdike area under sea level rise in the Western Scheldt. This is done for a system with large breach in the first dike, ranging from

50 to 500 meter. It shows that for open dynamic systems with sufficient sediment supply, the bed level accretion rate can keep up with sea level rise and even shows faster rates of accretion at the start for a bed level below MHWL. It follows that the rapid accretion scenario applied in this case study of the Western Scheldt as maximum morphology scenario is realistic.

7.3.3. Model uncertainties

The probabilistic FORM analysis is done with only one stochastic variable: the wind velocity. No actual uncertainty analysis can be done here. Such an analysis shows which uncertainties play an important role. The FORM analysis provides α-values as part of the output. These α-values serve as an indication of which uncertainties have more or less influence in the design point.

Uncertainty within the hydraulic boundary conditions is covered in section 7.3.1. However, the model allows for the implementation for more stochastic variables. Most important is the uncertainty in variation of maximum allowed overtopping discharge (resistance (R) of the limit state function), which is for this study assumed to be 10 l/s. In this uncertainty, variation in the current state of the inner slope (grass) revetment plays an important role.

In addition, uncertainties within the calculation of the transmission of loads. On can think of the application of the breakwater equations of d'Angremond (1996), which are deterministically fitted with a fitting parameter. These parameters can be implemented as a stochastic variable. This can also be done with bed level friction coefficient of Madsen (1988), the breaker parameter (Battjes & Janssen, 1978) and fitting parameters in the EurOtop formulas. A more comprehensive literature study should be done to determine the stochastic distributions which can be applied.

Of course, there is also a degree of uncertainty in the sea level rise and accretion rates assumed in the applied scenarios. However, these uncertainties cannot be applied as stochastic variable within the model, since it calculates with a situation independent of time. Nonetheless, the model can be used to quantify the impact of these uncertainties within the scenarios.

7.4. Financial feasibility

Application of a dynamic double dike system on the current situation shows that a second dike with considerable dimensions is needed, which gives the feeling that it is financially not the most effective alternative. However, a proper cost-benefit analysis should be done.

Investments of dike reinforcements can broken down into variable costs and overhead costs. Dike volumes are an example of variable costs. Overhead costs may include, for instance, dike revetments and do not depend on the required height of the dike reinforcement. These overhead costs are often substantial and the higher these are the less important dike volumes are within the feasibility considerations.

Possibly, a double dike system can be realized with grass-covered dike, whereas a single dike must be covered with a stone revetment. This last option is much more expensive. A grass-covered dike is an option, since the wave impact on the second dike is reduced for dynamic double dike systems.

In addition, the case study assumes the existing high single dike as first dike of the double dike system. However, the results of the sensitivity analysis show that if a dynamic double dike system is built from scratch, the first dike can be designed relatively lower and cheaper.

8

Conclusion and recommendations

This chapter presents the conclusions of the conducted research. First, the main research question is answered in section 8.1. Thereafter, the answers to the sub-questions in section 8.2 provide additional substantiation to the main conclusion. Finally, section 8.3 gives some recommendations on the applicability of dynamic double dike systems.

8.1. Answer to the main research question

The goal of this thesis was to provide an answer to the following research question:

Under which circumstances can a double dike system be an effective alternative to a regular dike reinforcement?

The effectiveness of a dynamic double dike system as an alternative to a regular dike reinforcement relies on three key location-specific factors:

1. ***Sufficient sediments present:*** The interdike area should experience a higher rate of sediment accretion compared to sea level rise. The accretion of the bed level offers two main advantages: 1) an increase in depth-induced wave damping and 2) a reduction in inflow through a dike breach.
2. ***Wave-dominant hydraulic conditions:*** The impact of the interdike area on the failure probability of a double dike system largely depends on water levels during extreme conditions. When storm surges prevail, the wave damping effect provided by the interdike area, in terms of depth-induced wave damping and additional friction from vegetation, becomes negligible.
3. ***Large hinterland area:*** There is a positive correlation between the effectiveness of a double dike system and the size of the inundated hinterland.

It is more advantageous to employ the local individual risk approach in comparative studies assessing the effectiveness of double dike systems than a comparison based on equal failure probabilities. Generally, the positive effect of bed level accretion on flood impact is significant. However, when considering only failure probabilities, this effect is overlooked.

8.2. Answer to the sub-questions

In this section, the answer to the sub-questions are provided.

What types of double dike systems can be defined?

A double dike system (DDS) is defined as a configuration of two parallel dikes separated by an interdike area. It is possible to distinguish three distinct systems based on the function of the seaward dike: dynamic open DDS, dynamic closable DDS, and static closed DDS. The effectiveness of the system under both normal and extreme conditions is determined by the degree to which water is permitted to pass through the first dike.

In the case of dynamic open DDS, the first dike is intentionally breached, allowing unobstructed inflow and outflow of water. Conversely, in the static closed DDS, a substantially sized first dike prevents any water passage. To achieve a more hybrid approach, dynamic closable DDS utilizes adjustable structures like tidal culverts to regulate the inflow.

Under normal tidal conditions, the permitted inflow governs the sediment supply and the potential for accretion within the interdike area. Moreover, during extreme circumstances, the function of the first dike transitions from acting as a breakwater in dynamic open DDS to serving as a retaining structure in static closed DDS and dynamic closable DDS when closed. The inflow of water and transmitted waves determine the hydraulic load on the second dike. The safety of the system fails when the second dike fails.

For this research, the analysis was conducted on an open system with a breached first dike and the potential of maximum accretion. This so-called dynamic double dike system focuses on wave damping. Since there is a free in and out flow, it is assumed that the water level in the interdike area is equal to the outer water level.

How to assess double dike systems on dike failure and flood risk?

The effectiveness of a double dike system was assessed using two distinct approaches: the failure probability approach and the local individual risk (LIR) approach. The first approach considers an equal probability of failure for the primary flood defense, while the second approach incorporates the Dutch local individual risk norm and includes the assessment of flood impact.

A transmission model was employed to describe the hydraulic conditions within the double dike system, focusing on wave transmission since the water level remains constant. Key factors in this load transmission include the height of the first dike and the length and depth of the interdike area, emphasizing wave damping or growth. The failure probability of a dike is evaluated for failure by overtopping and overflow with the help of EurOtop.

To assess the risk, a flood model was introduced to determine flood characteristics such as the rate of water level rise and maximum inundation depth. These characteristics were then used to calculate the mortality fraction. Crucial components of the flood model include breach hydrodynamics, breach growth, and consideration of storm boundary conditions over time, such as storm duration.

The accretion of the interdike area, resulting in a raised foreshore, leads to reduced inflow and slower breach growth. This effect was accounted for in the breach hydrodynamics model by primarily considering the water depth in front of the breach. However, the two tested methods, 1) Verheij & van der Knaap (2003) and 2) Van Damme (2020), to describe breach growth, do not accurately capture the limiting effect of a raised foreshore on the breach widening rate. The method of Verheij & van der Knaap was chosen for its ability to provide more

realistic and narrower breach widths.

How does the effectiveness of a double dike system compare to that of a single dike system for different morphological scenarios and sea level rise, under conditions present in the Western Scheldt?

This analysis investigates the effectiveness of a dynamic double dike system in the Western Scheldt with a simplified model based on the Eendragtspolder region. Various scenarios encompassing sea level rise (SLR) and morphology were examined. In the present situation, opening the existing dike requires the construction of a second dike that is only 1.7 meters lower than the single dike system.

When comparing the system based on equal failure probability, a single dike should be raised identically to the SLR that takes place. In the case of a double dike system and 1 meter SLR , this increase in height of the second dike should be approximately 1.15 meters to maintain the same failure probability. Sedimentation in the interdike area has a negligible impact on failure probabilities due to the dominant influence of water depth.

However, this comparison changes when based on equal flood risk. With 1 meter SLR, the additional required height of a single dike increases to 1.7 meters to prevent an increase in local individual risk. Applying this approach to a double dike system, the effect of the height of bed level of the interdike area on the breach flow does have influence. For instance, when combining 1 meter SLR with rapid bed level increase, raising the second dike by just 0.5 meters would be sufficient to maintain an equal level of LIR for the hinterland polder.

Examining the effectiveness of single and double dike systems in terms of total dike volumes strengthens the conclusions drawn above. The risk approach shows a more positive picture regarding the effectiveness of a dynamic double dike system in comparison to a single dike. In addition to the reducing effect of the bed level on breach flow, the increased height necessary of a single dike to meet the LIR norm due to sea level rise in the context of dike volumes can not be overlooked. For example, in the scenario involving a 1 meter SLR and rapid bed level increase, the failure probability approach requires 55% more dike volume for the implementation of a double dike system compared to a raised single dike, whereas the risk approach requires only an additional 31% in volume.

What is the sensitivity of influential system characteristics on the dynamic dike system?

Four influential parameters can be identified: dike height of the first dike, interdike area length and accretion, hydraulic boundary conditions, and size of the inundated hinterland. Additionally, vegetation has been incorporated into the model.

The impact of the first dike on failure probability is not dominant, as the required increase in height for the second dike is not proportional to a reduction in height of the first dike. In addition, a significant interdike area with adequate bed level accretion gradually reduces the influence of the first dike in time.

In situations with smaller storm surges or tidal conditions, the effectiveness of the double dike system is higher, both in terms of failure probability and local individual risk approaches. Accretion of the bed level influences wave heights due to decreased water levels. Both reductions in storm surge and tidal amplitude have a similar effect. However, it should be noted that interdike area accretion is directly related to tidal amplitude (sediment inflow), which makes these accretion scenarios in combination with a smaller tidal amplitude less likely.

A larger hinterland area size positively affects the effectiveness of a double dike system. The larger the area size, the longer the duration of the effect of the heightened foreshore on breach flow.

Vegetation does not have a significant effect on the system's failure probability. The increased dissipation of

wave energy is not yet noticeable under these hydraulic conditions, where storm surge dominates.

8.3. Recommendations

The recommendations made consist of four parts. The first three sub-sections elaborate on how this research provides a better understanding of the applicability of dynamic double dike systems. The last sub-section contains extra insight and recommendations for the implementation of more hybrid closable dynamic systems.

8.3.1. Highlighting the effect on the consequences of a flood

The conclusions demonstrate that the greatest potential for the implementation of dynamic double dike systems in comparison to a regular dike reinforcement lies in the impact of the elevated bed level of the interdike area on flood consequences. However, this study's flood simulation is limited to a 1D model and relies on certain basic assumptions. To gain a more comprehensive understanding of this specific potential and to effectively incorporate it into the Dutch flood risk approach, it is recommended to employ an enhanced flood model. This entails implementing a 2D flood model and considering the stabilizing effect of the foreshore on breach growth. The recommendation for a 2D model is further supported by the results, which indicate an increase in effectiveness as the flooded hinterland expands.

In addition to improving the flood model, it is advised to critically evaluate the current implementation of the Dutch flood risk approach. This approach reduces risk calculations to a failure probability norm per dike section, which is utilized in current dike evaluations. However, the implementation of these failure probability norms disregards the positive effect of dynamic double dike systems on flood consequences, as described earlier, as well as the additional negative impact of sea level rise on the flood impact of single dike systems. Therefore, it is essential to incorporate the influence of the system and its temporal development on flood characteristics into the risk approach.

Lastly, it is recommended to implement dynamic double dike systems in regions where LIR is considered normative within the risk approach. This is because the calculation of the mortality fraction is more sensitive to variations in flood characteristics compared to the flood damage calculations used in the MKBA approach.

8.3.2. Ideal conditions and implementation on other coastal regions

Based on the findings, it can be deduced that the combination of bed level height in the interdike area and hydraulic conditions plays a crucial role in determining the effectiveness of dynamic double dike systems under extreme conditions. Both factors determine the water depth in front of the second dike, influencing hydraulic loads and playing a significant role in flood simulations. Additionally, the most significant advantage of such systems lies in their potential for high rates of bed level accretion in the interdike area. This potential relies on sediment supply, which is influenced by sediment concentration and tidal range. By translating these insights into suitable locations for dynamic double dike systems, the following set of requirements can be outlined: high sediment concentrations, adequate tidal range, and a restriction on extreme water levels during extreme conditions, primarily referring to a mild storm surge.

This report focused on a case study conducted in the Western Scheldt, however it is worth considering implementing dynamic double dike systems in other parts of the Netherlands. In the Dutch province of Zealand, apart from the Western Scheldt, the Eastern Scheldt can also be considered, while in the northern part of the country, the Frisian coast of the Wadden Sea and the Ems-Dollard Estuary in the province of Groningen are notable areas. The findings of this report indicate that the effectiveness of the Western Scheldt is primarily influenced by the

occurrence of large storm surges. In contrast, due to the more enclosed nature of the Eastern Scheldt, extreme water levels are significantly lower. However, this enclosed nature also results in lower sediment concentrations, which adversely affects the morphological dynamics of these systems. In the case of the northern Dutch coast, we observe a combination of higher sediment concentrations and milder storm surges. Therefore, this location is ideal for implementing dynamic double dike systems. However, it is important to note that in the Wadden region, salt marshes are already commonly found in front of dikes. Therefore, the added value of such double dike systems compared to a single dike is significantly reduced in terms of flood risk.

8.3.3. Potential for smart management and design choices

The effectiveness of the dike volume is calculated in this case study under the assumption that the first dike is only breached while remaining stretches do not change. However, the sensitivity analysis reveals that the effectiveness in terms of volume increases with a decrease in the height of the first dike. This is because the primary function of the first dike is wave damping and does not have any retaining function. Also, it becomes less influential for interdike areas with greater length and reduced depth. Hence, the most effective scenario involves a long interdike area with a high bed level, placing greater emphasis on the safety of the second dike. So therefore, using this finding, it is recommended to make more efficient design and management decisions concerning the height of the first dike. For instance, potential options include reducing maintenance efforts and allowing controlled erosion of the first dike or re-purposing portions of the first dike to enhance the second dike. Furthermore, as wave impact is mitigated in a dynamic double dike system, it becomes feasible to consider more natural grass revetments instead of costly rock revetments.

8.3.4. Implementation of closable systems

This research assumes an open dynamic double dike system with unrestricted inflow and outflow, which cannot be closed during extreme conditions. However, for areas like the Western Scheldt or other coastal regions with significant storm surges, it is advisable to consider a closable system. This entails the ability to close the gaps in the first dike under specific conditions, such as utilizing tidal culverts. In this context, the first dike undergoes a functional transformation, retaining the water effectively constraining the water levels within the interdike area. Such systems offer the advantage of reducing the probability of extreme hydraulic loads on the second dike (only in the event of non-closure and failure of the first dike), potentially allowing for a reduction in its size. However, the use of tidal culverts should consider the potential decrease in sediment supply and subsequent reduction in morphological activity in comparison to a system with unrestricted inflow.

Implementing a closable system necessitates larger investments in modifications to the first dike. Additionally, the maintenance of the first dike becomes more crucial due to its retaining function. Therefore, it is recommended to conduct a comprehensive cost-benefit analysis to compare the open dynamic double dike system with the closable double dike system.

Bibliography

Battjes, J. A., & Janssen, J. (1978). Energy loss and set-up due to breaking of random waves. In *Coastal engineering 1978* (pp. 569–587).

Beckers, J., & de Bruijn, K. (2011). *Slachtofferrisico's waterveiligheid*. Deltares.

Bockarjova, M., Rietveld, P., & Verhoef, E. (2012). *Composite valuation of immaterial damage in flooding: Value of statistical life, value of statistical evacuation and value of statistical injury* (Tinbergen Institute Discussion Papers No. 12-047/3). Tinbergen Institute. https://EconPapers.repec.org/RePEc:tin:wpaper:20120047

Booij, N., Holthuijsen, L., & Ris, R. (1996). The" swan" wave model for shallow water, 668–676.

Bornschein, A., & Pohl, R. (2018). Land use influence on flood routing and retention from the viewpoint of hydromechanics. *Journal of Flood Risk Management*, *11*, 6–14. https://doi.org/10.1111/jfr3.12289

Boudewijn, T., Lenkeek, W., & Japink, M. (2008). *Mogelijkheden voor estuariene en integrale gebiedsontwikkeling in waterdunen*. Bureau Waardenburg bv.

d'Angremond, K., Meer, J. W. V. D., & Jong, R. J. D. (1996). Wave transmission at low-crested structures. *Coastal Engineering Proceedings*, *25*.

Deltares. (2011). *Maatschappelijke kosten-batenanalyse waterveiligheid 21e eeuw*.

EemsDollard2050. (n.d.). *Pilot dubbele dijk*.

EemsDollard2050. (2018). *Programma eems-dollard 2050 - meerjarig adaptief programma voor ecologische verbetering*.

Eijgenraam, C. J. (2006). Optimal safety standards for dike-ring areas. *Discussion paper nr. 62, ISBN 90-5833-267-5*.

Eurotop. (2018). Eurotop - manual on wave overtopping of sea defences and related structures.

Fan, D., Nguyen, D. V., Su, J., Bui, V. V., & Tran, D. L. (2019). Coastal morphological changes in the red river delta under increasing natural and anthropic stresses. *Anthropocene Coasts*, *2*, 51–71. https://doi.org/10.1139/anc-2018-0022

Gedan, K. B., Kirwan, M. L., Wolanski, E., Barbier, E. B., & Silliman, B. R. (2011). *The present and future role of coastal wetland vegetation in protecting shorelines: Answering recent challenges to the paradigm*. https://doi.org/10.1007/s10584-010-0003-7

Google maps [Accessed: March 21, 2023]. (n.d.).

Hinkel, J., Lincke, D., Vafeidis, A. T., Perrette, M., Nicholls, R. J., Tol, R. S. J., Marzeion, B., Fettweis, X., Ionescu, C., & Levermann, A. (2014). Coastal flood damage and adaptation costs under 21st century sea-level rise. *Proceedings of the National Academy of Sciences*, *111*, 3292–3297. https://doi.org/10.1073/pnas.1222469111

IPCC. (2013). Annex ii: Climate system scenario tables. In T. F. Stocker, D. Qin, G.-K. Plattner, M. Tignor, S. K. Allen, J. Boschung, A. Nauels, Y. Xia, V. Bex, & P. M. Midgley (Eds.). M. Prather, G. Flato, P. Friedlingstein, C. Jones, J.-F. Lamarque, H. Liao, & P. Rasch (Eds.), *Climate change 2013: The physical science basis. contribution of working group i to the fifth assessment report of the intergovernmental panel on climate change*. Cambridge University Press.

Jongejan, R. (2016). *Factsheet: Het lengte-effect*.

Jonkman, S., Steenbergen, R., Morales-Napoles, O., Vrouwenvelder, A., & Vrijling, J. (2020). Probabilistic design: Risk and reliability analysis in civil engineering. *Scientific reports*, *10*(1), 1–11.

Jonkman, S. N., Jorissen, R. E., Schweckendiek, T., & Bos, J. P. V. D. (2021). *Flood defences lecture notes CIE5314 4th edition*. Delft University of Technology.

Jonkman, S. N. (2007). *Loss of life estimation in flood risk assessment : Theory and applications*. S.N.

Jonkman, S. N., Hillen, M. M., Nicholls, R. J., Kanning, W., & Ledden, M. V. (2013). Costs of adapting coastal defences to sea-level rise - new estimates and their implications. *Journal of Coastal Research*, *29*, 1212–1226. https://doi.org/10.2112/JCOASTRES-D-12-00230.1

Jonkman, S., Bočkarjova, M., Kok, M., & Bernardini, P. (2008). Integrated hydrodynamic and economic modelling of flood damage in the netherlands. *Ecological Economics*, *66*, 77–90. https://doi.org/10.1016/j.ecolecon.2007.12.022

Kind, J. M. (2014). Economically efficient flood protection standards for the netherlands. *Journal of Flood Risk Management*, *7*(2), 103–117.

Kirwan, M. L., Guntenspergen, G. R., D'Alpaos, A., Morris, J. T., Mudd, S. M., & Temmerman, S. (2010). Limits on the adaptability of coastal marshes to rising sea level. *Geophysical Research Letters*, *37*, n/a–n/a. https://doi.org/10.1029/2010GL045489

Kirwan, M. L., Temmerman, S., Skeehan, E. E., Guntenspergen, G. R., & Fagherazzi, S. (2016). Overestimation of marsh vulnerability to sea level rise. *Nature Climate Change*, *6*, 253–260. https://doi.org/10.1038/nclimate2909

Klijn, F., Kolen, B., Knoop, J., Wagenaar, D., De Bruijn, K., & Bouwer, L. (2013). Maatschappelijke ontwrichting door overstromingen voorkomen. *Deltares Report*, *1208052*.

Maaskant, B. (2007). *Research on the relationships between flood characteristics and fatalities*. Master thesis - Delft University of Technology.

Maaskant, B., Jonkman, S. N., & Kok, M. (2009). Analyse slachtofferaantallen vnk-2 en voorstellen voor aanpassingen van slachtofferfuncties. *HKV lijn in water Rapport PR1669*, *10*.

Madsen, O. S., & Rosengaus, M. M. (1988). Spectral wave attenuation by bottom friction: Experiments. In *Coastal engineering 1988* (pp. 849–857).

Mal, S., Singh, R. B., & Huggel, C. (2018). *Climate change, extreme events and disaster risk reduction towards sustainable development goals*. https://doi.org/https://doi.org/10.1007/978-3-319-56469-2

Marijnissen, R. J. C. (2021). *Shared-use of flood defences*. Wageningen University and Research. https://doi.org/10.18174/549897

Marijnissen, R. J. C., Kok, M., Kroeze, C., & van Loon-Steensma, J. M. (2021). Flood risk reduction by parallel flood defences – case-study of a coastal multifunctional flood protection zone. *Coastal Engineering*, *167*. https://doi.org/10.1016/j.coastaleng.2021.103903

Mesel, I. D., Ysebaert, T., & Kamermans, P. (2013). *Klimaatbestendige dijken: Het concept wisselpolders*. IMARES Wageningen. Silhouette Books.

Möller, I., Kudella, M., Rupprecht, F., Spencer, T., Paul, M., Wesenbeeck, B. K. V., Wolters, G., Jensen, K., Bouma, T. J., Miranda-Lange, M., & Schimmels, S. (2014). Wave attenuation over coastal salt marshes under storm surge conditions. *Nature Geoscience*, *7*, 727–731. https://doi.org/10.1038/NGEO2251

Neumann, B., Vafeidis, A. T., Zimmermann, J., & Nicholls, R. J. (2015). Future coastal population growth and exposure to sea-level rise and coastal flooding - a global assessment. *PLOS ONE*, *10*, e0118571. https://doi.org/10.1371/journal.pone.0118571

Nguyen, Q. H., & Takewaka, S. (2020). Land subsidence and its effects on coastal erosion in the nam dinh coast (vietnam). *Continental Shelf Research*, *207*, 104227. https://doi.org/10.1016/j.csr.2020.104227

Pasche, E., Ujeyl, G., Goltermann, D., Meng, J., Nehlsen, E., & Wilke, M. (2008). Cascading flood compartments with adaptive response. *WIT Transactions on Ecology and the Environment*, *118*, 303–312. https://doi.org/10.2495/FRIAR080291

Provincie-Zeeland. (n.d.). *Beeldmateriaal waterdunen*.

Provincie-Zeeland. (2010). *Provinciaal inpassingsplan waterdunen*. Provinciale Staten van Zeeland.

Rijke, J., van Herk, S., Zevenbergen, C., & Ashley, R. (2012). Room for the river: Delivering integrated river basin management in the netherlands. *International Journal of River Basin Management*, *10*, 369–382. https://doi.org/10.1080/15715124.2012.739173

Rivierenland, W. (n.d.). *Waterbeheer buitenpolders*. https://www.waterschaprivierenland.nl/waterbeheer-buiten polders

Slobbe, E., Vriend, H. J., Aarninkhof, S., Lulofs, K., Vries, M., & Dircke, P. (2013). Building with nature: In search of resilient storm surge protection strategies. *Natural Hazards*, *65*, 947–966. https://doi.org/10.1007/s11069-012-0342-y

Stark, M., Ravenstijn, P., Korf, J., & Walraven, R. (2006). *Inlaatduiker waterdunen*. Oranjewoud.

Suzuki, T., Zijlema, M., Burger, B., Meijer, M. C., & Narayan, S. (2012). Wave dissipation by vegetation with layer schematization in swan. *Coastal Engineering*, *59*, 64–71. https://doi.org/10.1016/j.coastaleng.2011.07.006

Tijssen, A., & Diermandse, F. (2010). *Storm surge duration and storm duration at hoek van holland sbw-belastingen*. Deltares. https://www.helpdeskwater.nl/onderwerpen/waterveiligheid/primaire/beoordelen/@205885/storm-surge-duration/

Van Belzen, J., Rienstra, G., & Bouma, T. (2021). *Dubbele dijken als robuuste waterkerende landschappen voor een welvarende zuidwestelijke delta*. NIOZ Royal Netherlands Institute for Sea Research. https://doi.org/10.25850/nioz/7b.b.kb

Van Damme, M. (2020). An analytical process-based approach to predicting breach width in levees constructed from dilatant soils. *Natural Hazards*, *101*, 59–85. https://doi.org/10.1007/s11069-020-03862-8

Van den Hoven, K., van Belzen, J., Kleinhans, M., Schot, D., Merry, J., van Loon-Steensma, J., & Bouma, T. (submitted). How foreshores offer flood protection during dike breaches: A physical model study.

van der Meer, J. W., Briganti, R., Zanuttigh, B., & Wang, B. (2005). Wave transmission and reflection at low-crested structures: Design formulae, oblique wave attack and spectral change. *Coastal Engineering*, *52*, 915–929. https://doi.org/10.1016/j.coastaleng.2005.09.005

van Belzen, J., & Bouma, T. (n.d.). Tussenraport - samen leren over de weg naar dynamische dijkmogelijkheden: A casusstudie in de westerschelde.

van Dantzig, D. (1956). Economic decision problems for flood prevention. *Econometrica: Journal of the Econometric Society*, 276–287.

van Infrastructuur en Milieu, M. (2017a). *Regeling veiligheid primaire waterkeringen 2017 - bijlage i procedure*. http://www.helpdeskwater.nl/onderwerpen/waterveiligheid/pri

van Infrastructuur en Milieu, M. (2017b). *Regeling veiligheid primaire waterkeringen 2017 - bijlage i procedure*.

van Infrastructuur en Milieu, M. (2017c). *Regeling veiligheid primaire waterkeringen 2017 - bijlage iii sterkte en veiligheid*.

Verheij, J. H., & Van der Knaap, M. F. C. (2003). Modifying the breach growht model in his-om.

Vinh, T. T., Kant, G., Huan, N. N., & Pruszak, Z. (1996). Sea dike erosion and coastal retreat at nam ha province, vietnam. *Coastal Engineering Proceedings*, *25*.

Visser, P. J. (1998). *Breach growth in sand-dikes*.

VNK - Veiligheid Nederland in Kaart. (2014). *Eindrapportage veiligheid nederland in kaart* (tech. rep. HB 2540621). Rijkswaterstaat Projectbureau VNK. Nieuwegein.

Vuik, V., Borsje, B. W., Willemsen, P. W., & Jonkman, S. N. (2019a). Salt marshes for flood risk reduction: Quantifying long-term effectiveness and life-cycle costs. *Ocean and Coastal Management*, *171*, 96–110. https://doi.org/10.1016/j.ocecoaman.2019.01.010

Vuik, V., Borsje, B. W., Willemsen, P. W., & Jonkman, S. N. (2019b). Salt marshes for flood risk reduction: Quantifying long-term effectiveness and life-cycle costs. *Ocean and Coastal Management*, *171*, 96–110. https://doi.org/10.1016/j.ocecoaman.2019.01.010

Vuik, V., Heo, H. Y. S., Zhu, Z., Borsje, B. W., & Jonkman, S. N. (2018). Stem breakage of salt marsh vegetation under wave forcing: A field and model study. *Estuarine, Coastal and Shelf Science*, *200*, 41–58. https://doi.org/10.1016/j.ecss.2017.09.028

Vuik, V., Jonkman, S. N., Borsje, B. W., & Suzuki, T. (2016). Nature-based flood protection: The efficiency of vegetated foreshores for reducing wave loads on coastal dikes. *Coastal Engineering*, *116*, 42–56. https://doi.org/10.1016/j.coastaleng.2016.06.001

Wahl, T. L. (2004). Uncertainty of predictions of embankment dam breach parameters. *Journal of Hydraulic Engineering*, *130*, 389–397. https://doi.org/10.1061/(ASCE)0733-9429(2004)130:5(389)

Wauben, C. W. (2019). *Flood protection using multiple lines of dikes a case study of the twin dike eemshaven-delfzijl project*. http://repository.tudelft.nl/.

Zhu, Z., Vuik, V., Visser, P. J., Soens, T., van Wesenbeeck, B., van de Koppel, J., Jonkman, S. N., Temmerman, S., & Bouma, T. J. (2020). Historic storms and the hidden value of coastal wetlands for nature-based flood defence. *Nature Sustainability*, *3*, 853–862. https://doi.org/10.1038/s41893-020-0556-z

A

SWAN model - input

A SWAN one-dimensional wave model is used to calculate the propagation of the waves in the interdike area. For each run of modelling the wave attenuation using SWAN, a SWAN input file is created, for which an example can be found in Figure A.1.

```
PROJ 'Interdike' '0000'
SET NAUTICAL
MODE STATIONARY ONEDIMENSIONAL

$ CGRID REGULAR [xpc] [ypc] [alpc] [xlenc] [ylenc] [mxc] [myc]
CGRID REGULAR 0.0 0 0 1000.0 0 100 0 CIRCLE 36 0.14 2.80  31

$ INPGRID BOTTOM REGULAR [xpinp] [ypinp] [alpinp] [mxinp] [myinp] [dxinp] [dyinp]
INPGRID BOTTOM REGULAR 0.0 0 0 100 0 10.0 0
READINP BOTTOM -1 'bathy.txt' 5 0 FREE

INPGRID WLEVEL REGULAR 0.0 0 0 100 0 10.0 0
READINP WLEVEL 1 'wlevl.txt' 5 0 FREE

BOUND SHAPESPEC JONSWAP 3.3 PEAK DSPR POWER
BOUNDSPEC SEGMENT XY 0.0 0 UNIFORM PAR 0.06477426034692793 3.805685443900769 270 2

GEN3
BREAK CONstant alpha=1.00 gamma=0.65
WIND 15.596484681193889 270
QUAD
WCAP

$ VEGEtation < [height] [diamtr] [nstems] [drag]
VEGETATION 1 0.0 0.003 500 0.5

$ INPGRID NPLANTS REGULAR [xpinp] [ypinp] [alpinp] [mxinp] [myinp] [dxinp] [dyinp]
INPGRID NPLANTS REGULAR 0.0 0 0 100 0 10.0 0
READINP NPLANTS 1 'vegcover.txt' 5 0 FREE

FRICTION MADSEN 0.02

NUMERIC ACCUR 0.01 0.01 0.01 99 STAT 100 0.01

POINTS 'gauge' FILE   'gauges.loc'
$ CURve ♦sname♦ [xp1] [yp1] < [int] [xp] [yp] >
$ [int] = nr of locations
POINTS 'gauge' 990.0 0
CURVE  'curve' 0.0 0 100 1000.0 0
TABLE  'curve' HEAD   'curve.tab' HS TMM10
SPEC 'gauge' SPEC1D 'gauges.spec'

COMPUTE
STOP
```

Figure A.1: Example of a SWAN input file. For each run, the input file is replaced with the values applicable to that run, for example the bed level height.

B

Hydra-NL calculations - hydraulic boundary conditions

The hydraulic boundary conditions for the case study in Chapter 5 are obtained from HydraNL. HydraNL is a probabilistic assessment tool which can be used to assess design flood defences. An overview of the location can be found in Figure B.1.

This study used the possibility to calculate the hydraulic load level (Dutch: Hydraulisch Belastings Niveau or HBN), which is the required height of a dike at a certain location for hydraulic conditions with a given return period. These hydraulic conditions with a given return period are used as input for the transmission model. This data consists of water levels, significant wave heights, significant wave period and wind velocity. The data of HBN calculations is multi-directional. However, as a simplification, only the data of the most dominant wind direction (300 degrees North) is used. Figure B.2 gives an overview of used data. Figures B.3 to B.16 show the raw data sets from the HBN calculations.

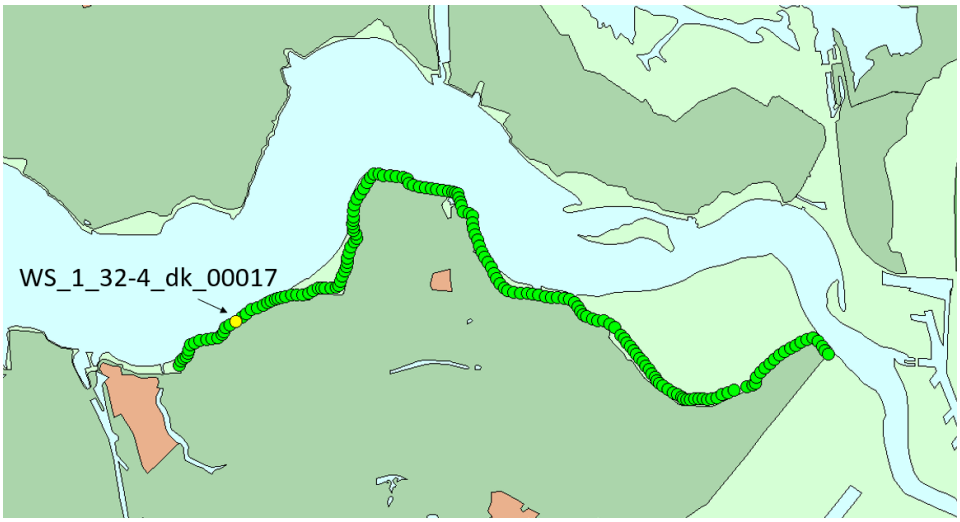

Figure B.1: Location of the extracted data in the Western Scheldt

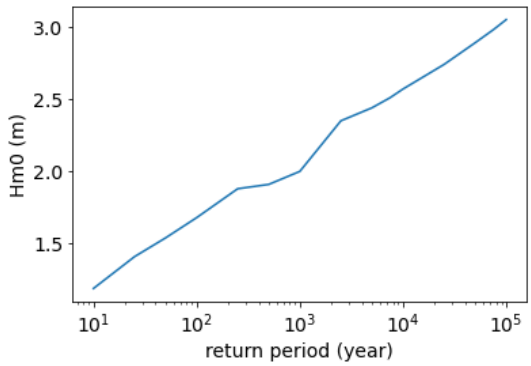

(a) Wave height (m)

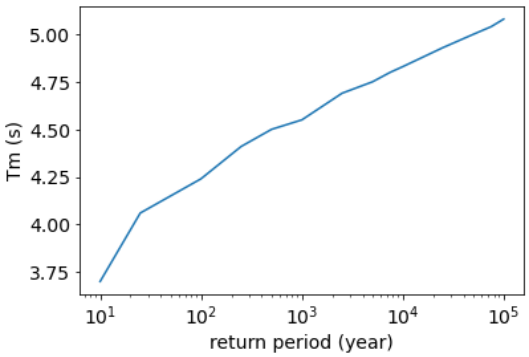

(b) Wave period (s)

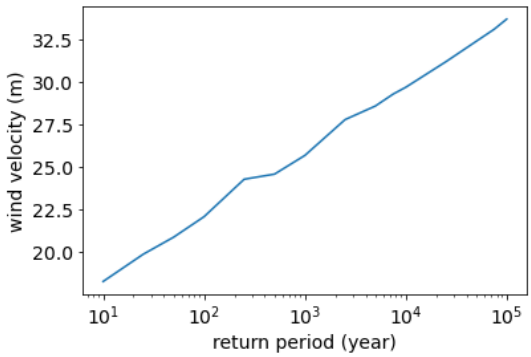

(c) Wind velocity (m/s)

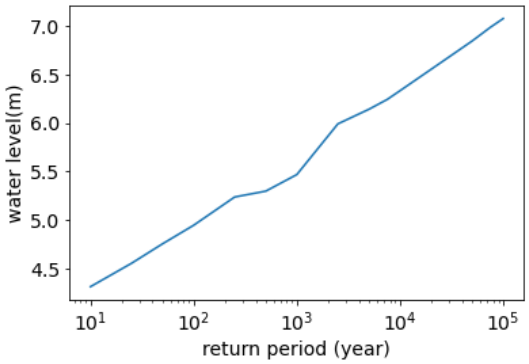

(d) Water level (m)

Figure B.2: The data of the hydraulic boundary conditions for a given return period

r	zeews. m+NAP	windsn. m/s	h,teen m+NAP	Hm0,teen m	Tm-1,0,t s	golfr graden	bijdrage ov. freq (%)
30.0	4.53	11.5	4.53	0.76	2.46	9.3	0.0
60.0	4.63	11.3	4.63	0.67	2.38	46.3	0.0
90.0	4.75	10.4	4.75	0.52	1.96	62.4	0.0
120.0	4.82	7.8	4.82	0.38	1.47	90.4	0.0
150.0	5.02	6.2	5.02	0.00	0.65	172.0	0.0
180.0	5.02	7.8	5.02	0.00	0.82	199.7	0.0
210.0	4.82	10.6	4.82	0.47	1.59	238.2	0.0
240.0	4.30	26.9	4.30	1.33	3.97	271.8	4.5
270.0	4.26	22.2	4.26	1.29	4.06	282.9	30.2
300.0	4.32	18.3	4.32	1.19	3.70	292.5	47.9
330.0	4.35	17.4	4.35	1.12	3.40	310.1	16.6
360.0	4.33	19.2	4.33	1.20	3.63	354.1	0.8
som							100.0

Figure B.3: Output of the HydraNL HBN calculation for a return period of 10 year.

r	zeews. m+NAP	windsn. m/s	h,teen m+NAP	Hm0,teen m	Tm-1,0,t s	golfr graden	bijdrage ov. freq (%)
30.0	4.73	13.3	4.73	1.04	2.86	6.0	0.0
60.0	4.94	12.3	4.94	0.78	2.63	45.7	0.0
90.0	5.02	10.2	5.02	0.64	2.19	63.2	0.0
120.0	4.94	12.4	4.94	0.78	2.65	67.3	0.0
150.0	--	--	--	--	--	--	0.0
180.0	--	--	--	--	--	--	0.0
210.0	5.19	10.4	5.19	0.47	1.58	237.6	0.0
240.0	4.55	29.7	4.55	1.53	4.12	270.2	2.9
270.0	4.52	24.2	4.52	1.48	4.19	281.8	26.9
300.0	4.56	19.9	4.56	1.41	4.06	291.5	52.6
330.0	4.61	18.8	4.61	1.31	3.70	308.2	17.1
360.0	4.59	20.7	4.59	1.37	3.86	353.9	0.5
som							100.0

Figure B.4: Output of the HydraNL HBN calculation for a return period of 25 year.

r	zeews. m+NAP	windsn. m/s	h,teen m+NAP	Hm0,teen m	Tm-1,0,t s	golfr graden	bijdrage ov. freq (%)
30.0	4.95	13.8	4.95	1.15	2.98	5.2	0.0
60.0	5.11	14.7	5.11	0.96	3.17	43.1	0.0
90.0	5.05	16.3	5.05	1.06	3.51	46.2	0.0
120.0	5.11	14.7	5.11	0.95	3.17	56.6	0.0
150.0	--	--	--	--	--	--	0.0
180.0	--	--	--	--	--	--	0.0
210.0	5.45	11.3	5.45	0.53	1.73	240.4	0.0
240.0	4.74	31.6	4.74	1.69	4.21	269.2	2.0
270.0	4.71	25.7	4.71	1.63	4.29	281.0	24.3
300.0	4.76	20.9	4.76	1.54	4.15	291.1	56.0
330.0	4.80	19.9	4.80	1.48	3.94	306.7	17.2
360.0	4.78	22.0	4.78	1.51	3.97	353.9	0.4
som							100.0

Figure B.5: Output of the HydraNL HBN calculation for a return period of 50 year.

r	zeews. m+NAP	windsn. m/s	h,teen m+NAP	Hm0,teen m	Tm-1,0,t s	golfr graden	bijdrage ov. freq (%)
30.0	4.95	18.6	4.95	1.56	4.02	356.7	0.0
60.0	5.11	21.3	5.11	1.40	4.43	37.2	0.0
90.0	5.03	23.3	5.03	1.50	4.60	37.4	0.0
120.0	5.03	23.2	5.03	1.50	4.59	37.3	0.0
150.0	--	--	--	--	--	--	0.0
180.0	--	--	--	--	--	--	0.0
210.0	5.74	10.8	5.74	0.52	1.67	239.2	0.0
240.0	4.93	33.5	4.93	1.84	4.30	268.0	1.5
270.0	4.90	27.2	4.90	1.77	4.37	280.1	22.1
300.0	4.95	22.1	4.95	1.68	4.24	290.7	59.1
330.0	4.99	21.2	4.99	1.62	4.06	306.5	17.0
360.0	4.95	23.5	4.95	1.66	4.08	353.7	0.3
som							100.0

Figure B.6: Output of the HydraNL HBN calculation for a return period of 100 year.

r	zeews. m+NAP	windsn. m/s	h,teen m+NAP	Hm0,teen m	Tm-1,0,t s	golfr graden	bijdrage ov. freq (%)
30.0	5.01	20.2	5.01	1.68	4.84	354.1	0.0
60.0	5.11	24.4	5.11	1.55	5.24	37.4	0.0
90.0	5.06	25.8	5.06	1.61	5.36	37.5	0.0
120.0	5.11	24.4	5.11	1.55	5.24	37.4	0.0
150.0	--	--	--	--	--	--	0.0
180.0	--	--	--	--	--	--	0.0
210.0	6.02	10.8	6.02	0.53	1.68	239.5	0.0
240.0	5.03	35.0	5.03	1.91	4.92	267.4	1.0
270.0	4.98	28.3	4.98	1.82	4.98	279.6	20.7
300.0	5.24	24.3	5.24	1.88	4.41	290.0	61.6
330.0	5.31	23.2	5.31	1.79	4.23	306.6	16.4
360.0	5.05	24.7	5.05	1.72	4.70	353.5	0.2
som							100.0

Figure B.7: Output of the HydraNL HBN calculation for a return period of 250 year.

r	zeews. m+NAP	windsn. m/s	h,teen m+NAP	Hm0,teen m	Tm-1,0,t s	golfr graden	bijdrage ov. freq (%)
30.0	5.02	23.4	5.02	1.80	5.10	353.7	0.0
60.0	5.12	28.3	5.12	1.70	5.57	38.0	0.0
90.0	5.09	29.1	5.09	1.72	5.63	38.1	0.0
120.0	5.12	28.3	5.12	1.70	5.57	38.0	0.0
150.0	--	--	--	--	--	--	0.0
180.0	--	--	--	--	--	--	0.0
210.0	6.21	10.6	6.21	0.53	1.66	239.2	0.0
240.0	5.23	37.3	5.23	2.07	5.02	266.5	0.7
270.0	5.16	30.2	5.16	1.96	5.09	278.6	19.4
300.0	5.24	24.6	5.24	1.87	4.99	290.1	63.7
330.0	5.54	24.5	5.54	1.94	4.34	306.6	16.0
360.0	5.25	26.4	5.25	1.84	4.82	353.6	0.2
som							100.0

Figure B.8: Output of the HydraNL HBN calculation for a return period of 500 year.

r	zeews. m+NAP	windsn. m/s	h,teen m+NAP	Hm0,teen m	Tm-1,0,t s	golfr graden	bijdrage ov. freq (%)
30.0	5.13	25.0	5.13	1.91	5.25	353.4	0.0
60.0	5.12	32.6	5.12	1.82	5.85	38.6	0.0
90.0	5.08	33.7	5.08	1.85	5.90	38.8	0.0
120.0	5.12	32.6	5.12	1.82	5.85	38.6	0.0
150.0	--	--	--	--	--	--	0.0
180.0	--	--	--	--	--	--	0.0
210.0	6.39	10.3	6.39	0.53	1.63	238.5	0.0
240.0	5.44	39.4	5.44	2.23	5.12	265.6	0.5
270.0	5.38	31.6	5.38	2.10	5.18	277.8	17.6
300.0	5.47	25.7	5.47	2.00	5.08	289.8	65.4
330.0	5.53	24.8	5.53	1.93	4.91	306.7	16.3
360.0	5.46	27.8	5.46	1.97	4.93	353.6	0.1
som							100.0

Figure B.9: Output of the HydraNL HBN calculation for a return period of 1000 year.

r	zeews. m+NAP	windsn. m/s	h,teen m+NAP	Hm0,teen m	Tm-1,0,t s	golfr graden	bijdrage ov. freq (%)
30.0	--	--	--	--	--	--	0.0
60.0	--	--	--	--	--	--	0.0
90.0	--	--	--	--	--	--	0.0
120.0	--	--	--	--	--	--	0.0
150.0	--	--	--	--	--	--	0.0
180.0	--	--	--	--	--	--	0.0
210.0	6.62	10.2	6.62	0.53	1.62	238.6	0.0
240.0	5.73	41.9	5.73	2.46	5.25	265.3	0.3
270.0	5.66	34.4	5.66	2.33	5.33	276.3	13.7
300.0	5.99	27.8	5.99	2.35	4.69	289.0	68.8
330.0	6.03	26.7	6.03	2.22	4.53	306.7	17.1
360.0	5.75	29.6	5.75	2.17	5.07	353.6	0.1
som							100.0

Figure B.10: Output of the HydraNL HBN calculation for a return period of 2500 year.

r	zeews. m+NAP	windsn. m/s	h,teen m+NAP	Hm0,teen m	Tm-1,0,t s	golfr graden	bijdrage ov. freq (%)
30.0	--	--	--	--	--	--	0.0
60.0	--	--	--	--	--	--	0.0
90.0	--	--	--	--	--	--	0.0
120.0	--	--	--	--	--	--	0.0
150.0	--	--	--	--	--	--	0.0
180.0	--	--	--	--	--	--	0.0
210.0	6.85	10.1	6.85	0.54	1.62	238.6	0.0
240.0	6.09	43.0	6.09	2.73	4.76	265.1	0.2
270.0	6.08	36.5	6.08	2.65	4.85	275.0	10.7
300.0	6.14	28.6	6.14	2.44	4.75	288.8	70.7
330.0	6.17	27.4	6.17	2.29	4.59	306.8	18.3
360.0	6.13	30.9	6.13	2.41	4.60	353.8	0.1
som							100.0

Figure B.11: Output of the HydraNL HBN calculation for a return period of 5000 year.

r	zeews. m+NAP	windsn. m/s	h,teen m+NAP	Hm0,teen m	Tm-1,0,t s	golfr graden	bijdrage ov. freq (%)
30.0	--	--	--	--	--	--	0.0
60.0	--	--	--	--	--	--	0.0
90.0	--	--	--	--	--	--	0.0
120.0	--	--	--	--	--	--	0.0
150.0	--	--	--	--	--	--	0.0
180.0	--	--	--	--	--	--	0.0
210.0	7.03	9.5	7.03	0.51	1.54	236.9	0.0
240.0	6.21	43.2	6.21	2.79	4.78	265.3	0.1
270.0	6.19	37.4	6.19	2.73	4.89	274.5	9.6
300.0	6.24	29.3	6.24	2.51	4.80	288.7	71.9
330.0	6.28	27.8	6.28	2.34	4.62	306.9	18.4
360.0	6.23	31.7	6.23	2.47	4.64	353.9	0.1
som							100.0

Figure B.12: Output of the HydraNL HBN calculation for a return period of 10000 year.

r	zeews. m+NAP	windsn. m/s	h,teen m+NAP	Hm0,teen m	Tm-1,0,t s	golfr graden	bijdrage ov. freq (%)
30.0	--	--	--	--	--	--	0.0
60.0	--	--	--	--	--	--	0.0
90.0	--	--	--	--	--	--	0.0
120.0	--	--	--	--	--	--	0.0
150.0	--	--	--	--	--	--	0.0
180.0	--	--	--	--	--	--	0.0
210.0	7.53	10.2	7.53	0.58	1.68	239.1	0.0
240.0	6.61	43.5	6.61	3.01	4.87	265.6	0.1
270.0	6.55	40.3	6.55	3.00	5.03	273.1	7.5
300.0	6.62	31.2	6.62	2.74	4.93	288.3	73.9
330.0	6.65	29.8	6.65	2.57	4.78	307.2	18.5
360.0	6.59	34.3	6.59	2.73	4.78	354.3	0.0
som							100.0

Figure B.13: Output of the HydraNL HBN calculation for a return period of 25000 year.

r	zeews. m+NAP	windsn. m/s	h,teen m+NAP	Hm0,teen m	Tm-1,0,t s	golfr graden	bijdrage ov. freq (%)
30.0	--	--	--	--	--	--	0.0
60.0	--	--	--	--	--	--	0.0
90.0	--	--	--	--	--	--	0.0
120.0	--	--	--	--	--	--	0.0
150.0	--	--	--	--	--	--	0.0
180.0	--	--	--	--	--	--	0.0
210.0	7.85	10.2	7.85	0.60	1.70	239.0	0.0
240.0	6.86	43.5	6.86	3.14	4.92	265.9	0.0
270.0	6.78	41.8	6.78	3.16	5.10	273.4	6.3
300.0	6.84	32.4	6.84	2.89	5.00	288.1	74.9
330.0	6.87	31.0	6.87	2.71	4.86	307.6	18.7
360.0	6.81	35.8	6.81	2.89	4.86	354.7	0.0
som							100.0

Figure B.14: Output of the HydraNL HBN calculation for a return period of 50000 year.

r	zeews. m+NAP	windsn. m/s	h,teen m+NAP	Hm0,teen m	Tm-1,0,t s	golfr graden	bijdrage ov. freq (%)
30.0	--	--	--	--	--	--	0.0
60.0	--	--	--	--	--	--	0.0
90.0	--	--	--	--	--	--	0.0
120.0	--	--	--	--	--	--	0.0
150.0	--	--	--	--	--	--	0.0
180.0	--	--	--	--	--	--	0.0
210.0	7.96	13.7	7.96	0.84	2.30	250.0	0.0
240.0	7.01	43.5	7.01	3.21	4.95	266.0	0.0
270.0	6.91	42.3	6.91	3.25	5.14	273.5	5.9
300.0	6.98	33.1	6.98	2.98	5.04	287.9	75.1
330.0	7.00	31.5	7.00	2.79	4.91	307.7	18.9
360.0	6.93	37.0	6.93	3.01	4.90	355.2	0.0
som							100.0

Figure B.15: Output of the HydraNL HBN calculation for a return period of 75000 year.

r	zeews. m+NAP	windsn. m/s	h,teen m+NAP	Hm0,teen m	Tm-1,0,t s	golfr graden	bijdrage ov. freq (%)
30.0	--	--	--	--	--	--	0.0
60.0	--	--	--	--	--	--	0.0
90.0	--	--	--	--	--	--	0.0
120.0	--	--	--	--	--	--	0.0
150.0	--	--	--	--	--	--	0.0
180.0	--	--	--	--	--	--	0.0
210.0	7.96	15.1	7.96	1.13	2.85	254.4	0.0
240.0	7.12	43.5	7.12	3.25	4.97	266.0	0.0
270.0	7.02	42.6	7.02	3.32	5.16	273.5	5.5
300.0	7.07	33.7	7.07	3.05	5.08	287.9	75.5
330.0	7.10	32.0	7.10	2.83	4.94	308.0	19.0
360.0	7.02	37.8	7.02	3.09	4.93	355.6	0.0
som							100.0

Figure B.16: Output of the HydraNL HBN calculation for a return period of 100000 year.

C

Sea level rise scenarios

The sea level rise scenarios are based IPCC (2013). Figure C.1 shows the median trend of the different sea level rise scenarios. The data of these scenarios including uncertainty range can be found Tables C.1 and C.2. For this study, the scenario of RCP8.5 is used.

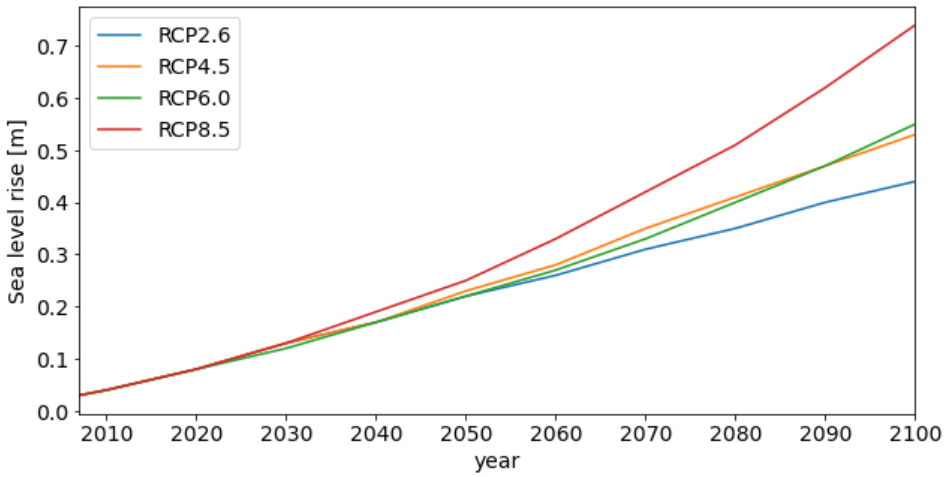

Figure C.1: IPCC (2013) sea level rise scenarios, median values

year	RCP2.6			RCP4.5		
	median	range min	range max	median	range min	range max
2007	0,03	0,02	0,4	0,03	0,02	0,04
2010	0,04	0,03	0,5	0,04	0,03	0,05
2020	0,08	0,06	0,1	0,08	0,06	0,1
2030	0,13	0,09	0,16	0,13	0,09	0,16
2040	0,17	0,13	0,22	0,17	0,13	0,22
2050	0,22	0,16	0,28	0,23	0,17	0,29
2060	0,26	0,18	0,35	0,28	0,21	0,37
2070	0,31	0,21	0,41	0,35	0,25	0,45
2080	0,35	0,24	0,48	0,41	0,28	0,54
2090	0,4	0,26	0,54	0,47	0,32	0,62
2100	0,44	0,28	0,61	0,53	0,36	0,71

Table C.1: Sea level rise in meter for different IPCC (2013) scenarios

year	RCP6.0			RCP8.5		
	median	range min	range max	median	range min	range max
2007	0,03	0,02	0,04	0,03	0,02	0,04
2010	0,04	0,03	0,05	0,04	0,03	0,05
2020	0,08	0,06	0,1	0,08	0,06	0,11
2030	0,12	0,09	0,16	0,13	0,1	0,17
2040	0,17	0,12	0,21	0,19	0,14	0,24
2050	0,22	0,016	0,28	0,25	0,19	0,32
2060	0,27	0,019	0,35	0,33	0,24	0,42
2070	0,33	0,24	0,43	0,42	0,31	0,54
2080	0,4	0,28	0,53	0,51	0,37	0,67
2090	0,47	0,33	0,63	0,62	0,45	0,81
2100	0,55	0,38	0,73	0,74	0,53	0,98

Table C.2: Sea level rise in meter for different IPCC (2013) scenarios

D

Data - polders Western Scheldt

Figure D.1 shows the bed level of polders in Zeeland on which the case study is based. For the case study a bed level of 1.5 meter is assumed.

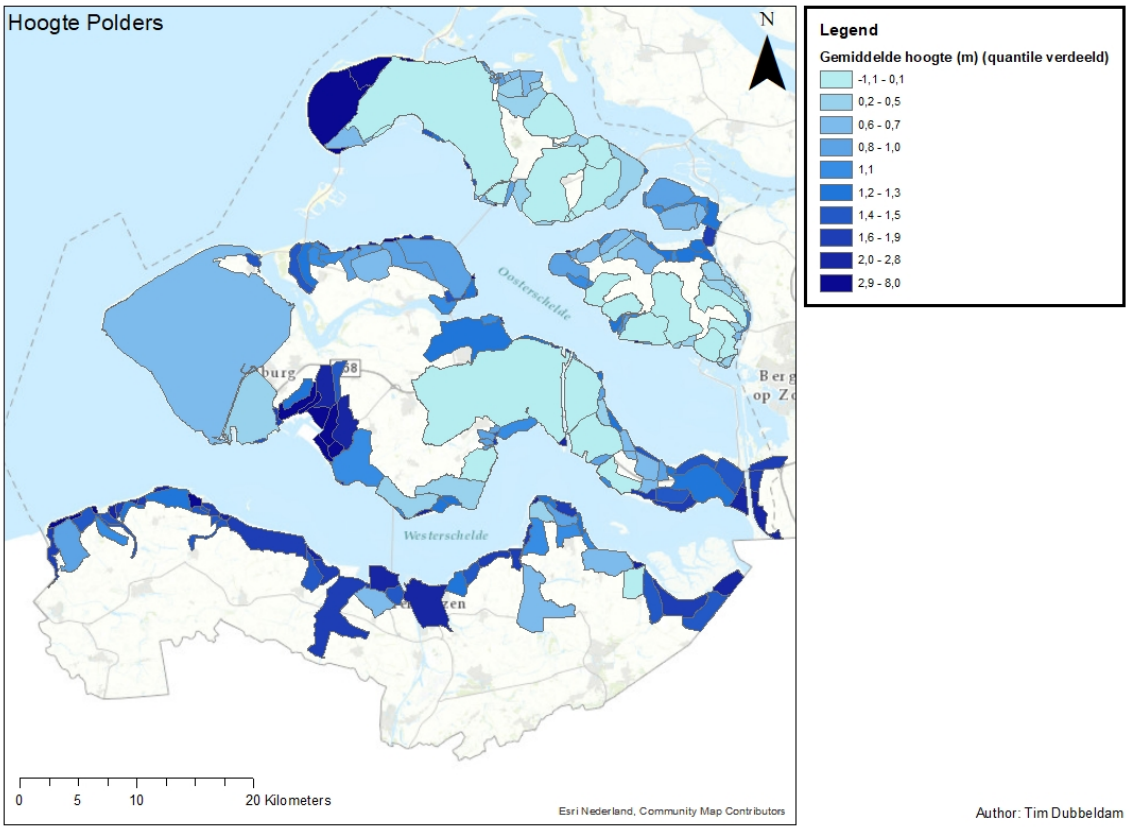

Figure D.1: Bed level height of polders in Zeeland (Van den Hoven et al., submitted)

E

Method for calculating dike volumes

For the calculation of the dike volumes, a single dike is schematized as depicted in Figure E.1. It is convenient to distinguish the volume of the following three parts: crest volume, slope volume and berm volume. The method for the calculation of a single dike is shown in Equation E.1. The calculation of the first and second dike in a double dike system does not differ. However, there is one exception. For the sensitivity analysis in which the height of the first dike is lowered, the berm is not included in the volume calculations.

$$V_{dike} = h_{crest} \cdot b_{crest} + \frac{1}{tan\alpha} \cdot h_{crest}^2 + h_{berm} \cdot b_{berm} \tag{E.1}$$

in which:

V_{dike} = volume of the dike (m^3)

h_{crest} = height of the crest (m)

b_{crest} = width of the crest (m)

$tan\alpha$ = slope of the dike (-)

h_{berm} = height of the berm (m)

b_{berm} = width of the berm (m)

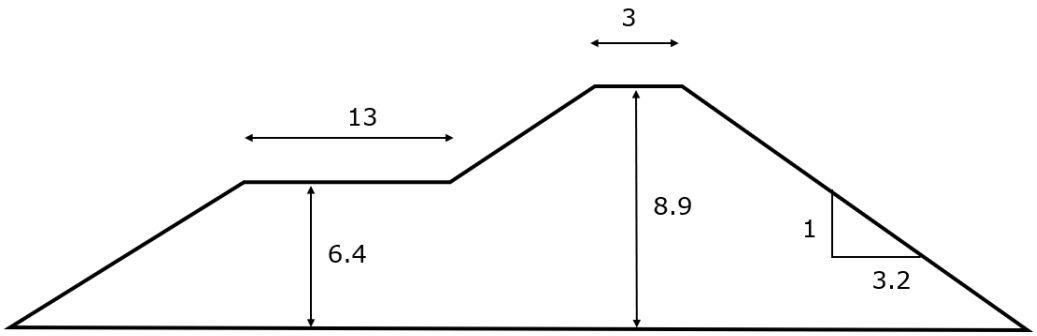

Figure E.1: Cross-section of a dike section

F

Results - Case study

The sections below show the results of the calculations done for the case study. The results are divided into dike heights, dike volumes and hydraulic conditions in the design point. A distinction is made between the failure probability approach and LIR approach.

F.1. Dike heights

failure probability approach			
	2020	**2070**	**2120**
SLR [m]	0	0,4	1
	height single dike [m]		
	8,9	9,3	9,9
	height double dike [m]]		
Scenario 1	7,2	7,62	8,36
Scenario 2	7,2	7,62	8,36
Scenario 3	7,2	7,62	8,34
Scenario 4	7,2	7,62	8,33
Scenario 5	7,2	7,56	8,32

Table F.1: Dike heights following the failure probability approach. The table contains both the height of the single dike system as the height of the second dike of the double dike system for the different morphological scenarios.

LIR approach			
	2020	**2070**	**2120**
SLR	0	0,4	1
	height single dike [m]		
	8,9	9,69	10,57
	height double dike [m]]		
Scenario 1	7,2	7,98	8,96
Scenario 2	7,2	7,93	8,89
Scenario 3	7,2	7,85	8,8
Scenario 4	7,2	7,76	8,63
Scenario 5	7,2	7,02	7,71

Table F.2: Dike heights following the LIR approach. The table contains both the height of the single dike system as the height of the second dike of the double dike system for the different morphological scenarios.

F.2. Dike volumes

	Failure	**LIR**
2020	261,1	261,1
2070	287,0	308,1
2120	327,7	367,2

Table F.3: Dike volumes $[m^3/m]$ of a single dike system in time for both the failure probability approach as LIR approach

	Volume h2		
	2020	**2070**	**2120**
Scenario 1	184,8	207,1	247,9
Scenario 2	184,8	207,1	247,9
Scenario 3	184,8	207,1	246,9
Scenario 4	184,8	207,1	246,5
Scenario 5	184,8	204,6	246,0
	Volume total		
	2020	**2070**	**2120**
Scenario 1	445,9	468,2	509,0
Scenario 2	445,9	468,2	509,0
Scenario 3	445,9	468,2	508,1
Scenario 4	445,9	468,2	507,6
Scenario 5	445,9	465,7	507,1

Table F.4: Dike volumes $[m^3/m]$ of double dike systems according the failure probability approach for the different morphological scenarios. A distinction is made between the volume of the second dike and the total volume of the system, which also includes the first dike of 8.9 meter.

	Volume dike 2		
	2020	**2070**	**2120**
Scenario 1	184,8	222,7	277,2
Scenario 2	184,8	220,5	273,6
Scenario 3	184,8	217,0	269,1
Scenario 4	184,8	213,1	260,8
Scenario 5	184,8	183,0	218,7
	Volume total		
	2020	**2070**	**2120**
Scenario 1	445,9	483,8	538,3
Scenario 2	445,9	481,6	534,8
Scenario 3	445,9	478,1	530,3
Scenario 4	445,9	474,2	521,9
Scenario 5	445,9	444,1	479,9

Table F.5: Dike volumes $[m^3/m]$ of double dike systems according the LIR approach for the different morphological scenarios. A distinction is made between the volume of the second dike and the total volume of the system, which also includes the first dike of 8.9 meter.

F.3. Hydraulic conditions in the design point

	Failure			LIR		
Wind velocity[m/s]	**2020**	**2070**	**2120**	**2020**	**2070**	**2120**
Scenario 1	31,7	31,7	31,7	31,7	33	33,8
Scenario 2	31,7	31,7	31,7	31,7	32,8	33,6
Scenario 3	31,7	31,7	31,7	31,7	32,6	33,2
Scenario 4	31,7	31,7	31,7	31,7	32,3	32,7
Scenario 5	31,7	31,7	31,7	31,7	29,2	31,9

Water level [m]	**2020**	**2070**	**2120**	**2020**	**2070**	**2120**
Scenario 1	6,71	7,11	7,71	6,71	7,36	8,07
Scenario 2	6,71	7,11	7,71	6,71	7,32	8,06
Scenario 3	6,71	7,11	7,71	6,71	7,28	7,99
Scenario 4	6,71	7,11	7,71	6,71	7,22	7,9
Scenario 5	6,71	7,11	7,71	6,71	6,63	7,75

Wave height [m]	**2020**	**2070**	**2120**	**2020**	**2070**	**2120**
Scenario 1	1,06	1,01	1,16	1,06	1,15	1,38
Scenario 2	1,06	0,99	1,16	1,06	1,13	1,34
Scenario 3	1,06	0,98	1,14	1,06	1,1	1,29
Scenario 4	1,06	0,98	1,12	1,06	1,08	1,22
Scenario 5	1,06	0,98	1,1	1,06	0,89	1,12

Wave period [s]	**2020**	**2070**	**2120**	**2020**	**2070**	**2120**
Scenario 1	2,72	2,79	3,19	2,72	3,09	3,6
Scenario 2	2,72	2,81	3,18	2,72	3,04	3,54
Scenario 3	2,72	2,81	3,16	2,72	2,99	3,46
Scenario 4	2,72	2,8	3,14	2,72	2,91	3,53
Scenario 5	2,72	2,74	3,13	2,72	2,56	3,17

Table F.6: Hydraulic conditions in the design point for the different morphological scenarios.

G

Results - sensitivity analysis

This appendix contains the quantitative results of the sensitivity analysis. G.1 shows the calculated dike heights and Section G.2 contains the corresponding volumes. This is done for the four different analyses: 1) Configuration of the first dike and interdike area, 2) Varying hydraulic boundary conditions, 3) Area size flooded hinterland and 4) Vegetation.

G.1. Dike heights and design points

Height dike 2 [m]

	Failure		LIR	
height dike 1 [m]	**2020**	**2120**	**2020**	**2120**
8,9	7,2	8,32	7,2	7,71
7,5	7,46	8,63	7,46	8,04
6	7,83	8,69	7,84	8,15
4,5	7,94	8,72	7,94	8,19

Wind velocity[m/s]

height dike 1 [m]	**2020**	**2120**	**2020**	**2120**
8,9	31,67	31,71	31,7	29,6
7,5	31,67	31,67	31,7	29,57
6	31,68	31,66	31,66	29,57
4,5	31,68	31,67	31,66	29,57

Water level [m]

height dike 1 [m]	**2020**	**2120**	**2020**	**2120**
8,9	6,7	7,7	6,7	7,3
7,5	6,7	7,7	6,7	7,3
6	6,7	7,7	6,7	7,3
4,5	6,7	7,7	6,7	7,3

Wave height [m]

height dike 1 [m]	**2020**	**2120**	**2020**	**2120**
8,9	1,05	1,10	1,05	0,91
7,5	1,23	1,34	1,23	1,16
6	1,57	1,38	1,57	1,23
4,5	1,67	1,38	1,67	1,23

Wave period [s]

height dike 1 [m]	**2020**	**2120**	**2020**	**2120**
8,9	2,72	3,13	2,72	2,63
7,5	3,39	3,8	3,39	3,51
6	4,04	3,94	4,04	3,77
4,5	4,19	4,05	4,19	3,88

Table G.1: Configuration of the first dike and interdike area - dike heights and design point

Single dike	Hydraulic conditions		Single dike height [m]			Opp [m2]
	tide %	surge %	2020	2120 failure	2120 LIR	
Conditions 0	100	100	8,9	9,9	10,57	8370082
Conditions 1	50	100	7,65	8,65	9,47	2606684
Conditions 2	100	50	6,8	7,8	8,54	416152

Table G.2: Varying hydraulic boundary conditions - approach and single dike results

Height dike 2 [m]

	Failure		LIR	
height dike 1 [m]	**2020**	**2120**	**2020**	**2120**
Conditions 0	7,2	8,32	7,20	7,71
Conditions 1	5,88	6,61	5,88	6,54
Conditions 2	5,00	5,95	5,00	6.20

Wind velocity[m/s]

height dike 1 [m]	**2020**	**2120**	**2020**	**2120**
Conditions 0	31,67	31,67	31,67	29,57
Conditions 1	31,67	31,67	31,67	30,16
Conditions 2	31,67	31,68	31,67	33,08

Water level [m]

height dike 1 [m]	**2020**	**2120**	**2020**	**2120**
Conditions 0	6,71	7,71	6,71	7,30
Conditions 1	5,46	6,45	5,46	6,17
Conditions 2	4,60	5,60	4,60	5,74

Wave height [m]

height dike 1 [m]	**2020**	**2120**	**2020**	**2120**
Conditions 0	1,06	1,10	1,06	0,91
Conditions 1	1,06	0,86	1,06	0,78
Conditions 2	0,87	0,70	0,87	0,75

Wave period [s]

height dike 1 [m]	**2020**	**2120**	**2020**	**2120**
Conditions 0	2,72	3,13	2,72	2,63
Conditions 1	3,01	2,58	3,01	2,50
Conditions 2	2,60	2,70	2,60	2,85

Table G.3: Varying hydraulic boundary conditions - dike heights and design point

	Opp		single dike height [m]			
	%	m2	2020 Failure	2020 LIR	2120 Failure	2120 LIR
area 0	100%	8377322	8,9	8,9	9,9	10,57
area 1	50%	4188661	8,9	9,56	9,9	10,89
area 2	25%	2094331	8,9	9,92	9,9	11,15
area 3	150%	12565983	8,9	8,15	9,9	10,23

Table G.4: Area size flood hinterland - approach and single dike results

Height dike 2 [m]

	Failure		LIR	
height dike 1 [m]	**2020**	**2120**	**2020**	**2120**
Area 0	7,20	8,32	7,2	7,71
Area 1	7,20	8,32	7,69	8,97
Area 2	7,20	8,32	7,99	9,27
Area 3	7,20	8,32	6,63	7,63

Wind velocity[m/s]

height dike 1 [m]	**2020**	**2120**	**2020**	**2120**
Area 0	31,67	31,67	31,67	29,55
Area 1	31,67	31,67	33,88	34,00
Area 2	31,67	31,67	34,99	35,05
Area 3	31,67	31,67	29,01	29,24

Water level [m]

height dike 1 [m]	**2020**	**2120**	**2020**	**2120**
Area 0	6,71	7,70	6,71	7,30
Area 1	6,71	7,70	7,08	8,11
Area 2	6,71	7,70	7,30	8,30
Area 3	6,71	7,70	6,21	7,23

Wave height [m]

height dike 1 [m]	**2020**	**2120**	**2020**	**2120**
Area 0	1,06	1,10	1,06	0,90
Area 1	1,06	1,10	1,14	1,33
Area 2	1,06	1,10	1,26	1,43
Area 3	1,06	1,10	0,93	0,89

Wave period [s]

height dike 1 [m]	**2020**	**2120**	**2020**	**2120**
Area 0	2,72	3,13	2,72	2,62
Area 1	2,72	3,13	3,02	3,60
Area 2	2,72	3,13	3,25	3,78
Area 3	2,72	3,13	2,59	2,56

Table G.5: Area size flooded hinterland - dike heights and design point

Heigh dike 1 [m]

	Failure		LIR	
Height dike 1 [m]	**2020**	**2120**	**2020**	**2120**
veg 0	7,2	8,32	7,2	7,71
veg 1	7,2	8,3	7,2	7,71
veg 2	7,2	8,27	7,2	7,71
veg 3	7,2	8,28	7,2	7,71
veg 4	7,2	8,23	7,2	7,69

Wind velocity[m/s]

Height dike 1 [m]	**2020**	**2120**	**2020**	**2120**
veg 0	31,67	31,67	31,67	29,57
veg 1	31,67	31,67	31,67	29,57
veg 2	31,67	31,67	31,67	29,57
veg 3	31,67	31,67	31,67	29,57
veg 4	31,67	31,67	31,67	29,57

Water level [m]

Height dike 1 [m]	**2020**	**2120**	**2020**	**2120**
veg 0	6,71	7,71	6,71	7,3
veg 1	6,71	7,71	6,71	7,3
veg 2	6,71	7,71	6,71	7,3
veg 3	6,71	7,71	6,71	7,3
veg 4	6,71	7,71	6,71	7,3

Wave height [m]

Height dike 1 [m]	**2020**	**2120**	**2020**	**2120**
veg 0	1,05	1,1	1,05	0,91
veg 1	1,05	1,06	1,05	0,89
veg 2	1,05	1,02	1,05	0,88
veg 3	1,05	1,04	1,05	0,89
veg 4	1,05	0,96	1,05	0,86

Wave period [s]

Height dike 1 [m]	**2020**	**2120**	**2020**	**2120**
veg 0	2,72	3,13	2,72	2,63
veg 1	2,72	3,11	2,72	2,62
veg 2	2,72	3,06	2,72	2,62
veg 3	2,72	3,08	2,72	2,62
veg 4	2,72	3,01	2,72	2,61

Table G.6: Vegetation - dike heights and design point

G.2. Double dike systems volumes

Total volume double dike (m3/m)				
	Failure		LIR	
	2020	2120	2020	2120
8,9	382,2	443,4	382,2	416,2
7,5	328,4	394,0	328,4	366,4
6	289,2	342,0	289,6	316,5
4,5	253,5	303,0	253,5	277,8

Table G.7: Configuration of the first dike and interdike area - total volumes

Tot volume double dike (m3)				
	Failure		LIR	
	2020	2120	2020	2120
Conditions 0	445,9	507,1	445,9	479,9
Conditions 1	315,4	352,8	315,4	350,3
Conditions 2	236,1	276,1	236,1	284,2

Table G.8: Varying hydraulic boundary conditions - total volumes

Total volume double dike (m3)				
	Failue		LIR	
	2020	2120	2020	2120
Area 0	445,9	507,1	445,9	479,9
Area 1	445,9	507,1	500,6	573,4
Area 2	445,9	507,1	533,8	609,0
Area 3	445,9	507,1	388,5	440,5

Table G.9: Area size flooded hinterland - total volumes

Total volume double dike (m3)				
	Failure		LIR	
	2020	2120	2020	2120
veg 0	445,9	507,1	445,9	479,9
veg 1	445,9	506,2	445,9	479,9
veg 2	445,9	504,8	445,9	479,9
veg 3	445,9	505,3	445,9	479,9
veg 4	445,9	503,0	445,9	479,0

Table G.10: Vegetation - total volumes